1997

Competition between Li+ and Mg2+ for Human RBCMembrane Phospholipids and Guanine Nucleotide Binding Proteins

Chandra Srinivasan
Loyola University Chicago

LOYOLA UNIVERSITY OF CHICAGO

COMPETITION BETWEEN Li^+ AND Mg^{2+} FOR HUMAN RBC MEMBRANE PHOSPHOLIPIDS AND GUANINE NUCLEOTIDE BINDING PROTEINS

A DISSERTATION SUBMITTED TO

THE FACULTY OF THE GRADUATE SCHOOL

IN CANDIDACY FOR THE DEGREE OF

DOCTOR OF PHILOSOPHY

DEPARTMENT OF CHEMISTRY

BY

CHANDRA SRINIVASAN

CHICAGO, ILLINOIS

JANUARY 1997

ACKNOWLEDGEMENTS

I am grateful to my mentor, Dr. Duarte Mota de Freitas for his guidance and generous financial support. I am indebted to him for giving me the opportunity to work in his research group and I am thankful to him for helping me with my organizational and communicational skills.

My sincere gratitude to our collaborators Drs. Carlos Geraldes (University of Coimbra, Portugal) and Daniel Graham (Loyola University) for their help and guidance with multiple quantum NMR experiments and data analysis. I would like to thank Dr. Margarida Castro, Rui Carvalho and others in Portugal for their friendship and hospitality during my stay in Portugal. Special thanks to our collaborators, Profs. Yee-Kin Ho and Heidi Hamm (University of Illinois, Chicago) for training me to carry out large scale G protein isolation and purification. I thank their lab members, especially, Dr. Andreas Loew, Joe Robello and Dr. Nick Skiba for their assistance and suggestions with protein purification. I would also like to thank Dr. Kenneth Olsen and Joe Brunzelle for their assistance with the figures on G proteins.

I am grateful to my committee members, Dr. David S. Crumrine, Dr. Evan B. Stubbs and Dr. Poluru L. Reddy for their time and help with my projects; their constructive criticism helped me to tie up the loose ends in the project.

Financial support from the Graduate School as well as generous travel grants for the conferences are grately appreciated by the author. I thank the Arthur J. Schmitt Foundation for awarding me a dissertation fellowship in the final year of my degree.

My sincere gratitude to Louis Amari, for his help and cooperation in the joint protein purification project; thanks for filling in when I was unable to work. Special thanks to my lab members Qinfen Rong, Dr. Elizabeth Dorus, Yuling Chi, Cherian Zachariah, Wanrong Lin, Hanan Hasan, Joyce Nikolakopoulos, Faiz Uddin, Loc Nuygen, Jason Toon, and Dr. Yang Nan for their cooperation and suggestions.

I would like to thank Dr. Mehboob Peeran (St. Joseph's College, Bangalore) for suggesting Loyola University Chicago for graduate studies. Special thanks to Ravi, Elias, Nachu and all my friends for their help and time. Finally, I would like to thank my mother and other family members for their love and encouragement.

To my dear father

TABLE OF CONTENTS

LIST OF FIGURES

LIST OF TABLES

LIST OF ABBREVIATIONS

AA	atomic absorption spectrophotometry
AT	acquisition time
ADP	adenosine 5'-diphosphate
ATP	adenosine 5'-triphosphate
BSA	bovine serum albumin
cAMP	cyclic adenosine monophosphate
$CDCl_3$	deuterated chloroform
cGMP	cyclic guanosine monophosphate
CL	cardiolipin
δ	chemical shift
DAG	diacylglycerol
D_2O	deuterium oxide
DPG	2,3-diphosphoglycerate
DTT	dithiothreitol
DQF	double quantum filtered
EDTA	ethylenediaminetetraacetic acid
EGTA	ethylene glycol-bis(β-aminoethylether) N,N,N',N'-tetraacetic acid
ESR	electron spin resonance
^{19}F	fluorine-19 isotope

G protein	guanine nucleotide binding protein
GDP	guanosine-5' diphosphate
G_i	G protein that inhibits adenylate cyclase
G_o	G protein that inhibits PI turnover
G_s	G protein that stimulates adenylate cyclase
Gpp(NH)p	guanosine-5'-(β,γ- imido)-triphosphate
GTP	guanosine-5' triphosphate
GTPγS	guanosine 5'-O-(3-thiotriphosphate)
HEPES	4-(2-hydroxyethyl)-1-piperazineethanesulfonic acid
HED (D_2O)	HEPES buffer (50 mM) at pH 8.0 containing 0.1 mM EDTA and 1 mM DTT in D_2O
HPLC	high performance liquid chromatography
ICP-ES	inductively coupled plasma emission spectroscopy
IOV	inside-out vesicle
IP_3	inositol 1,4,5-triphosphate
IPTG	isopropyl β-D-thiogalactoside
^6Li	lithium-6 isotope
^7Li	lithium-7 isotope
MOPS	(3-[N-Morpholino]propane-sulfonic acid)
NMR	nucleap magnetic resonance
MQF	multiple quantum filtered
NTA	nitrilotriacetic acid
PA	phosphatidic acid
^{31}P	phosphorous-31 isotope

PC	phosphatidylcholine
PDE	phosphodiesterase
PE	phosphatidylethanolamine
PE_p	plasmalogen PE
PG	phosphatidylglycerol
PI	phosphatidylinositol
PMSF	phenylmethylsulfonyl fluoride
PS	phosphatidylserine
PW	pulse width
RBC	red blood cell
rG_i	recombinant G_i
ROS	rod outer segment
ROV	right side-out vesicle
^{23}Na	sodium-23 isotope
SA	spectrin actin
SDS-PAGE	sodium dodecylsulfate polyacrylamide gel electrophoresis
Sph	sphingomyelin
SQ	single quantum
T_1	spin-lattice relaxation time
T_2	spin-spin relaxation time
T	heterotrimeric transducin
T_α-GDP	α-subunit of T bound to GDP
TMACl	tetramethylammonium chloride
TLC	thin layer chromatography

Tris	tris(hydroxymethyl)aminomethane
TQF	triple quantum filtered
UV-Vis	ultraviolet-visible spectroscopy

ABSTRACT

The mode of action of lithium ion (Li^+) in the treatment of manic-depression or bipolar illness is still under investigation although this inorganic drug has been in use for over forty years. Lithium ion was shown to block the activity of the enzyme inositol monophosphatase and also G_i and G_s, the guanine nucleotide binding (G) proteins that inhibit and stimulate the enzyme adenylate cyclase, respectively. As several enzymes in the signal transduction cascade require magnesium ions (Mg^{2+}) for their function, Li^+ could compete at the Mg^{2+}-binding sites. Li^+ and Mg^{2+} ions have similar ionic radii and hence competition between these two ions could occur. Several research reports have provided evidence for Li^+/Mg^{2+} competition in biomolecules. This present study was carried out in order to fully characterize the interactions of Li^+ and Mg^{2+} with red blood cells (RBCs) and purified G proteins to see whether Li^+/Mg^{2+} competition occurs for G proteins as this may explain the antimanic and antidepressant therapeutic effects of the lithium ion.

Low-temperature phosphorous-31 (^{31}P) nuclear magnetic resonance (NMR) studies with adenosine triphosphate (ATP) and RBC membranes confirmed the existence of Li^+/Mg^{2+} competition. To identify whether the RBC membrane cytoskeleton or the phospholipids provide major metal ion binding sites in the RBC membranes, sodium-23 (^{23}Na) multiple quantum filtered NMR studies were conducted. These NMR studies proved that the removal of the cytoskeleton did not affect metal ion binding to the membranes or competition between Li^+ and Mg^{2+}. However, ^7Li NMR relaxation measurements indicated that the removal of the cytoskeleton

increased Li^+ affinity for the membranes. ^{31}P NMR chemical shift measurements of the phospholipids extracted from the RBC membranes identified the anionic phospholipids, phosphatidylserine (PS) and phosphatidylinositol (PI), that bind Li^+ and Mg^{2+} most strongly. The Li^+ binding constant to the phospholipid extract was found to be $45 \pm 5\ M^{-1}$ ($r^2 > 0.90$). Thus these studies proved that the phospholipids, and not the cytoskeleton, play a major role in metal ion binding.

Similar multinuclear NMR methods were developed to probe Li^+ binding to various G proteins. ^7Li NMR relaxation measurements of bovine rod outer segment (ROS) membranes with transducin, and of recombinant $G_i\alpha_1$ in the GDP-bound conformation showed the existence of competition between Li^+ and Mg^{2+}. The Li^+ binding constants to these G proteins were also determined.

CHAPTER I

INTRODUCTION

I.1. History of Lithium in Psychiatry

Lithium salts have quite a few medical applications. Initially, they were used for the treatment of mania and depression. Less common medical applications of lithium salts include the treatment of patients suffering from depression (or unipolar disorder), schizophrenia, alcoholism, anemia, and cluster headaches (Schou, 1957). In an attempt to identify the toxins that cause mania, Cade gave guinea pigs lithium salt dissolved in uric acid and noticed that the animals became very sedated. The calming effect of lithium on the animals prompted Cade to test lithium in 10 patients with mania and he found some dramatic results (Cade, 1949). The same year, the Food and Drug Administration (FDA) banned the use of lithium due to the deaths of several patients. Since then it took nearly 20 years before the FDA approved lithium in the treatment of mania. Today, lithium salts in the form of citrate or carbonate are administered in the treatment of manic-depression (or bipolar disorder).

Manic-depression is a psychiatric illness characterized by severe mood swings, alternating between mania and depression. It is estimated that at least one in every thousand individuals in the United States, Great Britain and Scandinavian countries is undergoing lithium therapy (Jefferson et al., 1985). In the United States, lithium is marketed as a carbonate in tablets and as a citrate in a syrup. The uptake of lithium in the tissues is very slow; it takes 5-14 days to reach the therapeutic level of 0.3-1.0 mM in sera (Jefferson et al., 1985). In the initial stages of treatment, the daily dosage of lithium ranges from 1200-1800 mg per day in order to reach

plasma concentrations in the range of 0.8 to 1.4 mmol per liter; higher concentrations of lithium are associated with higher response rates as well as serious neurotoxicity. For mood maintenance therapy, doses of 900-1500 mg per day are usually given to attain plasma concentrations of 0.6-1.0 mmol per liter. The daily dose is soon consolidated into a single night time dose, which is supposed to decrease some of the long-term renal side effects.

Most patients undergoing lithium treatment experience side effects due to the narrow concentration range between therapy and toxicity (Jefferson et al., 1985). Common side effects of this drug are lethargy, excessive thirst and urination, skin disorders, weight gain due to water retention, hand tremor, and mild memory impairment. Serum and plasma lithium levels are monitored closely to distinguish the symptoms that are due to Li^+ toxicity. Severe toxic effects of lithium which occur when the plasma lithium level exceeds 2.5 mmol/liter are convulsions, ataxia, delirium, impaired renal function and impaired consciousness which progresses to coma.

Lithium has largely lived up to its initial promise as the first drug in the modern era of psychopharmacology. Although lithium has been in use for over forty years, its mode of action is not clearly understood.

I.2. Mode of Action of Lithium

There has been a lot of research done to solve the intriguing puzzle of where and how lithium acts. Increasing evidence points to signal transduction systems, especially the phosphoinositide second messenger system as the most important target of lithium action. In 1971, it was reported that lithium administered rats showed decreased brain inositol concentrations (Allison & Stewart, 1971). In 1974, lithium was shown to inhibit the enzyme inositol monophosphatase which catalyses the conversion of inositol monophosphate to inositol which in turn regenerates the phospholipid, phosphatidylinositol (PI) (Naccarato et al., 1974).

Since then there have been several reports on the actions of lithium on the phosphoinositide system (Baraban et al.,1989; Berridge et al., 1989; Mork, 1990; Pollack et al., 1994). The major drawback of this mechanism is that the evidence for *in vivo* brain inositol depletion at the therapeutic levels of Li^+ is still lacking (Jope & Williams, 1994). This hypothesis does not explain how Li^+ can be used to treat both mania and depression, which are two opposite effects. Because much of the emphasis in studies of the lithium action on phosphoinositide metabolism has been related to inositol phosphatases, significant gaps remain in the other actions of lithium.

The two inter-related hypotheses at the molecular level that we are currently investigating that complement the mechanistic studies of inositol monophosphatase are: competition between lithium and magnesium ions for the magnesium binding sites in biomolecules (Abraha et al., 1991; Frausto da Silva & Williams, 1976; Mota de Freitas et al., 1994a; Ramasamy & Mota de Freitas, 1989; Rong et al., 1992, 1994) and a cell membrane abnormality (Frazer et al., 1978; Meltzer, 1991).

The lithium ion (Li^+), the active species in drug formulations, may exert its pharmacological effects by regulating neurotransmitter systems through guanine nucleotide binding (G) proteins. A variety of other studies of lithium in neuronal and nonneuronal tissues provide evidence that lithium modulates G protein function and these effects may be related to its therapeutic effects in human patients (Manji, 1992). The latest study shows evidence that long term lithium treatment at therapeutic levels altered G protein function (Manji et al., 1995).

G proteins are localized in the inner surface of the plasma membrane, where they function as signal transducers, coupling diverse receptor to effector proteins. Once an extracellular agonist binds to a specific receptor, the receptor will stimulate the G proteins; the G protein will then undergo a conformational change, allowing GTP to bind to its α-subunit and become activated. The activated G protein interacts with adenylate cyclase and regulates the synthesis of cyclic

AMP (cAMP) from ATP. The activation of G proteins may also stimulate phospholipase C-mediated breakdown of phosphatidylinositol-4,5-biphosphate, leading to the formation of the intracellular second messengers diacylglycerol (DAG) and inositol-1,4,5-triphosphate (IP_3). IP_3 further interacts with its receptor and induces the release of intracellular stores of Ca^{2+} (Figure 1). The activation of G proteins, the synthesis of cAMP from ATP catalyzed by adenylate cyclase, and the dephosphorylation of inositol monophosphate catalyzed by inositol monophosphatase are all Mg^{2+}-dependent processes that are inhibited by Li^+ (Avissar et al., 1988; Mork, 1990; Pollack et al., 1994).

Avissar et al. (1991) found that G proteins were inhibited in the presence of lithium (*in vitro* or chronic *in vivo* treatment) and this effect was reversed by Mg^{2+}. These authors also showed that, within the therapeutic dosage range, lithium inhibits the activities of the G proteins, G_i and G_s (where G_i and G_s are two distinct G proteins that inhibit and stimulate the enzyme adenylate cyclase, respectively) and G_o, the neuronal G protein that mediates Ca^{2+} channel closure and inhibits the PI turnover. This inhibition is presumed to be occurring via the competition between lithium and magnesium ions for the Mg^{2+}-binding sites of the G protein complex. These two types of G proteins may provide a common site for the antimanic and antidepressant therapeutic effects of lithium (Avissar et al., 1988). The G protein hypothesis therefore explains the action of lithium salts, regulating both the manic and the depressive phases of bipolar illness, whereas the adenylate cyclase and PI turnover hypotheses only account for the effect of Li^+ in one of the mood disturbances. Several recent studies have provided evidence for the presence of hyperfunctional G proteins or abnormal amounts of G proteins in the membranes of bipolar patients relative to those present in normal individuals (Manji et al., 1995; Schreiber et al., 1991; Young et al., 1991; 1994).

Lithium belongs to group IA of the periodic table of elements. Its ionic radius is nearly

Figure 1. Modulation of adenylate cyclase and phosphoinositide turnover by guanine nucleotide binding (G) proteins (adapted from Campbell, 1995).

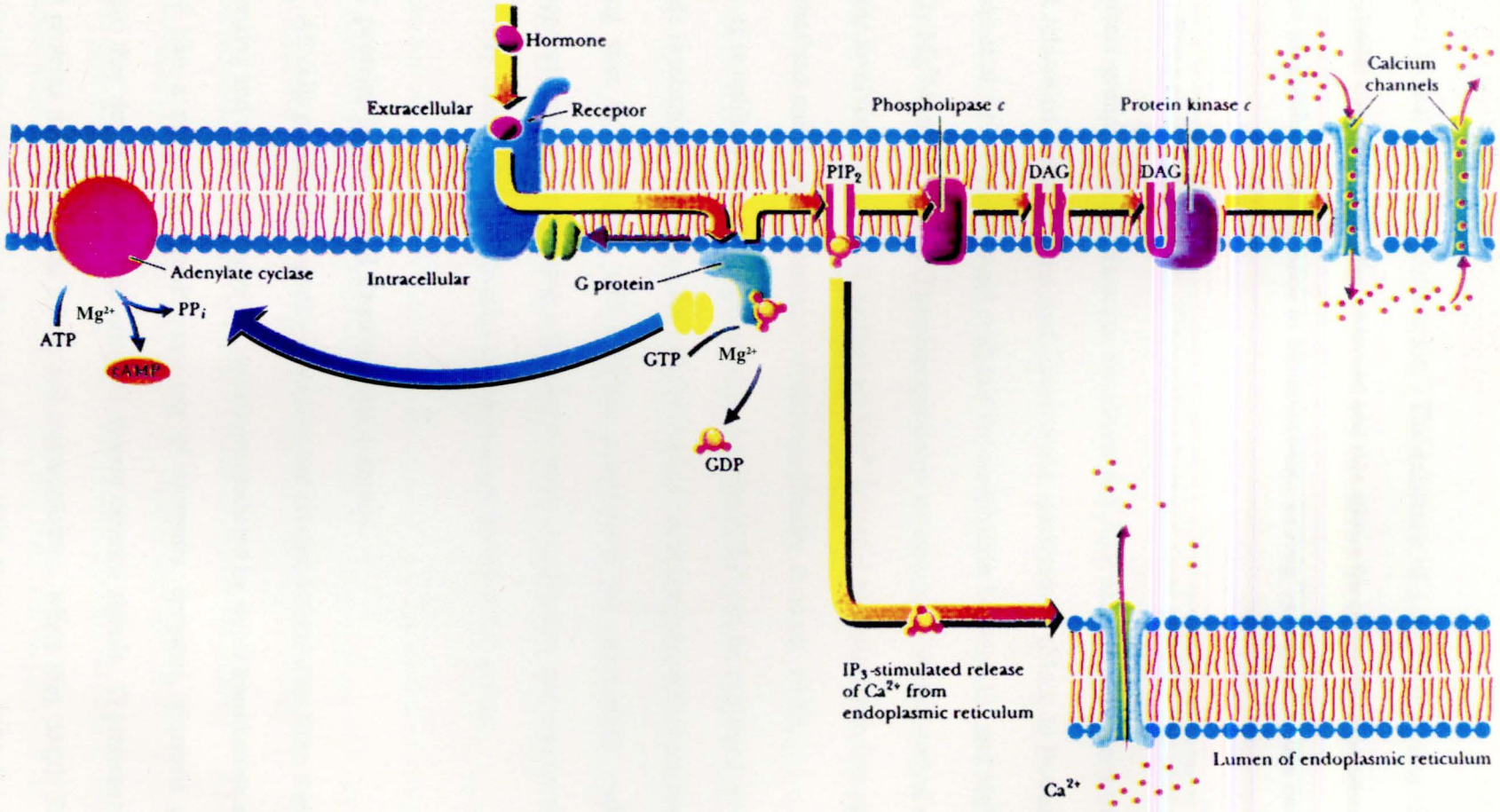
Hormone
Extracellular
Receptor
Phospholipase c
Protein kinase c
Calcium channels
PIP2
DAG
DAG
Adenylate cyclase
Intracellular
G protein
Mg2+
PPi
ATP
cAMP
GTP
Mg2+
GDP
IP3-stimulated release of Ca2+ from endoplasmic reticulum
Lumen of endoplasmic reticulum
Ca2+

identical to that of the magnesium ion. The existence of a diagonal relationship is consistent with similar chemical properties observed and this allows for competition between these two ions for the magnesium binding sites in biomolecules. Li^+/Mg^{2+} competition has been observed for the substrates of second messenger systems using multinuclear NMR methods (Abraha et al., 1991; Rong et al., 1992, 1994). Competition between these two ions was also reported for the phosphate groups in the erythrocyte membrane and ATP using low temperature ^{31}P NMR, ^{7}Li NMR relaxation measurements, and fluorescence spectroscopy (Mota de Freitas et al., 1994a). Avissar et al. (1991) have found evidence for competition between Li^+ and Mg^{2+} ions for low-affinity Mg^{2+}-binding sites in G proteins present in membranes from rat cerebral cortex. Several proteins involved in signal transduction are Mg^{2+} activated and could therefore participate in our hypothesized metal ion competition mechanism (Geisler & Mork, 1990).

It is unlikely that the pharmacological action of Li^+ can be explained solely in terms of a single mechanism. Our proposed investigation of metal ion competition mechanism for Mg^{2+}-binding sites in G proteins will therefore complement the mechanistic studies of inositol monophosphatase currently being conducted by other investigators, and the combination of these efforts may lead to the identification of the primary site(s) of Li^+ action.

I.3. G proteins in the Signal Transduction Cascade

All cells possess the capacity to receive and process information from their environment. The sensing and the processing of the signals are mediated by signal transduction cascades which behave like a molecular circuit consisting of receptors, enzymes, channels and regulatory proteins; they detect, amplify and integrate diverse external signals. G proteins are membrane-bound proteins that play a vital role in cell communication, where they couple first messengers to various intracellular effectors (Hepler & Gilman, 1992; Kaziro et al., 1991; Rawis, 1987). The

physiological role of G proteins in signal transduction may be perceived as that of a switch board.

I.4. Structure and Function of G Proteins

G proteins or GTPases are classified largely into two groups. One is the high-molecular weight or heterotrimeric G protein, consisting of three distinct subunits α (molecular mass in the range of 39-46 kDa), β (37 kDa), and γ (8 kDa). Another group is the low molecular weight, monomeric GTP binding proteins (abbreviated as "small Gs") (Bourne et al., 1991; Hall, 1990; Lacal & McCormick, 1993). The two groups, both growing in size, contain a large number of subgroups, each of which in turn contains large members.

In heterotrimeric G proteins, the α-subunits have a single, high affinity binding site for the guanine nucleotides (GTP or GDP). The GDP bound form of the α-subunit binds tightly to the βγ complex and this is the inactive conformation that turns off the signal transduction, whereas the active conformation that turns on the signal transduction is the GTP-bound form of the α-subunit and is dissociated from the βγ complex (Figure 2). All α-subunits are themselves enzymes since they possess intrinsic GTPase activity. In some cases, α-subunits possess specific residues that can be covalently modified by bacterial toxins. Cholera toxins catalyze the transfer of the ADP-ribose moiety of NAD to a specific Arg residue in certain α-subunits. Modifications of the α-subunit by cholera toxin activates these proteins by inhibiting their GTPase activity. In contrast, pertussis toxin ADP ribosylates those α-subunits that possess a specific Cys residue near the carboxyl terminus, thus preventing the receptor mediated activation of G proteins.

G proteins are localized in the inner surface of the plasma membrane. Association of the G proteins with the membrane is critical for ensuring high concentrations of signal transduction components and proper relative orientation. The primary sequence of each of the three G protein

Figure 2. Schematic representation of a signal transduction cascade involving G proteins (adapted from Campbell, 1995)

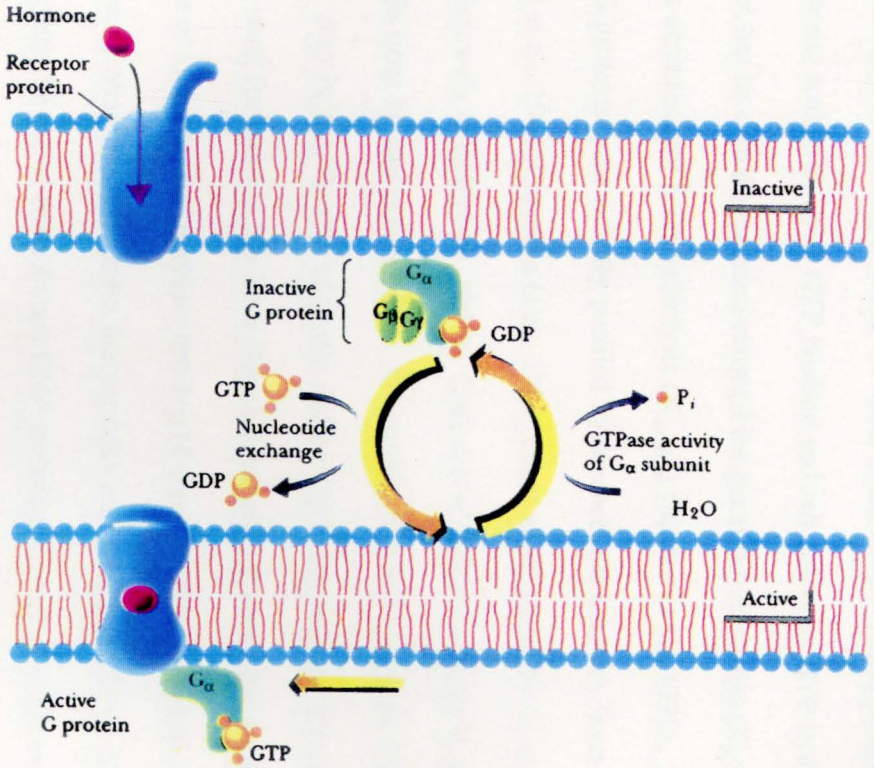
Hormone
Receptor protein
Inactive
Inactive G protein
G_α
$G_\beta G_\gamma$
GDP
GTP
Nucleotide exchange
GDP
P_i
GTPase activity of G_α subunit
H_2O
Active
Active G protein
G_α
GTP

subunits does not contain any lipid moiety or membrane spanning domains. However, it was shown recently that two distinct types of lipid modification of the G protein subunits, myristoylation and isoprenylation, play a role in membrane association of the G protein (Spiegel et al., 1991).

Although there are different kinds of G proteins, the basic principle of the function of GTP-binding proteins as molecular switches is universal. All G proteins utilize the same cycle of reactions, activation upon GTP binding and relaxation by GTP hydrolysis. Each G protein, however, has its own dissociation constant for guanine nucleotides (K_d value for GTP and GDP), and rate constants for GTP hydrolysis ($K_{cat.GTP}$) (Kaziro et al., 1991).

G proteins were initially purified by biochemical methods from different natural sources (Codina et al., 1984; Damonte et al., 1990; Evans et al., 1986; Ikeda et al., 1988; Kikuchi et al., 1988; Sternweis & Robishaw, 1984). Codina et al. (1984) isolated G_i and G_s to a purity greater than 90% from human erythrocytes. The purification of G proteins from different sources was the first step in the cloning of genes coding for these proteins (Northup et al., 1980). The strategy used for cloning has been the classical one of obtaining peptides through proteolytic digestion of Gα subunits, microsequencing of these peptides, synthesis of short oligonucleotide sequences (probes) deduced from the peptides and screening cDNA libraries with the probes. In 1985, with the use of recombinant DNA techniques it was possible to clone the first α subunit of a G protein (Lochrie et al., 1985; Medynski et al., 1985; Tanabe et al., 1985; Yatsunami & Khorana, 1985) corresponding to transducin, now called $G_t\alpha$. Following this, the number of cloned α, β and γ subunits has increased enormously. These recombinant DNA methodologies have helped the investigators to obtain large amounts of G proteins that are needed for structural studies.

The search for similarities of primary structures between various GTP-binding proteins has

revealed the presence of several regions of high degree of homology (Kaziro et al., 1991). Amino acid sequences of many G protein α-subunits are available and this allows for the comparison of the primary structures. Besides the striking overall structural homology, a strong conservation of the amino acid and nucleotide sequences in each group of G protein α-subunit is observed. The amino acid sequence of $G_s\alpha$ is strongly conserved between human and rat; only 1 out of 394 amino acid residues is different. There is 100% sequence homology between bovine and human $G_i\alpha_1$. For $G_i\alpha_2$, $G_i\alpha_3$ and $G_o\alpha$, more than 98% homology is present among different mammalian species. Among the 3 subfamilies of G protein α-subunits, it is remarkable that the homologies among the three $G_i\alpha$ species are higher than those of the $G_s\alpha$ and $G_t\alpha$ subfamilies (Kaziro et al., 1991).

Initially it was thought that the β-subunits of different G proteins were similar or identical in structure. This view changed in recent years and there are currently five different G_β subunits (Rens-Domiano & Hamm, 1995). It was found that there is a 90% amino acid sequence homology between β_1 and β_2 subunits of G proteins. The amino acid sequences of these two β-subunits are highly conserved among different mammalian species; the major differences between these two kinds of β-subunits are due to the distinct function performed (Olate & Allende, 1991).

It has been shown recently that the γ-subunit of G protein contains a 20-carbon isoprenoid group attached to the carboxyl terminal cysteine (Fukada et al., 1990). The isoprenylation of the γ-subunit is presumed to be responsible for the association of G proteins with membranes. The existence of more than one kind of γ subunit increases the number of βγ complexes and thus the number of G proteins.

Transducin (T), a signal transducing G protein, mediates visual excitation on vertebrate rod photoreceptor cells. This involves a light activated cyclic GMP (cGMP) cascade. When a photon of light is absorbed by the receptor molecule, rhodopsin, this leads to the activation of

a cGMP phosphodiesterase (PDE) which then hydrolyzes the cytosolic cGMP. The transient decrease in cGMP concentration causes the closure of cGMP-sensitive cation channels in the plasma membrane and results in hyperpolarization of the cell. Signal coupling between photolyzed rhodopsin (R^*) and PDE is mediated by transducin (Stryer, 1991).

Transducin is a trimeric protein composed of three polypeptides: T_α (39 kDa), T_β (37 kDa), and T_γ (8.5 kDa). In the dark-adapted state, transducin exists in the GDP-bound conformation (T_α-GDP.$T_{\beta\gamma}$); this complex strongly interacts with rhodopsin. Upon photoexcitation, R* catalyzes the GTP/GDP exchange reaction converting T_α-GDP to the active form T_α-GTP which dissociates from the $R^*/\beta\gamma$ complex and activates PDE. The inactivation is brought about by the natural GTPase activity of G proteins.

The purification procedure for transducin was originally developed by Fung et al. (1981). Transducin and PDE can be extracted from crude ROS membrane prepared from frozen dark-adapted bovine retinas (Ting et al., 1993). Transducin provides a good model system for metal binding studies since large amounts of protein can be easily obtained in a short period of time. Also, the amino acids involved in Mg^{2+} coordination are the same in most proteins in the G protein superfamily; there is also a 68% sequence homology between T_α and $rG_i\alpha_1$ outside the Mg^{2+} binding domain (Coleman et al., 1994a).

A great deal is known about the structure of wild type and mutants of $p21^{ras}$ from mutagenesis studies and from X-ray crystallography, which has provided a 3-D structure for both the GTP- and GDP-bound forms of the protein (Krengel et al., 1990; Milburn et al., 1990; Pai et al., 1990; Schlichting et al., 1990). After GTP hydrolysis, considerable structural changes are observed in parts of the molecule implicated in the interaction with GTPase-activating protein (GAP); the trigger for this process was from the change in coordination of the active-site Mg^{2+} ion as a result of the loss of the γ-phosphate of GTP (Schlichting et al., 1990).

Structural studies have also shown that the nucleotides with two or three phosphates bind to p21 with an affinity on the order of 10^{11} to 10^{12} M^{-1} in the presence of Mg^{2+} at 4 °C, whereas the affinity to GMP is six orders of magnitude lower (John et al., 1990). The high affinity for GTP and GDP is indicative of the large number of polar and nonpolar interactions between the protein and the nucleotide. The guanine base is sandwiched between the aromatic side chain of Phe 28 on one side and the aliphatic part of the side chain of Lys 117 on the other which is only 3.5 Å away from the endocyclic oxygen of the ribose (Pai et al., 1989; 1990). This is represented clearly in Figure 3. The interaction between the protein and the nucleotide is also very specific. p21 does not tolerate many substitutions on the guanine base, and it does not prefer the adenine nucleotides. The affinity of p21 for ATP has been estimated to be 10^4 M^{-1}, about six orders of magnitude smaller than for GTP (Lacal et al., 1993). The inability of ADP to bind to the nucleotide-binding site of G proteins could be due to stearic hindrance or another incompatibility of the 6-amino group with the nucleotide-binding site of p21.

From the three-dimensional structure of p21 complexed to GTP and Gpp(NH)p, information regarding the Mg^{2+} binding site has been obtained (Pai et al., 1989; 1990). In the highly refined 3-D structure, the Mg^{2+} ion is coordinated to 6 oxygen atoms in a perfect octahedral arrangement. This is shown in Figure 4. Mg^{2+} is complexed to two phosphate oxygens of Gpp(NH)p as a β,γ-bidentate complex. Two additional bonds are formed to the side chain oxygens of Ser-17 and Thr-35, both of which are highly conserved in all guanine nucleotide-binding proteins. The two apical positions of the octahedron are occupied by oxygens from water molecules. One of these water molecules is coordinated to the α-phosphate oxygen and the other to Asp-57, another highly conserved residue of G proteins. In the structure of p21.GDP, Ser-17, the β-phosphate, and four water molecules have been identified as the ligands of Mg^{2+} (Tong et al., 1991). The presence of four water molecules at the Mg^{2+}-binding site has

Figure 3. Schematic representation of the guanine nucleotide binding domain in G proteins. The nucleotide shown is the non-hydrolyzable analog of GTP, [Gpp(NH)p]. The broken line represents the hydrogen bonding interaction (adapted from the crystal structure of H-*ras* p21, Pai et al., 1990).

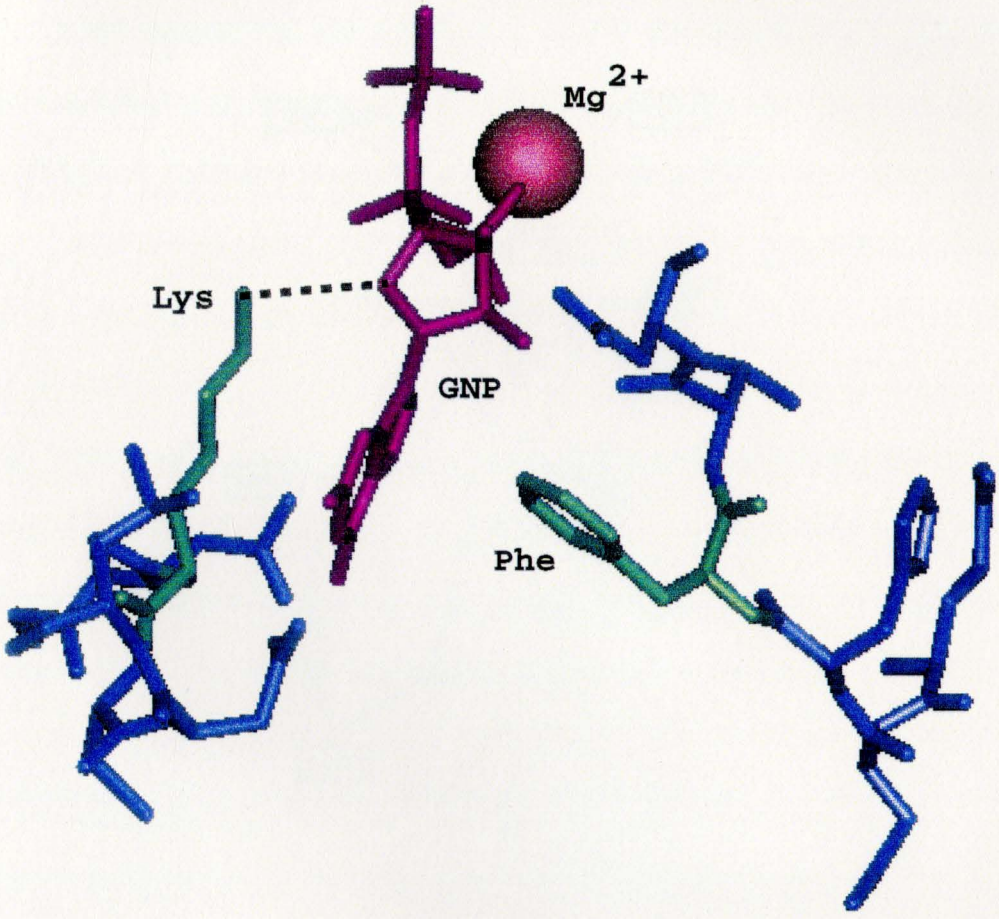
Mg2+
Lys
GNP
Phe

Figure 4. Schematic representation of the Mg^{2+}-binding domain of G proteins in the active conformation indicating the ligands in the first coordination sphere of the metal ion (from Pai et al., 1990).

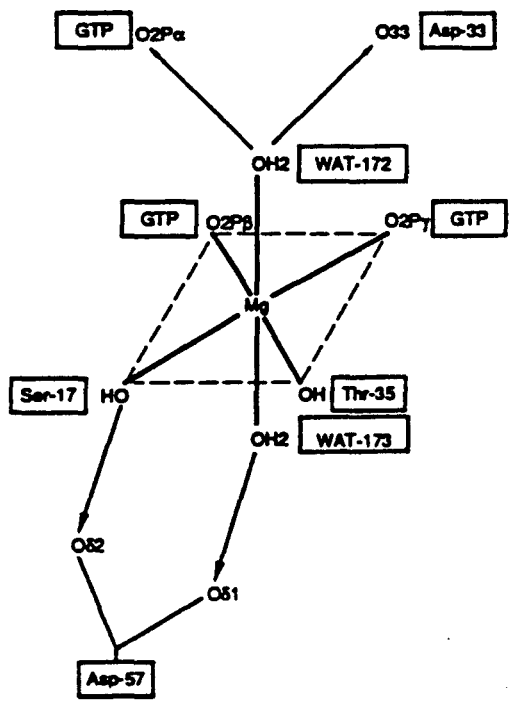
GTP
O2Pα
O33
Asp-33
OH2
WAT-172
GTP
O2Pβ
O2Pγ
GTP
Mg
Ser-17
HO
OH
Thr-35
OH2
WAT-173
O52
O51
Asp-57

been confirmed by ESR measurements using [^{17}O] H_2O (Smithers et al., 1990). The Mg^{2+}-binding site is one of the highly conserved region within the superfamily of G proteins (Table 1); the amino acids that co-ordinate Mg^{2+} are the same even in various conformations of this protein. However, the number of water molecules that are coordinated to the Mg^{2+} ion are different in different conformations (Table 1).

NMR methods have also been used to identify certain residues as in an N-RAS-encoded p21 study (Burk et al., 1989) or monitoring the conformational change between GDP-bound and GTPγS-bound forms of human N-ras p21 (Hu & Redfield, 1993; Miller et al., 1993).

Tetrafluoroaluminate (AlF_4^-) activates members of the heterotrimeric G-protein ($G_{\alpha\beta\gamma}$) family by binding to inactive G_α.GDP near the site occupied by the γ-phosphate in G_α.GTP. The crystal structure of T_α.GDP activated by aluminum fluoride at 1.7 Å has been reported by Sondek et al. (1994). AlF_4^- was found to activate G_α.GDP by binding with a geometry resembling a pentavalent intermediate for GTP hydrolysis. The stabilizing interactions were found to involve not only the residues that interact with the γ-phosphate in $G_{t\alpha}$.GDP.AlF_4-, but also conserved residues essential for GTPase activity. The presence of F^- ions in this form of G protein has allowed the observation of two ^{19}F NMR resonances by Higashijima et al. (1991). Since the two ^{19}F NMR resonances of free F^- and F^- bound to G protein α subunits of $rG_{s\alpha}$ and $G_{o\alpha}$ isolated from bovine brain are in slow exchange in the NMR time scale, the two resonances were clearly resolved. Titration with Al^{3+}, Mg^{2+}, and F^- indicated that each molecule of G_α binds 3-5 molecules of F^- (K_d = 0.47 mM), a single molecule of Al^{3+} (K_d less than 0.1 mM) and a single Mg^{2+} ion (K_d about 0.1 mM). Replacement of Mg^{2+} by Mn^{2+} caused a dramatic broadening of the NMR signal, indicating that the metal ion bound very close to the protein-bound F^-.

X-ray crystallographic data are available for the wild-type and some mutants of the highly homologous T_α and $rG_{i\alpha1}$ proteins in different conformations, i.e., in the presence of the non-

Table 1. Mg^{2+} ligands in the active and inactive conformations of T_α, $rG_i\alpha_1$ and *ras* p21.[a]

G protein	GDP bound (Inactive Conformation)	GTPγS / GPP(NH)p bound (Active Conformation)
T_α	phosphate oxygen (1)	phosphate oxygens (2)
	Ser-43 (1)	Ser-43 (1); Thr-177 (1)
	water (4)	water (2)
$rG_i\alpha_1$	phosphate oxygen (1)	phosphate oxygens (2)
	Ser-47 (1)	Ser-47 (1); Thr-181 (1)
	water (4)	water (2)
ras p21	phosphate oxygen (1)	phosphate oxygens (2)
	Ser-17 (1)	Ser-17 (1); Thr-35 (1)
	water (4)	water (2)

[a]The numbers in parentheses indicate the number of coordinations sites occupied by the ligand.

hydrolyzable GTP analog (GTPγS), of the GDP-AlF_4^- complex, and of GDP alone (Coleman et al., 1994a, b; Lambright et al., 1994; Noel et al., 1993). It was found, from the above studies, that the Mg^{2+} binding site was more exposed in the inactive conformation and also more water molecules were coordinated to Mg^{2+} in the GDP-bound conformation (Table 1). However in the GTPγS-bound conformation or in the transition state analog the Mg^{2+} was buried and the number of water molecules coordinated to Mg^{2+} was only two. Recently, the crystallographic structures of heterotrimeric G protein, $G_{i\alpha 1}\beta_1\gamma_2$ (Wall et al., 1995) as well as of the βγ dimer of G protein were resolved (Sondek et al., 1996). The availability of the crystal structures will aid in interpretation of our NMR results.

I.5. Interaction of Li^+ with Human RBC Membranes and Phospholipids

To test the Li^+/Mg^{2+} competition hypothesis, investigators have used small biomolecules or biomembranes as model systems. Often, human red blood cells (RBCs) were used because of their easy availability and relative simplicity. The lack of cell organelles and thus the presence of only a single membrane, the plasma membrane, has made RBC membrane the ideal model system for studies involving membranes. In the human body, blood transports Li^+ to the central nervous system (CNS); it is therefore important to understand the interaction of Li^+ with the RBCs and its components.

Human erythrocytes contain proteins, lipids, carbohydrates, and nucleotides. The most important task was to identify the major binding site(s) of Li^+. RBCs are thought of as packets of hemoglobin (Hb) and the intracellular Li^+ was thought to interact with the Hb. Many studies have indicated that Li^+-Hb interactions are weak (Bull et al., 1973; Pettegrew et al., 1987; Rong et al., 1993). Rong et al. (1993) using ^7Li relaxation measurements (T_1 and T_2) observed that the interaction of Li^+ with the blood cell components such as ATP, DPG, spectrin and different forms

of hemoglobin was very weak.

Pettegrew and co-workers (1987) measured the ^7Li T_1 and T_2 relaxation values for RBCs incubated with 50 mM Li^+ and found a large difference between the two relaxation times (T_1/T_2 = 34). They speculated that the large difference in the relaxation times observed in Li^+-loaded RBCs was due to diffusion of lithium ions across the heterogenous electrostatic field gradients generated by the spectrin-actin (SA) network. Their speculation was based on measurements obtained with agar gels. Rong et al. (1993) measured ^7Li relaxation times of Li^+-containing spectrin solution and found that the difference was, however, very small (T_1/T_2 = 4); the authors concluded that diffusion of the Li^+ ion through the SA network is not responsible for the large difference between T_1 and T_2 present in Li^+-loaded RBCs.

Li^+-treated RBC membranes, however, gave a very large difference between T_1 and T_2 (T_1/T_2 = 50) due to specific interactions between Li^+ and membrane binding sites. A systematic study was conducted using IOV and ROV which clearly indicated that the inner leaflet of the RBC membrane provided the major Li^+ binding site. Significant differences between T_1 and T_2 values were also observed for suspensions of phospholipids extracted from the RBC membrane, suggesting that phospholipids, but not the proteins in the membrane, provided the major Li^+ binding sites (Rong et al., 1993).

All biological membranes are sheetlike assemblies consisting of mostly proteins and lipids. The erythrocyte membrane, in particular, has very high mechanical stability and resilience which comes from a partnership between the plasma membrane and an underlying meshwork called the membrane cytoskeleton (Figure 5). The plasma membrane is essentially made up of proteins and lipids arranged in a bilayer as proposed by Singer and Nicolson (1972). The major constituent of the membrane cytoskeleton that provides the infrastructure is spectrin, which consists of a 260 KDa α-chain and a 225 KDa β-chain. Spectrin does not bind to the plasma membrane directly.

Figure 5. Model structure of human red blood cell membrane skeleton

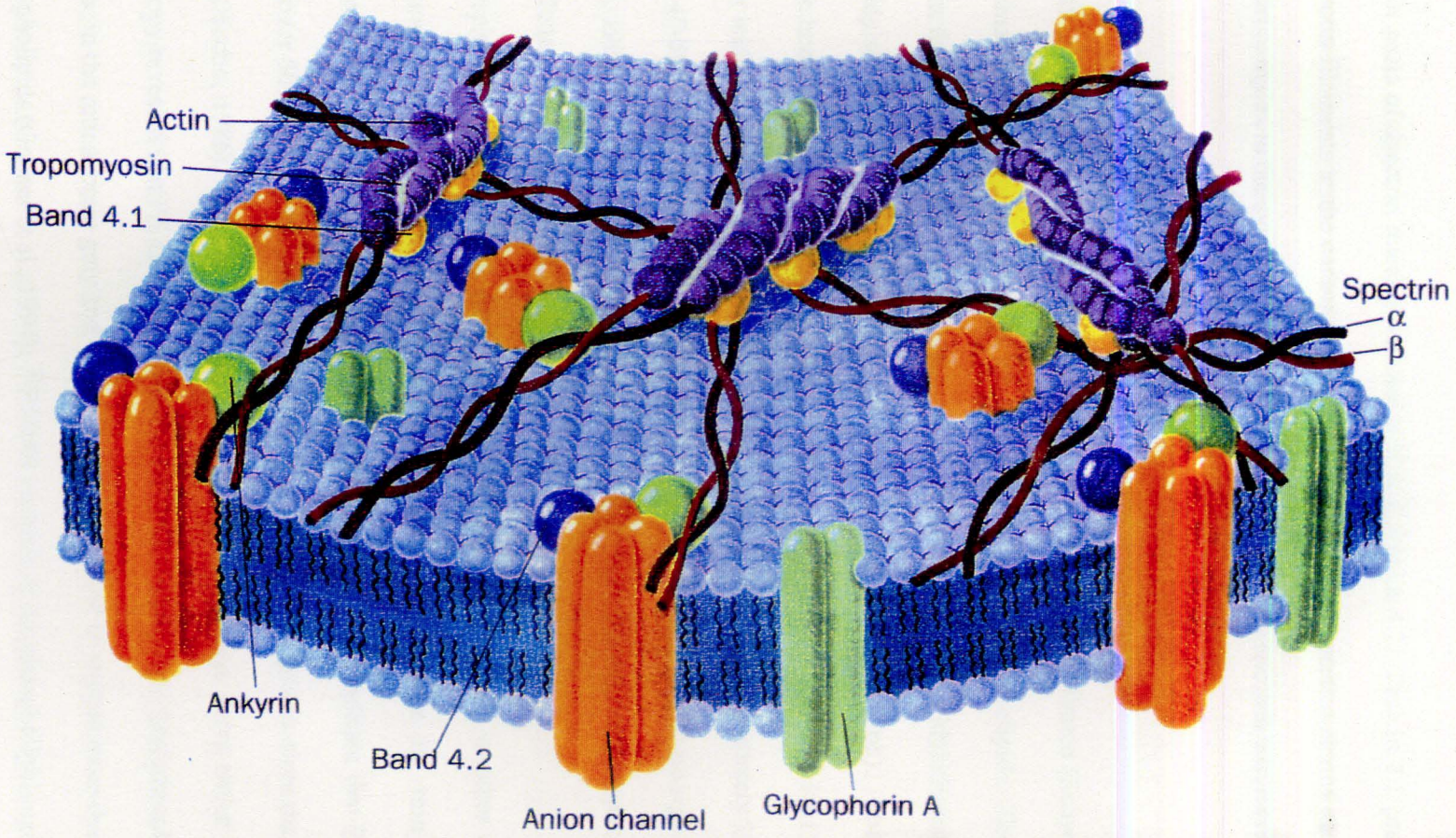
Actin
Tropomyosin
Band 4.1
Spectrin
α
β
Ankyrin
Band 4.2
Anion channel
Glycophorin A

Instead, different parts of spectrin interact with ankyrin and protein 4.1. Protein 4.1 promotes the binding of actin filaments to the carboxy-terminal portions of both spectrin chains and links this spectrin-actin complex to the cytosolic face of glycophorins. Several spectrin tetramers insert at each protein 4.1 junction complex to form a continuous meshwork underlying the plasma membrane (Stryer, 1995).

The lipids in the bilayer of RBC membranes are asymmetrically distributed (Schwartz et al., 1984). The major class of lipids present in the RBC membrane are phospholipids. The most common ones in the RBC membrane are phosphatidylcholine (PC), phosphatidylethanolamine (PE), phosphatidylserine (PS), phosphatidylinositol (PI) and sphingomyelin (Sph). The outer leaflet of mature human RBCs contain approximately 40-50% PC, 40-50% Sph, and 10-15% PE of the total outer leaflet phospholipids, whereas the inner leaflet contains approximately 10-20% PC, 10% Sph, 40-50% PE, 20-30% PS, and 1.4% PI of the total inner leaflet phospholipids (Cullis & Hope, 1985; Schwartz et al., 1984; Surgenor, 1974). Both the anionic phospholipids, PI and PS, are found only in the inner leaflet of the RBC membrane.

The phospholipid profile varies from one kind of cell membrane to another as the functions performed by the cells are different. Phospholipid analysis by thin layer chromatography (TLC) of axon membranes of the central nervous system indicate that PC and PE account for over 60% of the total phospholipids whereas the myelin contains more than 75% of PC and PE (Hucho, 1986). Phospholipid analysis of mammalian optic nerve tissue by ^{31}P NMR spectroscopy revealed that PE and PC account for more than 65% of the total phospholipid fraction whereas, in the retina, brain gray and white matter, PC and PE constitute more than 80% of the total phospholipids (Greiner et al., 1994). ^{31}P NMR analysis of the phospholipids extracted from SH-SY5Y neuroblastoma cell membrane indicated that PC and PE account for about 90% of the total phospholipids (Zachariah, 1996).

Variations in the phospholipid composition are also noticed for the same cell membrane from different species. For example, the erythrocyte membrane from humans contain about 39% PC whereas from sheep has about 1% PC. The phospholipids are continually modified, synthesized and degraded in the membrane and thus the phospholipid profile will indicate tissue pathology or aging; several diseases such as hypertension and manic-depression are also associated with cell membrane abnormalities which are due to altered phospholipid composition of the cell membrane (Chi et al., 1996; Mota de Freitas et al., 1994b). In manic depressive patients undergoing lithium therapy, the PS content from the phospholipid extract of the RBC membrane was found to be significantly higher than for normal individuals (17.0 ± 1.1 % vs 15.8 ± 1.2 %, paired student's t-test, $p < 0.05$, $n = 10$). However no significant changes were found between patients and normal individuals for other phospholipids present in RBC membranes. A later study using high performance TLC also confirmed PS to be higher in patients undergoing lithium therapy than the normal individuals (Bramham & Riddell, 1995).

The intrinsic binding constants for interactions between some alkali and alkaline earth metal ions and PS have been reported (Newton et al., 1988): 0.8 M^{-1} for PS-Na^+, 4.0 M^{-1} for PS-Mg^{2+}, and 35 M^{-1} for PS-Ca^{2+}. Evidence for Li^+ interactions with PS-containing liposomes was previously obtained from ^7Li relaxation data (Post & Wilkinson, 1991; Riddell & Arumugam, 1988; Roux & Bloom, 1990). Therefore, it is speculated that the anionic phospholipids, PS and PI present in the inner leaflet of the RBC membrane, contribute to Li^+ binding.

Merchant & Glonek (1992) used ^{31}P NMR to determine the relative interaction potentials of each of the phospholipids for each of the added cations. The cations used in this study were: Mg^{2+}, Ca^{2+}, Na^+ and K^+ ions. The ^{31}P NMR spectra of the phospholipids extracted from rat heart membranes gave a separate resonance for each phospholipid and the sample was titrated with a cation; the association of cations with individual phospholipids was indicated by ^{31}P NMR

chemical shift changes, signal broadening, signal quenching or a combination of these. The titrations of rat heart membrane lipid extract revealed that cardiolipin (CL) had the highest, followed by phosphatidic acid (PA) with the next highest, interaction potential for Mg^{2+} cations. In contrast, PS and PA had the highest, and CL the next highest, interaction potential for Ca^{2+}. The two phospholipids with the least interaction potential for either of the alkaline-earth cations were PC and Sph. The three anionic phospholipids, CL, PI and PG, interact with Na^{+} in a characteristic manner that is similar among these three phospholipids and yet different from Na^{+} interactions with all of the other phospholipids (Merchant & Glonek, 1992). Similar studies involving interactions with Al^{3+} have already been carried out (Panchalingam et al., 1991).

Mota de Freitas et al. (1994a) reported an increase in the ^{31}P NMR chemical shift anisotropy (CSA) parameter for increasing concentrations of either Li^{+} or Mg^{2+} in the presence of human RBC membrane. These results suggested metal ion binding to the phosphate head groups in the membrane; the study however, did not identify which phospholipids were predominantly involved in the Li^{+}/Mg^{2+} competition mechanism. This is because the ^{31}P NMR spectrum of the human RBC membranes is not resolved into many resonances, each corresponding to a particular phospholipid, without extraction of phospholipids using a suitable organic solvent mixture.

One of the useful features of NMR spectroscopy is that complex mixtures can be directly analyzed (Merchant & Glonek, 1992). Thus, for example, in examining the spectrum of rat heart membrane phospholipids, all of the common phospholipids can be qualitatively and quantitatively analyzed in a single sample after extraction, without carrying out a separation. This method has not been previously employed to human RBC membrane phospholipids; we have utilized this method to test Li^{+}/Mg^{2+} competition for human RBC membrane phospholipids and also to identify the phospholipids in the RBC membrane that interacts strongly with Li^{+} and Mg^{2+} ions.

Li^+ binding to RBC anionic phospholipids is very important since it may affect the extent of lipid-protein interactions in the RBC membrane. Since the Na^+-Na^+ exchange protein, which mediates RBC Na^+-Li^+ countertransport, is a membrane protein, it is possible that different extents to which Li^+ bind to phospholipids, and in turn different extents of interactions between anionic phospholipids and the membrane bound Na^+-Na^+ exchange protein, could be responsible for the variations in RBC Na^+-Li^+ countertransport rates reported for bipolar (Frazer et al., 1978; Mota de Freitas et al., 1990; Ramsey et al., 1979) and hypertensive (Canessa et al., 1980; Chi et al., 1996; Ramasamy et al., 1990) patients relative to normal individuals. Hence it is very important to understand the interactions of Li^+ with the phospholipids present in human RBC membranes.

In previous NMR studies based on Li^+ binding to agar gels (Pettegrew et al., 1987), or on Na^+ binding to human RBC membranes measured by double-quantum experiments (Shinar et al., 1993), investigators have speculated that the cytoskeletal proteins provide binding sites for alkali metal ions in human RBC membranes. An NMR study with purified spectrin, however, did not show evidence for Li^+ binding to cytoskeleton (Rong et al., 1993). This controversy needs to be addressed. The contribution of the SA network towards Li^+ and Na^+ binding and Li^+/Mg^{2+} competition can be tested by conducting ^7Li NMR relaxation measurements as well as ^{23}Na MQF NMR experiments with the unsealed and cytoskeleton-depleted RBC membranes. SA network depletion can be attained without altering the dimension of the membrane ghost by washing the RBC membrane with a low ionic strength buffer as previously reported (Fairbanks et al., 1971).

It is well known that quadrupolar nuclei with spin I = 3/2, such as ^{23}Na, ^{39}K and ^{87}Rb, can exhibit biexponential spin relaxation when in environments away from motional extreme narrowing ($\omega\tau_c \geq 1$) (Hubbard, 1970), as the outer transitions (-3/2 $\leftrightarrow$ -1/2 and 1/2 $\leftrightarrow$ 3/2) decay at a rate faster than that of the inner transition (-1/2 $\leftrightarrow$ 1/2). In macromolecular and biological

systems, these quadrupolar nuclei exchange rapidly between bound and free states and relax as the sum of two exponentials (Bull, 1972). This biexponential relaxation behavior allows the creation and detection of multiple quantum coherences (Pekar & Leigh, 1986). Thus, MQF NMR spectroscopy of quadrupolar I = 3/2 alkali metal nuclei has been studied extensively in macromolecular model systems (Knubovets et al., 1996; Shinar et al., 1993), in perfused organs (Jelicks & Gupta, 1993; Lyon & McLaughlin, 1994; Navon et al., 1994) as well as in human brain and skeletal muscle *in vivo* (Reddy et al., 1995).

MQF NMR studies are used mainly to study the nuclei in intracellular environments and of their binding to biological molecules in solution. As the appearance of the MQF NMR signal is due to motional restriction of the nuclei, the observance of the MQF NMR signal is indicative of ion binding to the biological molecule in solution. This technique can also differentiate between anisotropic and isotropic motion of the ions when bound to biological molecules. Anisotropic motion of Na^+ has been detected using this method in a variety of biological systems, such as RBCs (Knubovets et al., 1996; Shinar et al., 1993), connective tissues, cartilage, tendon and skin (Eliav et al., 1992; Eliav & Navon, 1994). In RBCs the anisotropic sodium binding sites are present at the membrane level and depend on the integrity of the cytoskeleton (Knubovets et al., 1996; Shinar et al., 1993).

The DQ behavior of ^{23}Na NMR signals of intracellular and extracellular sodium ions of human RBCs in the presence of increasing concentrations of Li^+ has been investigated (Gullapalli et al., 1992). The ^{23}Na DQ signal was quenched in both the intra- and extracellular compartment of the RBCs upon Li^+ addition providing evidence for Li^+/Na^+ competition for the intra- and extracellular binding sites in RBCs. Similar approach with DQF and TQF ^{23}Na NMR can be used for unsealed and cytoskeleton-depleted membranes to study the involvement of cytoskeleton towards Li^+/Na^+ competition. Thus these MQF NMR studies can provide a much more complete

picture of the molecular sites of Li^+/Na^+ competition for the RBC membrane sites and of the role played by the cytoskeleton on the binding of these ions and their competition for the membrane binding sites.

Information on Li^+/Mg^{2+} competition and Li^+ binding to biomolecules cannot be obtained by any other techniques commonly used for Li^+ analysis. The Li^+ and Mg^{2+} ions have no unpaired d electrons and therefore cannot be detected by standard spectroscopic techniques, such as electron spin resonance and visible spectroscopy. However, the ^7Li isotope is highly abundant (92.6%) and is a high-receptivity NMR nucleus. These properties of the ^7Li nuclide make ^7Li NMR methods highly selective and sensitive tools for monitoring Li^+ binding and Li^+/Mg^{2+} competition (Mota de Freitas, 1993).

CHAPTER II

STATEMENT OF THE PROBLEMS

The specific aims of this thesis are two fold. The first aim is to probe Li^+ and Mg^{2+} binding to G proteins using multinuclear NMR methods developed earlier for small biomolecules (Abraha et al., 1991; Mota de Freitas, 1993) and to test whether or not there is competition between these two ions for the Mg^{2+}-binding sites in G proteins. The second aim is to study the interactions of Li^+ and Mg^{2+} ions with the human RBC membrane phospholipids and to investigate the role of the RBC membrane cytoskeleton towards alkali metal ion binding, as well as the competition between these ions using NMR methods.

Lithium and magnesium ions have similar ionic radii, which results in similar chemical properties observed between these two ions; hence these two ions compete for Mg^{2+} binding sites on biomolecules (Abraha et al., 1991; Avissar et al., 1991; Mota de Freitas et al., 1994a; Rong et al., 1992; 1994). The exact mode and site(s) of Li^+ action in the treatment of manic-depression is still unclear. However, recent studies have shown the involvement of G proteins and the signal transduction system in bipolar disorder and in lithium therapy (Jope & Williams, 1994; Manji et al., 1995). Therapeutic concentrations of lithium were shown earlier to block the activities of G_s and G_i, the G proteins that stimulate and inhibit the enzyme adenylate cyclase respectively and G_o, the G protein that modulates PI turnover (Avissar et al., 1988). These findings suggest that G proteins (G_s and G_i or G_o) may provide a common site for both the antimanic and antidepressive therapeutic effects of lithium (Avissar et al., 1988). G proteins

require Mg^{2+} for their function (Gilman, 1987) and Mg^{2+} ions are shown to interact at multiple sites on G proteins (Avissar et al., 1991). It is possible then that lithium might compete with Mg^{2+} ions on these multiple Mg^{2+}-binding sites on G proteins. Multinuclear NMR spectroscopy will be used to investigate the interactions of Li^+ and Mg^{2+} with G proteins and to test whether there is Li^+/Mg^{2+} competition. This metal ion competition investigation would complement the inositol monophosphatase studies conducted by other investigators; these studies may lead to the understanding of the pharmacological action of Li^+ in the treatment of bipolar illness.

Transducin (T), a retinal G protein, and recombinant $G_i\alpha_1$ were chosen as model systems to test the Li^+/Mg^{2+} competition hypothesis. The availability of the X-ray crystallographic data on the Mg^{2+} and guanine nucleotide binding sites for transducin and $rG_i\alpha_1$ (Coleman et al., 1994b; Noel et al., 1993; Rens-Domiano & Hamm, 1995) will aid in the interpretation of data for the proposed study. The metal binding domain on the G proteins is highly conserved; however, the distinct functions performed by various members in the G protein superfamily are due to the low sequence homology outside the metal binding domain. The proposed study on these two types of G proteins will aid in determining if the extent of Li^+ binding and the competition is the same or different for $rG_i\alpha_1$ and transducin. Retinal rod outer segment (ROS) membranes are abundant in tansducin and studies with isolated transducin and transducin embedded in ROS membranes will be conducted to address questions concerning the effect of Li^+ on G protein function.

^7Li spin-lattice (T_1) and spin-spin (T_2) NMR relaxation measurements and ^{23}Na MQF NMR provide a good method for monitoring Li^+ and Na^+ binding as well as competition between these ions. Several studies from our lab have utilized this method successfully (Mota de Freitas et al., 1994a; Rong et al., 1993). Since Li^+, Na^+, and Mg^{2+} ions have no unpaired d-electrons, methods such as ESR and visible spectroscopy are not useful to address the above questions.

In human RBCs, the inner leaflet of the membranes was identified as the major site of Li^+ binding (Rong et al., 1993). It was also shown that the cytoskeletal protein spectrin in solution did not bind Li^+ strongly. Since membranes are made up of proteins and lipids, it is important to study the interaction of Li^+ with the lipids and to check if Li^+/Mg^{2+} competition is present for the phospholipids; this study will also identify the individual phospholipids that interact with Li^+ and Mg^{2+} most strongly. To achieve this goal, ^{31}P NMR chemical shift measurements along with lithium relaxation measurements will be used. The ^{31}P NMR spectra of phospholipid extracts from human RBC membranes are well resolved, providing a ^{31}P NMR resonance for each individual phospholipid present in the RBC membrane (Meneses & Glonek, 1988). Metal ion titrations cause a change in the chemical shift or linewidth of the resonances, which yields a quantitative measure of the interaction between the lipids and the metal ions (Merchant & Glonek, 1992). This ^{31}P NMR technique is unique, since no separation of the phospholipid mixture is needed to monitor the interaction of metal ions with the individual phospholipids.

Li^+-loaded RBCs gave a large difference in ^7Li NMR T_1 and T_2 values, and it was proposed that the differences were due to the electric field gradient caused by the spectrin-actin (SA) network underlying the plasma membrane of the RBCs (Pettegrew et al., 1987). It was later proved that the large T_1/T_2 difference observed was due to Li^+ binding to the inner leaflet of the RBC membranes and purified spectrin in solution bound Li^+ very weakly (Rong et al., 1993). The role played by the RBC membrane cytoskeleton towards Li^+ and Na^+ binding as well as Li^+/Na^+ competition will be investigated using ^{23}Na MQF NMR methods. As the observance of the MQF NMR signal is due to bound Na^+, this technique is of great value for the proposed metal ion-binding studies.

CHAPTER III

EXPERIMENTAL APPROACH

III.1. Materials

III.1.1. Reagents

Aluminum chloride ($AlCl_3$), sodium fluoride (NaF), lithium chloride (LiCl), magnesium chloride ($MgCl_2$), sodium chloride (NaCl), potassium chloride (KCl), tetramethylammonium chloride (TMACl), tetramethylammonium hydroxide, nickel sulfate ($NiSO_4$), imidazole, ethylenediaminetetraacetate (EDTA), 2-mercaptoethanol, glycerol, phosphoric acid and trifluroacetic acid were purchased from Aldrich Chemical Company (Milwaukee, WI). Buffers such as HEPES, MOPS, Trizma base, Trizma hydrochloride were obtained from Sigma Chemical Company (St. Louis, MO). Sodium salts of nucleotides, such as adenosine triphosphate (ATP), guanosine diphosphate (GDP) and guanosine triphosphate (GTP), were supplied by Sigma. Phenylmethylsulfonyl fluoride (PMSF), ampicillin, isopropylthiogalactoside (IPTG) were purchased from Boehringer Mannheim (Indianapolis, IN). Yeast extract and tryptone were obtained from Curtin Matheson Scientific Inc. (Houston, TX). His-binding resin used for the purification of His_6-$rG_i\alpha_1$, and hexylagarose used for the purification of heterotrimeric transducin were purchased from Novagen Inc. (Madison, WI) and ICN Pharmaceuticals Inc. (Costa Mesa, CA), respectively. Solvents used for phospholipid extraction such as chloroform and methanol were from Sigma and they were used without further purification. Pure phospholipids were obtained from Sigma or Avanti polar lipids (Alabaster, AL). Deuterated chloroform ($CDCl_3$) was

obtained from Aldrich; deuterium oxide (D_2O) used for NMR experiments was bought from Cambridge Isotopes (Cambridge, MA). The dye reagent used for protein determination was from Bio-Rad Laboratories (Hercules, CA). Pre-cast gels, bufferstrips, and blue-R dye were purchased from Pharmacia Biotech (Uppsala, Sweden) for SDS-PAGE using the phast system. High molecular and low molecular weight markers for SDS were obtained from Sigma. All chemicals were used without further purification.

III.1.2. Blood and Biological Samples

Human red blood cells, typically 3-5 days after they were withdrawn from healthy individuals, were obtained from the blood bank (Life Source, IL) and they were used prior to the expiration date. *Eschericia Coli* cells harboring the His_6-$G_i\alpha_1$ were a gift from Dr. Heidi Hamm (Department of Physiology and Biophysics, University of Illinois, Chicago). Bovine retinas were purchased from Dr. Yee-Kin Ho (Department of Biochemistry, University of Illinois, Chicago).

III.2. Sample Preparation

III.2.1. Preparation of Unsealed RBC Membranes

RBCs were washed once in an isotonic choline wash solution (100 mM choline chloride, 10 mM glucose, 85 mM sucrose, and 10 mM HEPES at pH 7.4) to remove plasma and buffy coat. The washed, packed cells were lysed in 20 to 40 volumes of hypotonic 5 mM HEPES buffer at pH 8.0 and centrifuged at 22,000 g and 4 °C for 10 min. The supernatant was removed by aspiration and the pellet was washed 3-4 times until pale white membranes were obtained (Mota de Freitas et al., 1994a; Steck & Kant, 1974). The membranes were stored at -20 °C for no more than a week before they were used.

III.2.2. Preparation of Cytoskeleton-depleted RBC Membranes

Cytoskeleton-depleted unsealed RBC membranes were obtained by incubating 2 mL of unsealed membranes in 18 mL of 0.1 mM EDTA at pH 8.0 and at 37 °C for 30 min (Fair banks et al., 1971). The suspension was centrifuged at 22,000 g and 4 °C for 20 min. The supernatant was removed by aspiration and checked for the presence of spectrin and actin, the major cytoskeletal proteins by SDS-PAGE to confirm the removal of the cytoskeleton. The pellet was washed 3-4 times with 5 mM HEPES buffer at pH 8.0 to obtain cytoskeleton-depleted RBC membranes.

III.2.3. Metal ATP Complexes with and without RBC Membranes in Aqueous Solution

The ATP concentration was maintained at 3 mM to prevent base stacking of the nucleotides (Corfu et al., 1990). As the binding of metal cations to nucleotide is dependent on pH, temperature and ionic strength (Sontheimer et al., 1986), in all NMR experiments with ATP the pH was adjusted to 7.0 at room temperature and the ionic strength was maintained at 0.15 M using Tris-Cl buffer. All samples contained 20% D_2O to lock the frequency of the ^{31}P NMR spectra. The temperature of the samples was maintained at 0 ± 1 °C by the variable-temperature unit of the NMR spectrometer. The low temperature was attained by passing a stream of dry nitrogen gas at the appropriate temperature. Before the start of the experiment the variable temperature unit was calibrated by using the chemical shift separation between the ^{1}H NMR resonances of methanol. For ATP samples containing human RBC membrane, appropriate amounts of membrane were added so that the final membrane protein concentration of the sample was 2.7 ± 0.1 mg/mL. All samples with and without RBC membrane contained 1.0 mM $MgCl_2$ and the samples were titrated with 0 to 80 mM LiCl.

III.2.4. Extraction of Phospholipids from Human RBC Membranes

RBC membranes (1-1.5 mL, membrane protein concentration 5.2 ± 0.4 mg/mL) were added slowly to anhydrous methanol (17 mL) and the mixture was stirred for 15 min. Chloroform (33 mL) was then added, and the sample was stirred for an additional 15 min at room temperature. The resulting extract with celite was filtered through a sintered glass funnel and the solids were washed with 50 mL of a 2:1 chloroform/methanol solvent mixture. The filtrate was thoroughly mixed in a separatory funnel with 20 mL of 0.1 M KCl to remove non-lipid impurities. The bottom chloroform layer was separated and the solvent was removed using a rotary evaporator at 30 °C (Meneses & Glonek, 1988) to form a lipid film. The dried lipid film was suspended in a solvent mixture of chloroform/methanol/aqueous 0.2 M EDTA reagent in a ratio of 125:8:3 for ^{31}P NMR experiments. For Li^+ relaxation measurements, the extracted dried phospholipid film was dissolved in a chloroform/methanol solvent mixture in a ratio of 5:2. The purpose of the aqueous EDTA phase was to remove the paramagnetic impurities which will otherwise cause the ^{31}P NMR resonances to broaden and this will interfere with the resolution of the various classes of phospholipid. The EDTA phase is not necessary for ^6Li or ^7Li NMR relaxation measurements.

III.2.5. Phospholipid-Metal Ion Titration

Prior to metal ion addition, a ^{31}P NMR spectrum of the sample was recorded by adjusting the spinning turbine so that only the organic phase of the sample was exposed to the receiver coil of the NMR spectrometer. The EDTA phase was then removed and appropriate amounts of 1 M $MgCl_2$ or LiCl solution were added directly into the organic phase (Merchant & Glonek, 1992) and the sample was mixed thoroughly and the spectrum was recorded with the organic phase in the NMR window. Addition of 3 mM $MgCl_2$ or 20 mM LiCl to the phospholipid suspension

caused precipitation. Metal ion titration was stopped when precipitation occurred or when one of the signals quenched. All NMR spectra were recorded by spinning the sample at 16 Hz and the probe temperature was maintained at 27 ± 1 °C.

III.2.6. Preparation of ROS Membranes from Bovine Retinas

Fresh bovine eyes were collected from local packing companies and kept on ice in a dark room for several hours prior to dissection. Dissection of the eyes to collect retinas were done in a dark room under a dim red light (Kodak, Rochester, NY, red No. 2 safety light filter). Retinas from 400 bovine eyes were suspended and stirred for 20 min in MOPS isolation buffer (10 mM Mops, 60 mM KCl, 30 mM NaCl, 2 mM $MgCl_2$, 0.1 mM PMSF and 1 mM DTT at pH 7.5) containing 50% sucrose. The retinal suspension was homogenized to break the tissue and it was centrifuged at 15,000 rpm (27,000 g) for 15 min at 4 °C. This centrifugation step causes the ROS membranes to float while the other retinal membranes pellet to the bottom. ROS membranes along with the supernatant were transferred into another set of centrifuge tubes and diluted with isolation buffer to obtain a sucrose concentration of 28%. The tubes when centrifuged at 18,000 rpm (38,000 g) for 15 min pellet ROS membranes leaving the lipids floating on top. The lipids along with the supernatant were discarded and the ROS membranes were further purified by varying the sucrose concentration in the isolation buffer (Ting et al., 1993). The final ROS membranes were suspended in 40 mL of isolation buffer and stored overnight in the dark over ice.

III.2.7. Extraction of cGMP Phosphodiesterase (PDE) from ROS Membranes

All extraction procedures from this point on were carried out in room light. The ROS membranes were resuspended in low ionic strength extraction buffer (5 mM Tris-Cl at pH 7.5,

0.5 mM $MgCl_2$, 0.1 mM PMSF and 1 mM DTT) and homogenized with a teflon-glass homogenizer, and the homogenate on ice was photolyzed under room light for 15-20 min. The samples changed color from red to bright orange, indicating the conversion of rhodopsin to meta-II-state (R^*). Under these conditions most peripheral proteins including PDE can be easily extracted by low ionic strength buffers. However, transducin remains very tightly bound to R^*-containing membrane. After photolysis, the ROS membrane suspension was centrifuged at 19,000 rpm (42,000 g) for 30 min. The supernatant contains PDE and the pellet contains transducin bound to ROS membranes. The pellet was suspended and homogenized in the extraction buffer and once again subjected to centrifugation. The supernatant was saved for purification of PDE. This procedure was repeated 6 times to remove PDE from the ROS membrane containing transducin.

III.2.8. Extraction of Transducin from ROS Membranes

ROS membranes stripped of PDE were homogenized in extraction buffer containing 0.1 mM GTP. Centrifugation at 19,000 rpm for 30 min pellets ROS membranes and the transducin remains in the supernatant. This procedure of homogenization and centrifugation was repeated 3 times to extract all the transducin from the ROS membranes. Prior to each centrifugation 50 μL of 10 mM GTP was added to all tubes as a precaution since transducin hydrolyses GTP in the presence R^*. The supernatants from the extractions were combined and an excess of GTP was added prior to column chromatography.

III.2.9. Purification of Transducin

The combined supernatant from the transducin extraction (approximately 300 mL in volume) was applied immediately to a hexylagarose column (6 X 1.5 cm) equilibrated with

MOPS buffer (10 mM MOPS at pH 7.5, 2 mM $MgCl_2$, 1 mM DTT) at 4 °C. After loading, the column was washed with 300 ml of MOPS buffer to remove unbound contaminants and GTP. Elution of transducin was performed with MOPS buffer containing 0.3 M NaCl. Fractions of 5 mL were collected and the protein concentration was determined by using the Bio-Rad Bradford dye reagent. Fractions containing transducin were combined and concentrated using an Amicon (Danvers, MA) concentrator with a YM 10 membrane to 5 mL and stored in 40% glycerol at 4 °C. The purity of transducin was checked by SDS-PAGE gel electrophoresis using a Pharmacia Phast system. Isolation from 400 retinas usually yielded 20-30 mg of pure transducin. This yield is consistent with previous reports (Ting et al., 1993).

III.2.10. Preparation of ROS Membranes Depleted of All Soluble Proteins without and with Transducin

Unbleached ROS membranes prior to transducin extraction were washed in the dark at 4 °C a total of 6 times with MOPS buffer containing 4 M urea and 1 mM EDTA to deplete transducin and other peripheral proteins. The membrane suspension was centrifuged at 19,000 rpm and 4 °C for 10 min and the supernatant was discarded. After 6 washes with EDTA and urea, membranes were further washed with MOPS buffer to remove urea and EDTA. The final pellet was stored at -80 °C in the dark. This membrane readily binds transducin when added and thus provides a reconstituted ROS membranes containing transducin without other soluble proteins.

III.2.11. *E.Coli* Culture

A single colony of *Escherichia Coli* cells harboring His_6-$G_i\alpha_1$ vector was used to inoculate the growth medium (1.6% yeast extract, 1% tryptone, 0.5% NaCl) containing 100 μg/mL

ampicillin. A 100 mL culture was grown at 37 °C for 5-6 h with shaking at 250-300 rpm. This culture was used to inoculate overnight cultures of 4 L (4 X 1 liter in 4-liter Erlenmeyer flasks) containing growth medium and 100 μg/mL ampicillin. The cultures are maintained at room temperature in a rotary air shaker (250-300 rpm). When the OD_{600} reached 0.6, IPTG (30 μM), an inducer of gene expression, was added and the incubation was continued for 16-18 h with shaking to obtain optimal cell densities.

III.2.12. Harvesting of Cells

Bacterial cells were collected by centrifugation at 4 °C in a Beckman JA-14 rotor for 10 mins at 7,000 rpm (7,500 g). The cells were then suspended in 150 mL of cold lyse buffer (50 mM NaCl, 5 mM $MgCl_2$, 50 mM Tris-Cl at pH 7.9, 0.1 mM PMSF and 10 mM β-mercaptoethanol) and the pellet was dislodged using a rubber policeman to obtain a homogeneous cell suspension. The cell suspension on ice was sonicated and the cell suspension was centrifuged for 1 h using an ultra centrifuge at 100,000 g at 4 °C. The supernatant containing His_6-$G_i\alpha_1$ was removed carefully and the pellet was discarded (Lee et al., 1994).

III.2.13. Purification of $rG_i\alpha_1$ Using a Ni^{2+}-NTA Affinity Column

The crude lysate (approximately 175 mL in volume) was applied to the column (1.5 X 10 cm) packed with the His-binding resin charged with Ni^{2+}. After loading, the column was washed with 15 column volumes of binding buffer (20 mM imidazole, 1 M NaCl, 20 mM Tris-Cl at pH 7.9). The column was then washed with 10 volumes of I-60 washing buffer (60 mM imidazole, 1 M NaCl, 20 mM Tris-Cl at pH 7.9). Elution was performed with 5 volumes of I-100 buffer (100 mM imidazole, 1 M NaCl, 20 mM Tris-Cl, pH 7.9). $rG_i\alpha_1$ eluted when the I-100 wash was performed (pET system manual, 1995). The I-100 fraction was dialyzed overnight against lyse

buffer containing 5% glycerol and 10 μM GDP to remove sodium chloride and imidazole. The presence of $rG_i\alpha_1$ in the I-100 fraction was confirmed by SDS-PAGE electrophoresis. The protein at this stage was about 70-80% pure as indicated by electrophoresis. The I-100 fraction after dialysis was further purified using a Pharmacia FPLC system with a Protein Pak-Q Column (Waters). Gradient elution with NaCl eluted $rG_i\alpha_1$ between 9-10 min. The protein at this stage had a purity greater than 95%. The protein sample was stored at -20 °C after adding 10 μM GDP, 2 mM β-mercaptoethanol, 0.1 mM PMSF and 40% glycerol until NMR experiments were performed. The activity of $rG_i\alpha_1$ was checked by adding aluminum fluoride to the sample and monitoring the change in the fluorescence emission intensity with time. A 30-50% increase in emission intensity upon addition of aluminum fluoride indicated that $rG_i\alpha_1$ was functionally active (Skiba et al., 1996).

Typical yields from 4 L cultures are 20-30 mg of $rG_i\alpha_1$. This method of purifying hexahistidine tagged to the protein using affinity chromatography on a resin containing chelated Ni^{2+} is rapid and results in the isolation of relatively large amounts of protein in a very short time. Since the hexahistidine tagged $rG_i\alpha_1$ is similar to that of the untagged $rG_i\alpha_1$ (Lee et al., 1994), no effort was made to remove the tag at the end of the purification.

III.2.14. Preparation of $rG_i\alpha_1$ Sample for ^{7}Li NMR Relaxation Measurements

Prior to ^{7}Li NMR relaxation measurements the protein in glycerol was dialyzed against 50 mM Tris-Cl buffer containing 0.025 mM EDTA at pH 7.9 for 10-12 h to remove glycerol which will otherwise affect the relaxation measurements. The sample was concentrated using an Amicon stirred cell with an YM-10 membrane and centricon-10 to obtain 10-12 mg of protein in 0.4-0.5 mL. To this sample appropriate amounts of LiCl or $MgCl_2$ were added.

III.2.15. Replacement of Bound Mg^{2+} by Mn^{2+} in $rG_i\alpha_1$

$rG_i\alpha_1$ sample stored at -20 °C was dialyzed for 4 h at 4 °C against 50 mM Tris-Cl buffer at pH 7.9 to remove the added glycerol. This sample was then dialyzed for 4 h, against 2 L of Tris-Cl buffer at pH 7.9 containing 0.005% *n*-octyl-β-D-glucopyranoside, 1 mM EGTA, 1 mM EDTA, 0.02 mM GDP, 10 mM β-mercaptoethanol and 0.1 mM PMSF; the protein was dialyzed against Tris-Cl buffer overnight. The dialyzed protein solution was concentrated to about 1 mL using an Amicon stirred cell with an YM-10 membrane and centricon-10. $MnSO_4$ was added (0.9 moles per mole of protein) to the concentrated protein to obtain the Mn^{2+} derivative of the protein (Smithers et al., 1990). Incorporation of Mn^{2+} was confirmed by ESR measurements.

III.2.16. Preparation of Mg^{2+}-bound $rG_i\alpha_1$.GDP Sample for ^{31}P and ^{19}F NMR

The protein sample in glycerol was dialyzed against 5 L of 50 mM Tris-Cl buffer at pH 7.9 to remove the added glycerol. The sample was concentrated to about 1.0 mL; the protein sample was diluted to 8.0 mL using HED(D_2O) buffer and it was concentrated to about 1.0 mL using centricon-10. This procedure was repeated 3-4 times so that most of the water in the sample was replaced by D_2O (Higashijima et al., 1991). The replacement of water by D_2O was done to obtain a good lock signal so that the changes in the chemical shift values are not due to field drift.

III.3. Data Analysis

III.3.1. Calculation of $[Mg^{2+}]_f$ Values from the Low-temperature ^{31}P NMR Spectra of ATP

At low temperature (0 °C), the ^{31}P NMR resonance of β-phosphate is in slow exchange with Mg^{2+}, giving rise to two separate signals for the Mg^{2+}-free and Mg^{2+}-bound forms of ATP.

This is in contrast with Li^+, which is in fast exchange giving rise to only one signal for the free and bound species. The $[Mg^{2+}]_f$ values from the low-temperature ^{31}P NMR spectra of ATP were calculated using the equation

$$[Mg^{2+}]_f = (\delta_{\alpha\beta}{}^f - \delta_{\alpha\beta}{}^b) / [K_\beta \text{ (area ratio) } (\delta_{\alpha\beta}{}^{obs} - \delta_{\alpha\beta}{}^b)] \qquad (1)$$

where $\delta_{\alpha\beta}{}^f$ and $\delta_{\alpha\beta}{}^b$ are the chemical shift separations between the α-phosphate and the β-phosphate resonances of Mg^{2+}-free ATP in the absence and presence of 150 mM LiCl, and $\delta_{\alpha\beta}{}^{obs}$ is the chemical shift separation observed in ATP samples containing both LiCl and $MgCl_2$. The value of 1563 M^{-1} was used for the Mg^{2+}-binding constant to the β-phosphate of ATP (K_β) at 0 °C and pH 7.5; this value was calculated from previously reported values at 37 °C and 25 °C and pH 7.5 (Abraha et al., 1991; Bock et al., 1985; Prigodich & Haake, 1985). The area ratio was obtained by dividing the area of the Mg^{2+}-free β-phosphate resonance by that of the Mg^{2+}-bound β phosphate signal. Areas were obtained by conducting a deconvolution of the partially overlapped Mg^{2+}-free and Mg^{2+}-bound β-phosphate resonance by using the Marquardt peak-fitting menu of the NMR-286 software provided by Softpulse Software Co. (Guelph, Ontario, Canada).

III.3.2. Calculation of Li^+ and Mg^{2+} Binding Constants from ^7Li NMR T_1 Measurements

The calculation of the binding constants, K_{Li}, of Li^+ to the biomolecules, such as RBC membranes, ROS membranes and phospholipid extracts, from ^7Li T_1 measurements assumed a two-state (free, f, and bound, b, metal ions) model undergoing fast exchange and a total Li^+ concentration, $[Li^+]_t$, that is large with respect to the binding site concentration, [B] (Urry et al., 1989):

$$\Delta R^{-1} = (R_{obs} - R_f)^{-1} = K_{Li}{}^{-1} \{[B](R_b - R_f)\}^{-1} + [Li^+]_t\{[B](R_b - R_f)\}^{-1} \qquad (2)$$

where R_{obs}, R_f, and R_b are the reciprocals of T_{1obs}, T_{1f}, and T_{1b}, respectively. K_{Mg}, the binding

constant of Mg^{2+} to biological membranes and phospholipids, and K_{Li} were calculated from the apparent Li^+-binding constants, K_{app}, which were in turn determined from ^7Li T_1 values measured in the presence of increasing Mg^{2+} concentrations:

$$1 / K_{app} = 1 / K_{Li} (1 + K_{Mg} [Mg^{2+}]) \quad (3)$$

These equations assume 1:1 stoichiometry for Li^+ and Mg^{2+} binding to biomembranes and phospholipids.

III.3.3. Calculation of Mg^{2+} and Li^+ Binding Constants from ^{31}P NMR Spectroscopy

The Mg^{2+}-binding constants, K_{Mg}, to individual phospholipids were calculated from the chemical shift changes, $\Delta\delta$, observed in Mg^{2+}-containing suspensions (no Li^+) of phospholipids extracted from human RBC membranes according to the following equation.

$$1/\Delta\delta = 1/(\delta_{obs}-\delta_{free}) = 1/\{K_{Mg}[Mg^{2+}](\delta_{bound}-\delta_{free})\} + 1/(\delta_{bound}-\delta_{free}) \quad (4)$$

where δ_{obs}, δ_{free}, and δ_{bound} are the chemical shifts of the observed, Mg^{2+}-free, and Mg^{2+}-saturated ^{31}P NMR resonances of the individual phospholipids. From a linear plot of $1/\Delta\delta$ versus $[Mg^{2+}]$, K_{Mg} can be determined by taking either the ratio of the slope by the y-intercept or the reciprocal of the x-intercept. The Li^+ binding constants, K_{Li}, to individual phospholipids were obtained from the chemical shift changes, $\Delta\delta$, observed in Li^+-containing suspensions (no Mg^{2+}) of phospholipids extracted from human RBC membranes according to the following equation.

$$1/\Delta\delta = 1/(\delta_{obs}-\delta_{free}) = 1/\{K_{Li}\,[Li^+](\delta_{bound}-\delta_{free})\} + 1/(\delta_{bound}-\delta_{free}) \quad (5)$$

The phospholipid samples used for ^{31}P NMR have two phases (aqueous and organic). Since it is the organic phase that contains the phospholipids, attempts were made to measure the amount of metal ions (Li^+ and Mg^{2+}) in the organic phase (see Chapter V).

III.3.4. Protein Concentration Determination

Protein concentration was determined by "Bio-Rad Bradford" method using bovine serum albumin as a standard to generate the calibration curve (Bollag & Edelstein, 1991). For membrane-bound protein samples, a modified procedure with detergent was used (Fanger, 1987). For pure $rG_i\alpha_1$, the absorbance at 280 nm was measured and the protein concentration was determined using the calculated extinction coefficient, $\varepsilon_{280} = 40$ (Skiba et al., 1996).

III.3.5. SDS-PAGE Gel Electrophoresis

The purity of the protein samples was determined by SDS-PAGE using a Pharmacia Phast system. A homogeneous phastgel (12.5%) was used, and the lower molecular weight marker kit from Sigma was used to reconfirm the molecular weight of the proteins. Staining of the gel was achieved by using either Coomassie Blue or blue R dye.

III.3.6. Tryptophan Fluorescence Assay

The activity of the purified $rG_i\alpha_1$ samples was checked by monitoring the changes in the fluorescence emission intensity of 5-10 μM $rG_i\alpha_1$ at 340 nm (excitation at 280 nm) and at room temperature in a 50 mM Tris-Cl buffer at pH 8.0 containing 50 mM NaCl, and 2 mM $MgCl_2$ upon addition of 20 μM $AlCl_3$ and 10 mM NaF; a 30-50% increase in emission intensity is indicative of the activated state of G protein α-subunit (Gilman, 1987; Higashijima et al., 1991; Skiba et al., 1996).

III.4. Instrumentation

III.4.1. Nuclear Magnetic Resonance Spectrometers

NMR experiments were conducted using Varian VXR-300, VXR-400 NMR, or Varian Unity 500 NMR spectrometers equipped with multinuclear probes. The NMR parameters of the

nuclei used in this study are listed in Table 2. A 5 or a 10 mm broad band probe was used depending on the availability of the sample. All samples were run by spinning the sample at 16-18 Hz. A variable temperature unit with the NMR spectrometer was used to maintain the probe temperature at 0, 27 or 37 ° C. Spin-lattice (T_1) relaxation measurements were conducted using the inversion recovery pulse sequence. Spin-spin (T_2) relaxation measurements were performed using the Carr-Purcell-Meiboom-Gill pulse sequence. The relaxation measurements are often accompanied by a 10% uncertainty and the reported values represent the range or the standard deviation obtained by averaging the values from 2 or 3 separately prepared samples, respectively. Binding constants were calculated from T_1 or T_2 values using at least 5 data points using James-Noggle (1969) plots. Experiments with ROS membranes were conducted in the dark under a dim red light to avoid the photo bleaching of the membranes.

Sodium-23 single quantum (SQ) NMR experiments were conducted using either a Varian VXR 300 or a Varian Unity 500 NMR spectrometer operating at 79.354 and 132.212 MHz, respectively, using a broad band 10 mm probe tuned for sodium, and 10 mm o.d. sample tubes. ^{23}Na MQF NMR spectra were measured at 132.212 MHz using a Varian Unity 500 NMR spectrometer. The double (DQF) and triple (TQF) quantum T_2 measurements were performed using the pulse sequence

$$90^\circ - \tau/2 - 180^\circ - \tau/2 - \theta^\circ - \delta - \theta^\circ - t_{acq} \qquad (6)$$

with $\theta = 90^\circ$ and 54.7° for DQF and $\theta = 90^\circ$ for TQF. In this sequence τ is the creation or preparation time, δ is the evolution time, and t_{acq} is the acquisition time (Jaccard et al., 1986; Pekar & Leigh, 1986). A fixed evolution time of 10 μs was used, while the creation time was varied typically in 20 steps from 0.1 to 300 ms. Although the same pulse sequence was used for both DQF and TQF experiments, by using a suitable phase cycling either a DQF or a TQF spectrum was obtained (Shinar et al., 1993). Special care was taken to measure the 90° pulse

Table 2. List of NMR parameters for various nuclei investigated in this study

Parameters	Nuclei				
	^{6}Li	^{7}Li	^{23}Na	^{31}P	$^{19}F^{a}$
Frequency (MHz)	44.2	116.6	79.4	121.4	376.3
SW (KHz)	5.9	4.5	2.5	10.0	50.0
AT (s)	2.0	1.0	0.4	1.5	0.6
PW 90 (μs)	39	27[b], 32[c], 14[d]	23	12	9.0
Flip angle (°)	45	45	45	45	45

[a]^{19}F NMR parameters are for a Varian VXR-400 MHz instrument. [b]PW 90 in a 10 mm probe for low ionic samples. [c]PW 90 in a 10 mm probe for highly ionic samples. [d]PW 90 for samples in 5 mm probe.

width accurately for each sample and the carrier frequency was selected to coincide with the SQ signal. All MQF NMR spectra were recorded at 37 °C without spinning the samples. The performance of the DQ and the TQ filter was checked for any SQ signal leakage by running a 150 mM NaCl sample in D_2O, by observing the absence of DQF and TQF signals from monoexponential free Na^+ (aq.) ions. This experiment however did not confirm the performance of the DQ and TQ filter in the RBC membrane preparations.

The effects of missettings of the 90° pulse width on the line shape and intensity of the DQF and TQF signals was checked by using a sample of RBC membrane containing 5 mM NaCl and 10 mM LiCl. A change of up to 2 μs in the PW 90° did not affect significantly the shape or the intensity of the MQF signal.

Postprocessing of all FIDs included baseline correction before Fourier transformation. For DQF and TQF spectra, a magnitude calculation was done after Fourier transformation. The areas under the resultant peaks were determined by point-to-point integration between user-defined break points. Correction factors were applied to count for non-zero mean noise in the magnitude calculation spectra (Hutchinson et al., 1993). The values of T_{2f}, T_{2s} and ω_Q were obtained by fitting the DQF or TQF signal peak intensity versus the τ value to the appropriate function using a Marquart-Levenberg non-linear optimization algorithm.

III.4.2. Atomic Absorption Spectrophotometer

A Perkin-Elmer spectrophotometer (model 5000) equipped with a flame source was used for lithium and magnesium ion concentration determinations.

III.4.3. UV-Vis Spectrophotometer

All absorbance measurements were conducted using a Jasco spectrometer. For the Bio-

Rad Bradford assay, the absorbance was measured at 595 nm, and for $rG_i\alpha_1$ protein concentration determinations, the absorbance was measured at 280 nm.

III.4.4. Fast Protein Liquid Chromatography (FPLC)

Purification of $rG_i\alpha_1$ was achieved using a Pharmacia FPLC system with a Waters Protein-Pak Q column. The protein solution from the Ni^{2+}-NTA column was dialyzed to remove excess NaCl and imidazole; this solution was concentrated to 10 mL and it was loaded on to the Protein-Pak Q column. A flow rate of 1 mL/min was used and the purification was carried out at 4 °C. A NaCl gradient in the lyse buffer was applied to the column and when the NaCl concentration was approximately 0.1 M, $rG_i\alpha_1$ was eluted. This protein sample was stored at -20 °C after adding 10 μM GDP, 2 mM β-mercaptoethanol, 0.1 mM PMSF and glycerol so that the final concentration of glycerol was about 40%. The $rG_i\alpha_1$ sample at this stage was found to have a purity greater than 95% as shown by SDS-PAGE.

III.4.5. Sonicator

Lysis of *E. Coli* cells was achieved by sonication of the cell suspension using a sonic 300 dismembrator (Artek Systems, Farmindale, NY) equipped with an intermediate tip. A 20 pulse sonication was performed with 30 s pulsing followed by a 30 s break to prevent heating of the sample.

III.4.6. Centrifuges

General low speed centrifugation was performed using a temperature controlled Savant (model HSC 10000) centrifuge. The RBC membrane preparations were done using a Beckman J2-21 centrifuge with JA-14 and JA-20 fixed angle rotors. Ultra centrifugation used to pellet the

E. Coli membranes was performed using a Dupont RC 60 Ultra centrifuge with a T-865 rotor. The concentration of protein samples using a Centricon-10 was performed using a Savant refrigerated centrifuge at 5,000 rpm (3,000 g).

CHAPTER IV

RESULTS

IV.1. Competition Between Li^+ and Mg^{2+} for the Phosphate Groups in ATP, Human RBC Membranes and Phospholipids

IV.1.1. Competition Between Li^+ and Mg^{2+} for ATP and Human RBC Membranes

This study was conducted using low temperature ^{31}P NMR to reinvestigate if there is competition between Li^+ and Mg^{2+} for ATP (Brown et al., 1993). The experiments were conducted at 0 °C and this enabled the calculation of $[Mg^{2+}]_f$ values as a function of added LiCl. ATP samples with and without RBC membranes were used in this study.

Figure 6 shows the ^{31}P NMR spectra of an aqueous solution containing 3.0 mM ATP (in sodium form) and 1 mM $MgCl_2$ at 0 °C and pH 7.5 titrated with varying amounts of LiCl. Whereas the addition of up to 40 mM LiCl did not cause a significant change in the ratio of the areas of the Mg^{2+}-free and Mg^{2+}-bound β-phosphate resonances in the absence of human RBC membrane, the addition of 20 mM LiCl to an ATP-containing membrane suspension was sufficient to cause a significant increase in the area ratio (Table 3). However, significant downfield shifts of the Mg^{2+}-free β-phosphate resonance upon the addition of 20 mM LiCl to ATP solutions in both the presence and absence of RBC membrane were noticed. In both the presence and absence of RBC membrane, the $[Mg^{2+}]_f$ values increased with an increase in the Li^+ concentration. In the absence of RBC membranes, the values of $[Mg^{2+}]_f$ increased for $[Li^+] \leq 40$ mM when no changes in the area ratio were apparent from the ^{31}P NMR spectra (Figure 6); these

Figure 6. ^{31}P NMR spectra, at 0 °C and pH 7.5, of 3 mM ATP (in sodium form) in the presence of 1.0 mM $MgCl_2$ and (A) 0, (B) 20, (C) 40, (D) 60, and (E) 80 mM LiCl. The ionic strengths of all samples was adjusted to 0.15 M by using Tris-Cl. The assignment of the phosphate resonances are indicated in spectrum E; the subscripts f and b refer to Mg^{2+}-free and Mg^{2+}-bound forms of β-phosphate, respectively. Line broadening was 8 Hz.

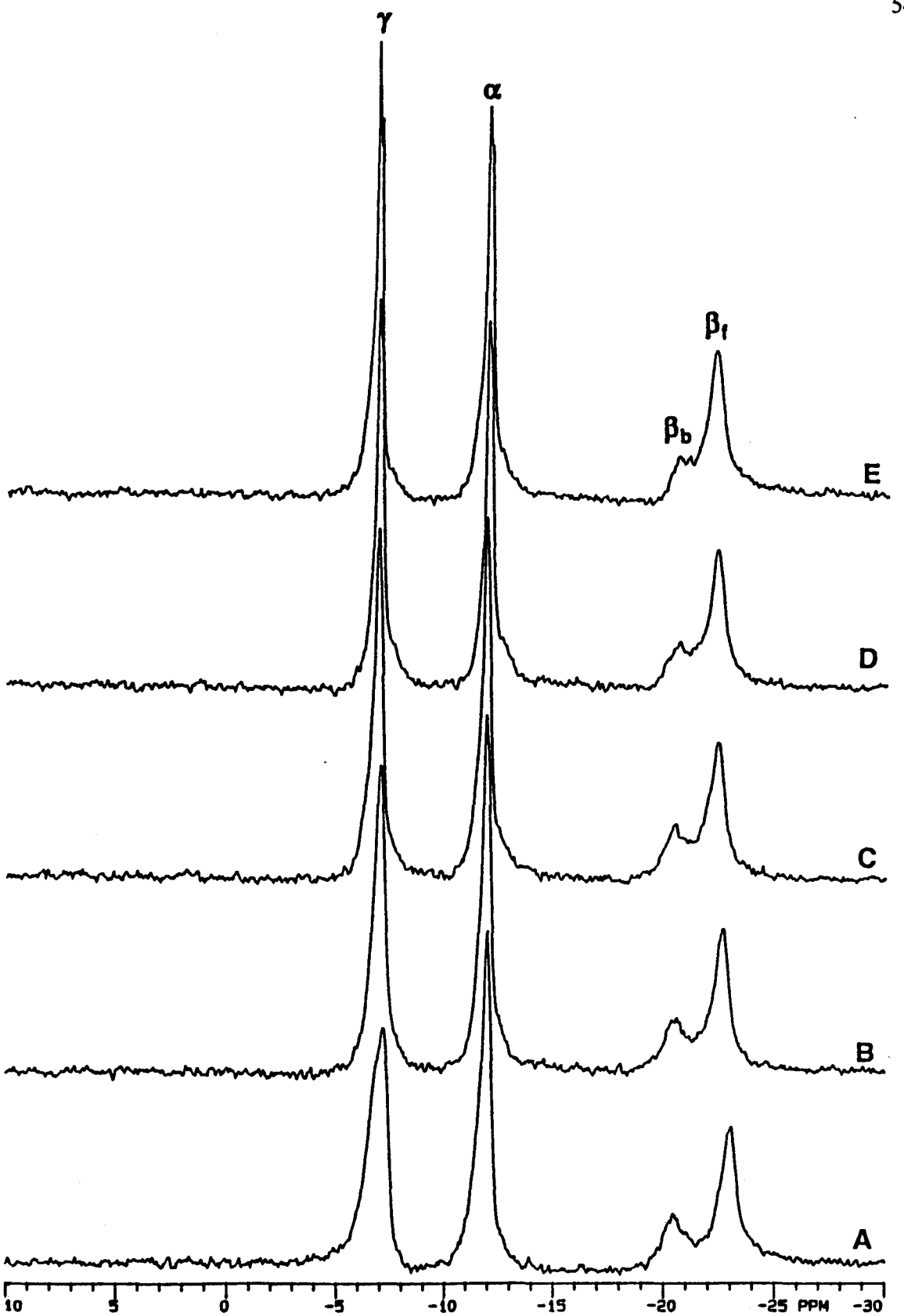
γ
α
βf
βb
E
D
C
B
A
10
5
0
-5
-10
-15
-20
-25 PPM
-30

Table 3. ^{31}P NMR-determined $[Mg^{2+}]_f$ values for ATP solutions in the presence and absence of RBC membrane[a]

	Without membrane			With membrane[b]		
$[Li^+]$/mM	Area ratio[c]	$\delta_{\alpha\beta}$ /ppm[d]	$[Mg^{2+}]_f$ /μM[e]	Area ratio[c]	$\delta_{\alpha\beta}$ /ppm[d]	$[Mg^{2+}]_f$ /μM[e]
0	1.5	10.9	380	1.9	11.0	280
20	1.5	10.8	490	2.2	10.7	360
40	1.5	10.5	800	2.6	10.5	410
60	1.8	10.4	890	2.8	10.4	710
80	2.5	10.3	960	3.1	10.3	770

[a]The reported values represent an average of measurements conducted in two separately prepared samples. All samples contained 3.0 mM NaATP, 1.0 mM $MgCl_2$, and 0.15 M Tris-Cl, pH 7.5 at 0 °C. [b]The membrane protein concentration was 2.7 ± 0.1 mg/mL. [c]The area ratios were obtained by dividing the area of the Mg^{2+}-free-β-phosphate resonance by that of the Mg^{2+}-bound-β-phosphate signal. The errors in the determination of the area ratios were less than 5%. [d]The errors are less than 0.1 ppm. [e]The $[Mg^{2+}]_f$ values were calculated from eq. (1), and the errors are less than 10%.

increases in free Mg^{2+} concentration originate from a decrease in free [ATP], as manifested by the downfield shifts observed in the Li^+ concentration range of 0-40 mM. For every Li^+ concentration studied, the $[Mg^{2+}]_f$ values were lower in the presence of membrane than in its absence (Table 3) because of the additional Mg^{2+}-binding sites in the membrane. This was however not the case when the samples contained 5 mM NaATP and 2.5 mM Mg^{2+}. The area ratios were comparable for samples with and without RBC membranes (Table 4).

IV.1.2. Interactions of Li^+ and Mg^{2+} with Human RBC Membrane Phospholipids

This investigation was conducted using ^{31}P NMR chemical shift measurements, and ^{31}P and Li^+ relaxation measurements. The ^{31}P NMR chemical shift variation upon metal ion addition was used to identify the phospholipids that interact most strongly with the metal ion added. ^7Li and ^6Li T_1 measurements were used to compute the Li^+ association constant to the phospholipid extract. Both these studies were also used to investigate if Li^+/Mg^{2+} competition is present for the phosphate head group of the phospholipids.

IV.1.2a Comparison of the Phospholipid Extraction Procedures for ^{31}P NMR

Figure 7 shows the ^{31}P NMR spectra of phospholipids extracted from human RBC membranes using different extraction procedures. The purpose of this experiment was to identify the extraction procedure that yields a well resolved spectrum which can then be used for metal binding studies. The ^{31}P NMR resonances of various phospholipids shown in the figure are found within a 1 ppm chemical shift range. The NMR parameters of the instrument must be optimized as well as the samples should contain no paramagnetic impurities which will otherwise broaden the resonances; this can lead to overlapping of several resonances. When the extraction solvent contained HCl (Mallinger et al., 1993), which was used to neutralize the charge on the

Table 4. ^{31}P NMR-determined β-P area ratios of 5 mM ATP (in sodium form) containing 2.5 mM $MgCl_2$ in the presence and absence of RBC membranes containing varying amounts of LiCl

	Without membrane	With membrane
$[Li^+]$/mM	Area ratio	Area ratio
0	0.95 ± 0.03	0.96 ± 0.05
20	1.01 ± 0.05	1.05 ± 0.09
40	1.18 ± 0.03	1.19 ± 0.02
60	1.53 ± 0.04	1.46 ± 0.08

The reported values represent an average of measurements conducted in two separately prepared samples. Variance reported here are a range and not a standard deviation. All samples contained 5.0 mM ATP (in sodium form), 2.5 mM $MgCl_2$, and 0.15 M Tris-Cl, pH 7.5 at 0 °C. The membrane protein concentration was 2.7 ± 0.1 mg/mL.

Figure 7. ^{31}P NMR spectra of phospholipids extracted from human RBC membrane using different extraction procedures. The extraction solvent mixture contained (A) methanol:$CHCl_3$ in a ratio of 1:2 without HCl and 0.74% KCl was used to remove non-lipid impurities, (B) methanol-$CHCl_3$-HCl in a ratio of 100:50:1 to which 1:1 of $CHCl_3$-H_2O was added prior to the separation of the organic layer, and (C) methanol-$CHCl_3$-HCl in a ratio of 100:50:1 with 0.74% KCl to remove non-lipid impurities. All samples contained the same amount of membrane ([protein] = 5.3 ± 0.8 mg/mL) from which the phospholipids were extracted. The dried phospholipids in all the samples were suspended in $CDCl_3$:methanol:EDTA reagent in a ratio of 125:8:3. All samples were run at 27 °C in a 10 mm NMR tube with sample spinning at 16 Hz. All spectra were weighted averages of an overnight accumulation. The peak assignments are indicated in spectrum A.

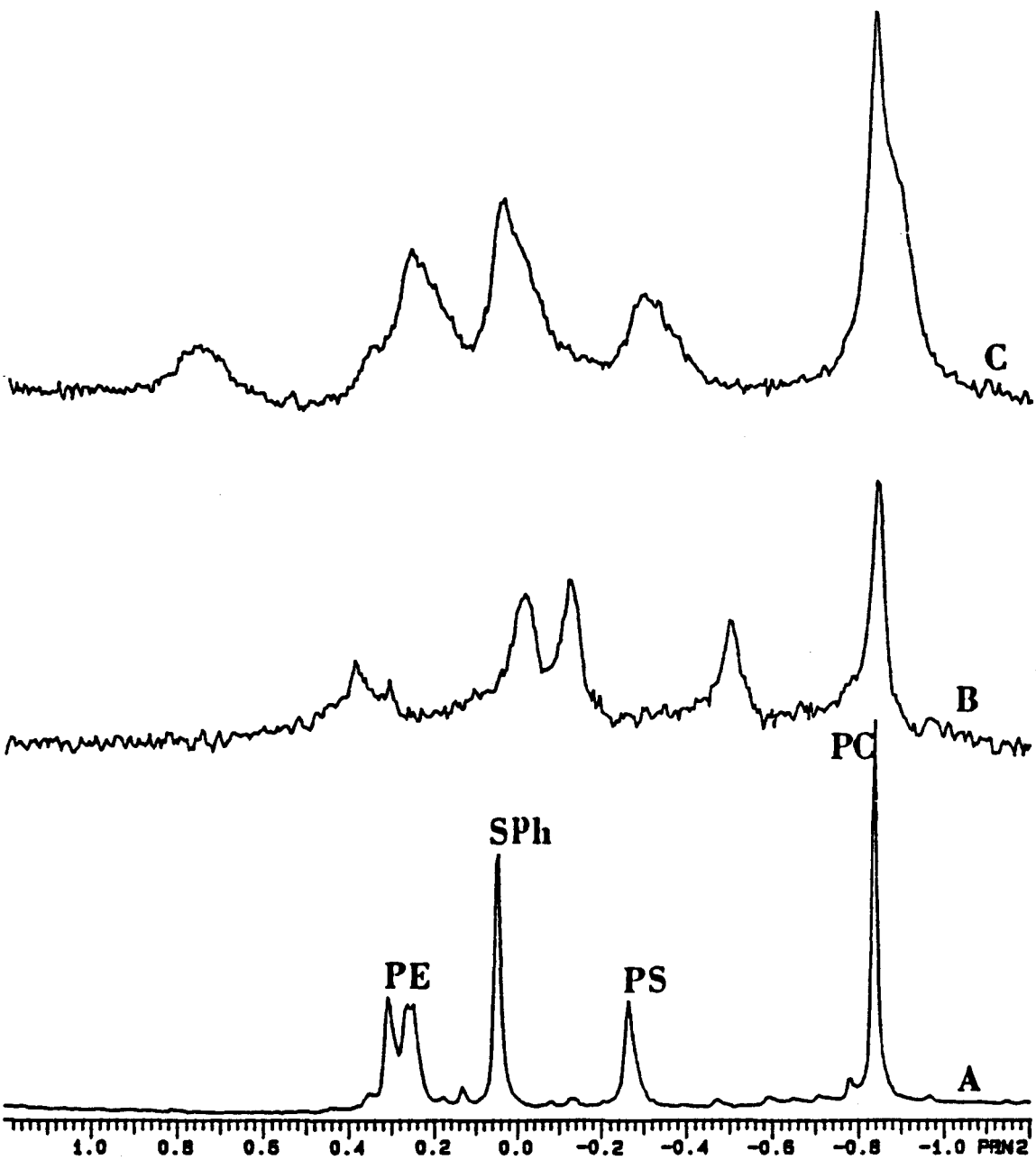
C
B
PC
SPh
PE
PS
A
1.0
0.8
0.6
0.4
0.2
0.0
-0.2
-0.4
-0.6
-0.8
-1.0
PRN2

anionic phospholipid, the resonances were broad and the signal to noise of the spectrum was not good for quantitative measurements (spectra B and C). However, the extraction solvent containing no acid (spectrum A) gave sharper resonances which were used to determine the phospholipid composition (Meneses & Glonek., 1988; Mota de Freitas et al., 1994b).

IV.1.2b. ^{31}P NMR Chemical Shift Measurements

The phospholipids extracted from the human RBC membranes were titrated with varying amounts of magnesium chloride and the variation of the chemical shifts with Mg^{2+} addition are presented in Table 5 and Figure 8. Upon Mg^{2+} addition the ^{31}P NMR resonances of all the phospholipids shifted upfield and the extent was different for the various phospholipids. The changes in the chemical shift upon metal ion addition is indicative of metal ion binding to the phosphate head group of the phospholipids; the changes in the chemical shift are dependent on the extent of interaction. The change in ^{31}P NMR chemical shift was largest for the anionic phospholipid PS at 0.5 ppm when 1.96 mM Mg^{2+} was added (Figure 8A); while the other phospholipids, phosphatidylethanolamine (PE), PE_p (plasmalogen PE) and sphingomyelin (Sph), resonances shifted upfield to a lesser extent than PS (about 0.1 ppm) when 1.96 mM Mg^{2+} was added. The phosphatidylcholine (PC) resonance did not show any appreciable change in the chemical shift upon metal ion addition.

The effect of Mg^{2+} addition on PI could not be investigated as the percentage of PI in the RBC membranes is under 2 % and to be able to observe this resonance clearly overnight accumulations of the ^{31}P NMR spectrum should be carried out (Mota de Freitas et al., 1994b). As the interaction of PI with the metal ion will cause broadening of the PI signal, with 2% abundance it will be impossible to observe the signal after metal ion addition. Hence to the human RBC membrane phospholipid extract a known amount of PI was added and the Mg^{2+}

Table 5. ^{31}P NMR chemical shifts of human RBC membrane phospholipids as a function of added $MgCl_2$

$[Mg^{2+}]$ / mM	^{31}P NMR Chemical Shift (ppm)				
	PE_p	PE	Sph	PS	PC
0.00	0.32 ± 0.0	0.27 ± 0.00	0.05 ± 0.01	-0.24 ± 0.01	-0.84 ± 0.00
0.49	0.29 ± 0.02	0.24 ± 0.02	0.03 ± 0.01	-0.41 ± 0.05	-0.85 ± 0.00
0.98	0.26 ± 0.02	0.21 ± 0.02	-0.01 ± 0.01	-0.60 ± 0.08	-0.86 ± 0.01
1.47	0.24 ± 0.02	0.18 ± 0.02	-0.03 ± 0.01	-0.65 ± 0.05	-0.87 ± 0.00
1.96	0.21 ± 0.02	0.16 ± 0.01	-0.06 ± 0.02	-0.74 ± 0.05	-0.87 ± 0.00

All samples were run at 27 °C in a 10 mm NMR tube with sample spinning at 16-18 Hz. The chemical shifts were referenced to 85% phosphoric acid. At the beginning of each titration the δ value of the PC resonance was referenced to -0.84 ppm. Reported chemical shifts are average values ± standard deviations obtained from three separate trials. The Mg^{2+} ion concentrations are the amount added to the suspension and not the amount present in the organic phase.

Figure 8. Plot of the changes in ^{31}P NMR chemical shifts of human RBC membrane phospholipids upon addition of varying amounts of chloride salts of (A) Mg^{2+} and (B) Li^{+}. Same experimental conditions as in Table 5.

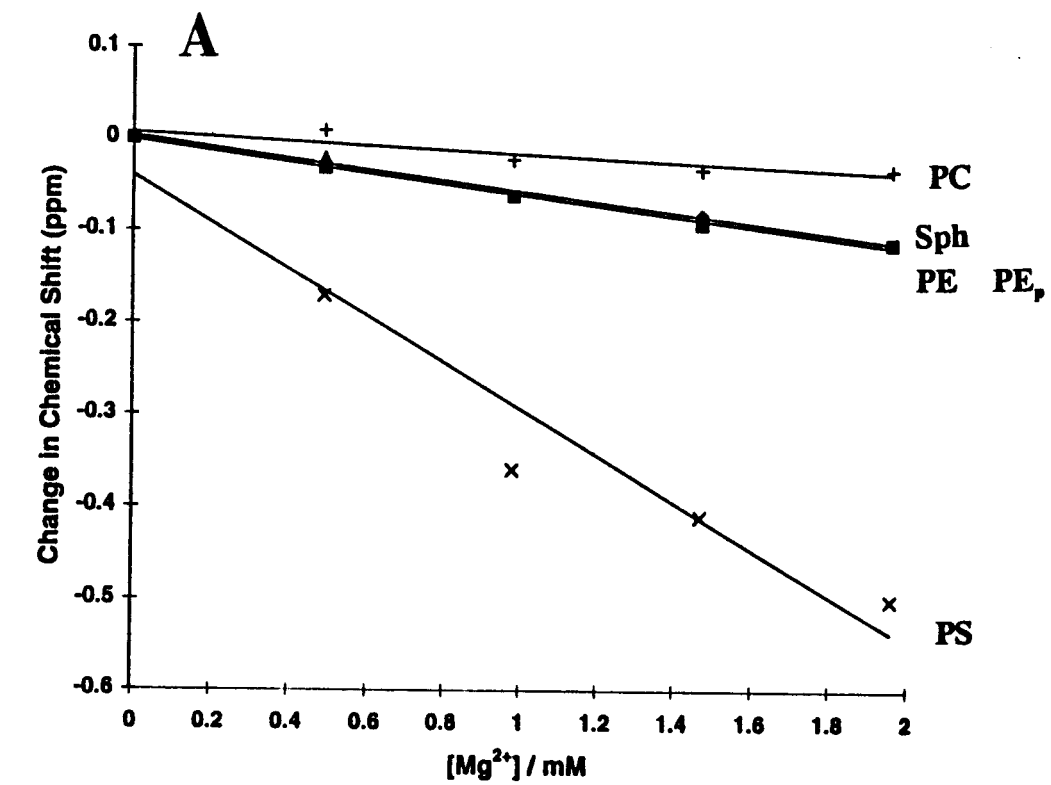
A
0.1
0
-0.1
-0.2
-0.3
-0.4
-0.5
-0.6
Change in Chemical Shift (ppm)
0
0.2
0.4
0.6
0.8
1
1.2
1.4
1.6
1.8
2
[Mg2+] / mM
PC
Sph
PE
PEp
PS

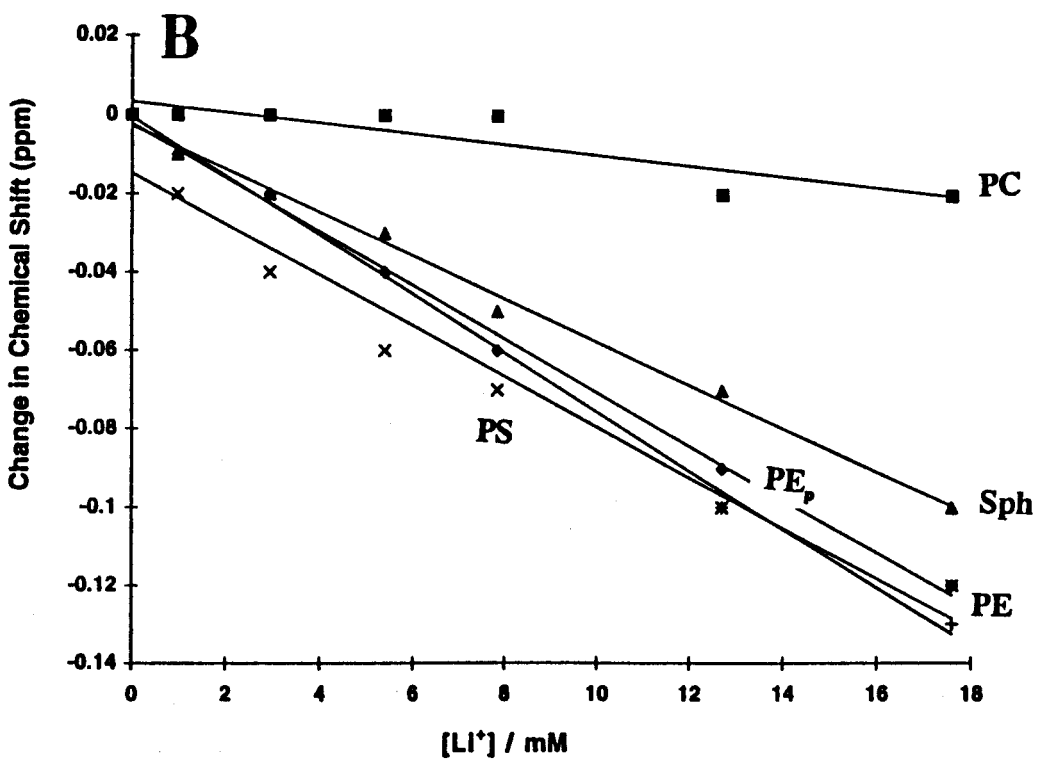
B
0.02
0
-0.02
-0.04
-0.06
-0.08
-0.1
-0.12
-0.14
Change in Chemical Shift (ppm)
0
2
4
6
8
10
12
14
16
18
[Li+] / mM
PC
PS
PEp
Sph
PE

titration was carried out. The addition of up to 1.96 mM Mg^{2+} caused the ^{31}P NMR resonances of PI and PS resonance to move upfield by 0.56 and 0.43 ppm, respectively (Table 6). These results suggest that the anionic phospholipids PI and PS interact most strongly with Mg^{2+}. Figure 8B and Table 7 show the changes in the ^{31}P NMR δ values as a function of added LiCl. Addition of up to 17.6 mM LiCl caused the δ values of PS, Sph, PE and PE_p to change by 0.1 ppm while the δ value of the PC resonance did not change appreciably with Li^+ titration. When compared with the Mg^{2+} titration larger amounts of Li^+ were needed to see an effect on the ^{31}P NMR spectrum of human RBC membrane phospholipids. This may be due to the difference in charge between lithium and magnesium ions. In order to characterize the interaction between PI and Li^+, the phospholipid extract from human RBC membranes was spiked with known amounts of pure PI (1.0 mg / 4.0 mL extract) and this sample was titrated with LiCl. Addition of up to 18.0 mM LiCl caused the PI resonance to move downfield by 0.18 ppm while the Sph resonance shifted upfield by 0.08 ppm; the δ value for all other resonances including PS changed by only 0.03 ppm.

^{31}P NMR chemical shift changes of the phospholipid extracts containing both lithium and magnesium ions are shown in Figure 9. The addition of 0.5 mM $MgCl_2$ caused the ^{31}P NMR resonances to move upfield while the ^7Li titration of this phospholipid sample caused the resonances to move downfield. This effect is clearly seen for the anionic phospholipid PS where addition of 0.5 mM $MgCl_2$ caused the resonance to move by 0.2 ppm upfield and addition of 7.8 mM LiCl caused the resonance to move downfield by 0.03 ppm.

IV.1.2c. ^{31}P NMR T_1 Measurements

^{31}P NMR T_1 measurements of phospholipid extract with and without metal ions were carried out to quantify metal ion binding to the phosphate head groups of the phospholipids.

Table 6. ^{31}P NMR chemical shifts of human RBC membrane phospholipids spiked with PI as a function of added $MgCl_2$[a]

$[Mg^{2+}]$ / mM	^{31}P NMR Chemical Shift (ppm)					
	PE_p	PE	Sph	PS	PI	PC
0.00	0.29	0.24	0.04	-0.22	----	-0.84
0.00 / with PI[b]	0.25	0.20	0.02	-0.29	-0.59	-0.84
0.49	0.23	0.18	0.00	-0.40	-0.70	-0.85
0.98	0.20	0.16	-0.03	-0.55	-0.86	-0.86
1.47	0.18	0.14	-0.06	-0.64	-1.01	-0.87
1.96	0.15	0.11	-0.09	-0.72	-1.15	-0.89

[a]All samples were run at 27 °C in a 10 mm NMR probe with sample spinning at 16-18 Hz. The chemical shifts were referenced to 85% phosphoric acid. At the beginning of each titration the δ value of the PC resonance was referenced to -0.84 ppm. Reported chemical shifts are average values obtained from two separate trials. The error in the δ values is under 5%. The $[Mg^{2+}]$ concentrations are the amount added to the suspension and not the amount in the organic phase. [b]The phospholipid extract was spiked with PI so that the NMR sample contained 0.25 mg of PI/mL of the sample.

Table 7. ^{31}P NMR chemical shifts of human RBC membrane phospholipids as a function of added LiCl

$[Li^+]$ / mM	^{31}P NMR Chemical Shift (ppm)				
	PE_p	PE	Sph	PS	PC
0	0.32 ± 0.01	0.27 ± 0.01	0.05 ± 0.01	-0.24 ± 0.00	-0.84 ± 0.01
0.98	0.31 ± 0.01	0.26 ± 0.01	0.04 ± 0.00	-0.26 ± 0.01	-0.84 ± 0.00
2.94	0.30 ± 0.00	0.25 ± 0.01	0.03 ± 0.00	-0.28 ± 0.00	-0.84 ± 0.00
5.39	0.28 ± 0.00	0.23 ± 0.00	0.02 ± 0.00	-0.30 ± 0.00	-0.84 ± 0.00
7.84	0.26 ± 0.01	0.21 ± 0.01	0.00 ± 0.01	-0.31 ± 0.01	-0.85 ± 0.00
17.6	0.20 ± 0.01	0.14 ± 0.01	-0.05 ± 0.01	-0.36 ± 0.00	-0.86 ± 0.00

All samples were run at 27 °C in a 10 mm NMR tube with sample spinning at 16-18 Hz. The chemical shifts were referenced to 85% phosphoric acid. At the beginning of each titration the δ value of the PC resonance was referenced to -0.84 ppm. Reported values are average values obtained from two different sample preparations and the variances represented are the ranges of values observed. The above $[Li^+]$ are the amount added to the phospholipid suspension and not the amount present in the organic phase.

Figure 9. ^{31}P NMR spectra of human RBC membrane phospholipids with (A) no metal ions added, (B) 0.5 mM Mg^{2+}, (C) 0.5 mM Mg^{2+} and 1.96 mM Li^{+}, (D) 0.5 mM Mg^{2+} and 3.92 mM Li^{+} and (E) 0.5 mM Mg^{2+} and 7.84 mM Li^{+}. Same experimental conditions as in Tables 5 and 7. The peak assignments are indicated in spectrum E.

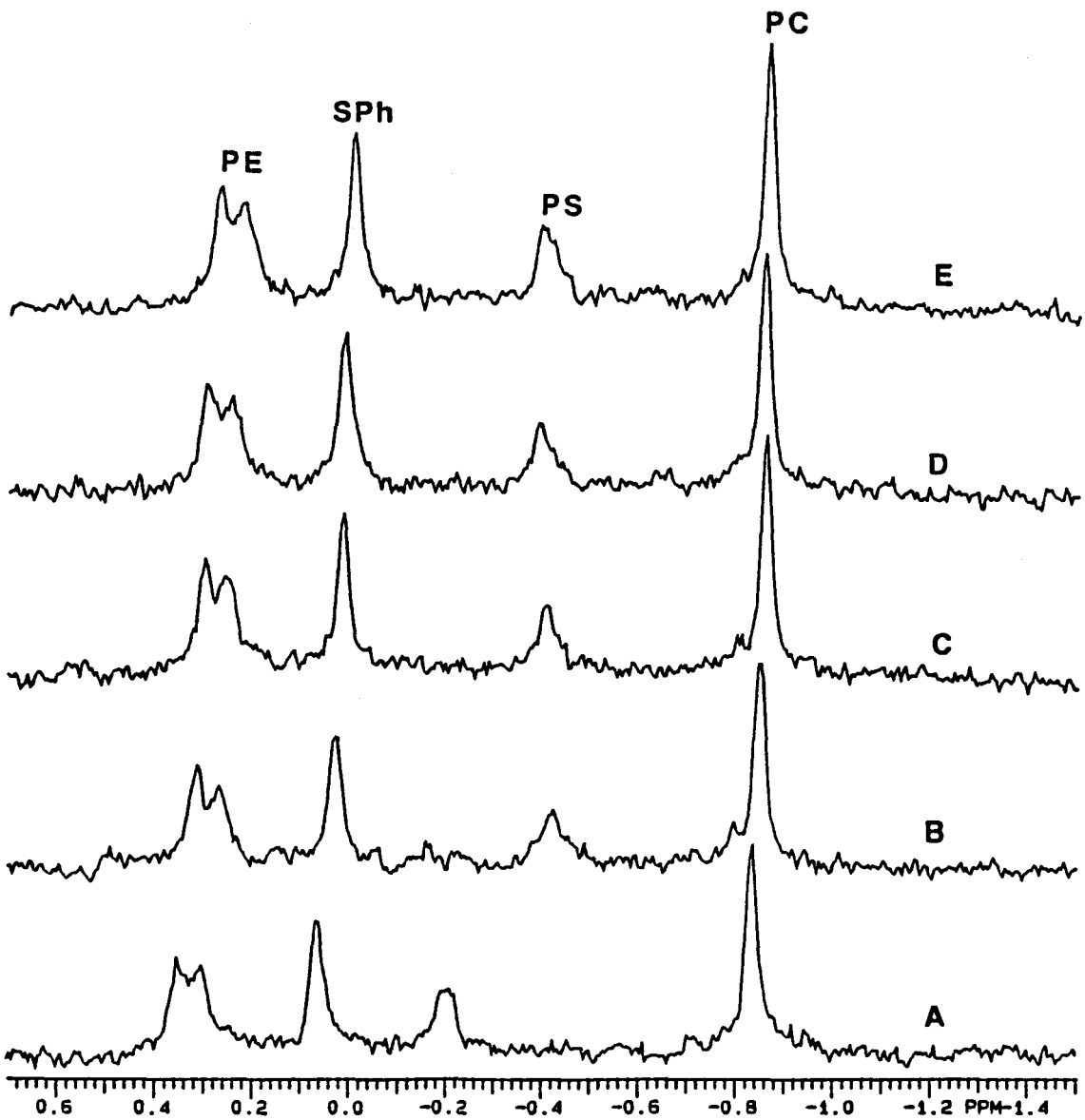
PC
SPh
PE
PS
E
D
C
B
A
0.6
0.4
0.2
0.0
-0.2
-0.4
-0.6
-0.8
-1.0
-1.2
PPM-1.4

However, the T_1 variations within each class of phospholipids were very small (0.1 s) to be measured accurately (Table 8). The addition of metal ions also did not cause any significant changes in the ^{31}P NMR T_1 values and hence this technique could not be used for any quantitative measurements.

IV.1.2d. ^7Li and ^6Li NMR T_1 Measurements

Lithium NMR relaxation measurements have been used previously by us and others to probe Li^+ binding and competition mechanism between Li^+ and Mg^{2+} for biomolecules (Rong et al., 1993). In this study we used both ^6Li and ^7Li spin-lattice (T_1) relaxation time measurements to determine the lithium binding constant to the phospholipid extract. Lithium ions are in fast exchange in the NMR time scale and hence the observed lithium NMR signal is a weighted average of the free and bound Li^+. As the Li^+ nucleus has a narrow chemical shift range the chemical shifts do not change upon Li^+ binding to substrates. However, the lithium T_1 values are sensitive to motion with free nuclei having longer T_1 values than tightly bound nuclei, and hence ^7Li or ^6Li T_1 measurements provide good tools to monitor the interaction of Li^+ with biomolecules.

The phospholipid extract in a chloroform-methanol solvent system was titrated with increasing amounts of LiCl; as the $^7Li^+$ concentration increased from 3 to 20 mM, the ^7Li T_1 values increased from 0.75 ± 0.16 s to 1.81 ± 0.13 s (Table 9). However, for each ^7Li addition of 3 mM, the T_1 changes were very small (0.2 s) and only slightly sensitive to variations in Li^+ concentration. As the changes in T_1 are very small, this method is unreliable for quantitative analysis. To see if this effect was a mere ionic strength effect, the phospholipid extract containing 6.0 mM LiCl was titrated with TMACl. Addition of up to 20 mM TMACl caused the ^7Li T_1 to change by only 0.2 s and therefore the changes in the ^7Li T_1 noticed are due to

Table 8. ^{31}P NMR T_1 measurements of human RBC membrane phospholipids with and without metal ions

Phospholipid	^{31}P NMR T_1 / s		
	without metal ions	with 0.5 mM $MgCl_2$	with 7 mM LiCl
PE_p	1.36 ± 0.16	1.43 ± 0.08	1.49 ± 0.13
PE	1.35 ± 0.15	1.43 ± 0.08	1.49 ± 0.13
Sph	1.50 ± 0.36	1.68 ± 0.06	1.73 ± 0.17
PS	1.63 ± 0.26	1.68 ± 0.06	1.73 ± 0.17
PC	1.66 ± 0.25	1.68 ± 0.06	1.73 ± 0.17

The reported T_1 values are the average values ± range from two separately prepared samples. The sample contained extracted dried phospholipids suspended in 4.08 mL of $CDCl_3$:methano:EDTA in a ratio of 125:8:3. The relaxation measurements were conducted at 27 °C in a 10 mm probe. Each sample was run for 5-6 h to obtain a good signal to noise so that accurate T_1 values could be obtained.

Table 9. ^{7}Li T_1 measurements of phospholipids extracted from human RBC membranes

$[^{7}Li^{+}]$ / mM	^{7}Li T_1 / s
3.0	0.75 ± 0.16
6.0	1.04 ± 0.14
9.0	1.20 ± 0.16
12.0	1.38 ± 0.20
15.0	1.47 ± 0.15
20.0	1.81 ± 0.13
500.0 (free)	3.67 ± 0.23

The reported T_1 values are average values and the variance indicates the range obtained from two different samples. ^{7}Li T_1 measurements were conducted at 27 °C in a 10 mm probe. The extracted dried phospholipids were dissolved in a chloroform:methanol solvent mixture in a ratio of 5:2.

binding of the Li^+ to the phospholipids and are not due to ionic strength effects.

The ^6Li nucleus exhibits much larger relaxation values than the ^7Li nucleus. Hence, ^6Li T_1 measurements were used to quantify Li^+ binding to the phospholipids (Table 10). Unlike ^7Li, the ^6Li T_1 values increased from 7.63 ± 0.76 to 16.18 ± 0.69 s upon addition of 5-40 mM ^6LiCl. The increase in ^6Li T_1 values with an increase in LiCl concentration is due to the increase in the fraction of free Li^+ in solution. The lithium binding constant to the phospholipid extract was calculated to be 45 ± 5 M^{-1} ($n=2$, $r^2 > 0.90$) by using a James-Noggle (1969) plot.

The phospholipid extract was titrated with ^6LiCl in the presence and absence of 0.1 mM Mg^{2+}. Addition of $^6Li^+$ caused an increase in the ^6Li T_1 values for both samples (Figure 10) indicating Li^+ binding. However, at a given $^6Li^+$ concentration the T_1 values were much higher for the sample containing 0.1 mM $MgCl_2$ and this is probably due to Mg^{2+} replacing the Li^+ that is bound to the phosphate head group of the phospholipids.

IV.1.3. Contribution of RBC Membrane Cytoskeleton towards Na^+ and Li^+ Binding

To identify if the cytoskeleton plays a major role in metal ion binding and competition, NMR studies were conducted with the unsealed and cytoskeleton-depleted RBC membranes. ^7Li T_1 measurements along with ^{23}Na multiple quantum filtered NMR measurements were used to address the involvement of the cytoskeleton in metal ion binding as well as competition between these metal ions.

IV.1.3a. ^7Li NMR T_1 Measurements

To help understand the involvement of the cytoskeleton towards Li^+ binding, ^7Li T_1 measurements were conducted with samples of unsealed and cytoskeleton-depleted RBC membranes. The T_1 and T_2 of the intracellular ^7Li resonance of frog hearts perfused with Li^+-

Table 10. ^{6}Li NMR T_1 measurements and the calculation of Li^+ binding constant to the human RBC membrane phospholipids as a function of $^{6}LiCl$ addition

[^{6}Li] / mM	^{6}Li T_1 (s)	R (s^{-1})	ΔR (s^{-1})	$(\Delta R)^{-1}$
5	7.63 ± 0.76	0.13	0.11	9.43
10	9.03 ± 0.28	0.11	0.09	11.66
15	9.74 ± 0.64	0.10	0.08	12.87
20	11.21 ± 0.78	0.09	0.07	15.57
25	12.02 ± 0.11	0.08	0.06	17.18
30	13.13 ± 1.3	0.08	0.06	19.54
40	16.18 ± 0.69	0.06	0.04	27.16
500 (free)	40.03 ± 4.30	0.02 (R_f)	0.00	---

The T_1 values reported are avarage values obtained from two different sample preparations and the variance indicates the range. The symbol R indicates the relaxation rates which are reciprocal of the T_1 values. ΔR is the difference of R_{obs} and R_f values. The Li^+ binding constant (K_{Li}) to the phospholipid extract was calculated from slope/intercept ratio of the linear James-Noggle plot of [Li^+] vs ΔR^{-1}. The K_{Li} value to the phospholipid extract was calculated to be 45 ± 5 M^{-1} (n=2, $r^2 > 0.90$) using the James-Noggle plot.

Figure 10. Variations in ^{6}Li T_1 values of the phospholipids extracted from human RBC membranes in the absence (■) and presence of 0.1 mM Mg^{2+} (▲). The extracted dried phospholipids were suspended in a chloroform-methanol solvent mixture in a ratio of 5:2. The relaxation measurements were carried out at 27 °C in a 10 mm NMR probe. The reported values are average values obtained from two separate measurements.

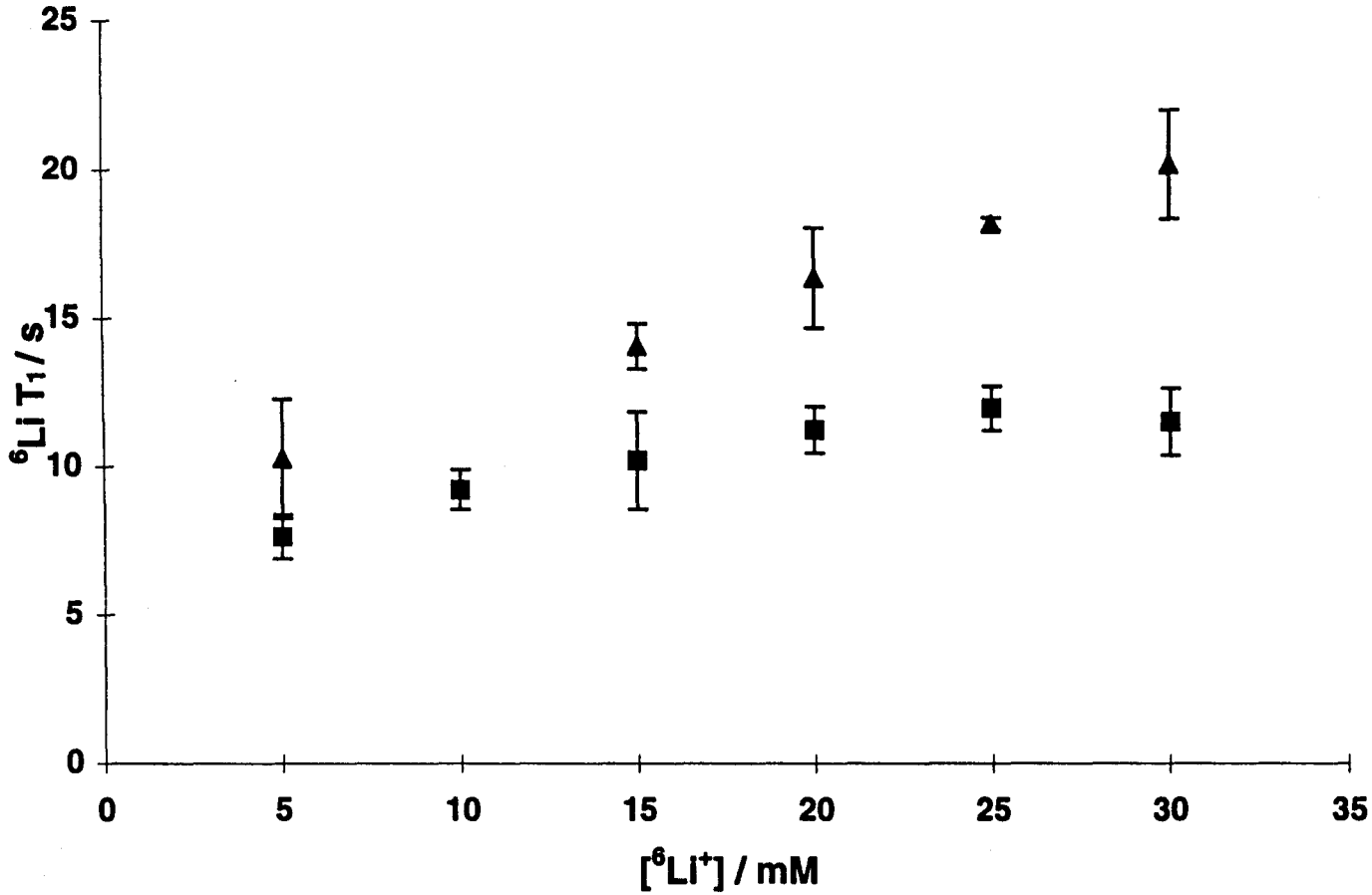
25
20
15
10
5
0
^{6}Li T_1 / s
0
5
10
15
20
25
30
35
[^{6}Li$^+$] / mM

containing buffer have been found to be monoexponential (Burstein & Fossel, 1987), whereas for 20 mM LiCl in the presence of unsealed RBC membrane both the relaxation parameters are biexponential (Rong et al., 1993). In our experiments as the membrane samples were titrated up to 10 mM LiCl, the monoexponential approximation for ^{7}Li T_1 values for these samples was justified. A plot of the variation of ^{7}Li T_1 values of the unsealed and cytoskeleton-depleted membranes is presented in Figure 11. As the $^7Li^+$ concentration increased from 2.0 to 10.0 mM, the ^{7}Li T_1 values for both samples increased. The slopes of the two plots are however different; the plot for the cytoskeleton-depleted membrane has a significantly larger slope than the unsealed membrane. The Li^+ binding constants calculated using the James-Noggle plots are independent of membrane concentrations and the K_{Li} for the cytoskeleton-depleted RBC membranes was calculated to be 333 ± 33 M^{-1} ($n=4$, $r^2 > 0.88$). This value is at least two-fold higher than the K_{Li} value of 161 ± 19 M^{-1} ($n=4$, $r^2 > 0.96$) obtained for the unsealed RBC membranes.

Table 11 shows the ^{7}Li T_1 values for the Li^+-treated membrane samples containing varying amounts of $MgCl_2$. As the Mg^{2+} concentration increased from 0.0 to 0.6 mM, the ^{7}Li T_1 values increased for both membrane samples. However, at a given Mg^{2+} concentration the T_1 values for the cytoskeleton-depleted membranes were significantly larger than for the unsealed membranes. Similar results were obtained when unsealed and cytoskeleton-depleted RBC membranes containing 4.0 mM LiCl was titrated with increasing amounts of NaCl; as the Na^+ concentration increased from 0 mM to 7.0 mM, the ^{7}Li T_1 values for the unsealed membranes increased from 8.22 ± 0.40 to 11.20 ± 0.40 s. Whereas for the cytoskeleton-depleted membranes the ^{7}Li T_1 values increased from 8.39 ± 0.52 to 11.98 ± 0.60 s indicating competition between Li^+ and Na^+ for both the membrane samples.

Figure 11. Plot of ^{7}Li T_1 measurements of Li^+-treated unsealed (■) and cytoskeleton-depleted (o) human RBC membranes as a function of added LiCl. The reported values are average values obtained from two separately prepared samples. The NMR measurements were carried out at 37 °C in a 10 mm NMR probe with sample spinning at 16 Hz.

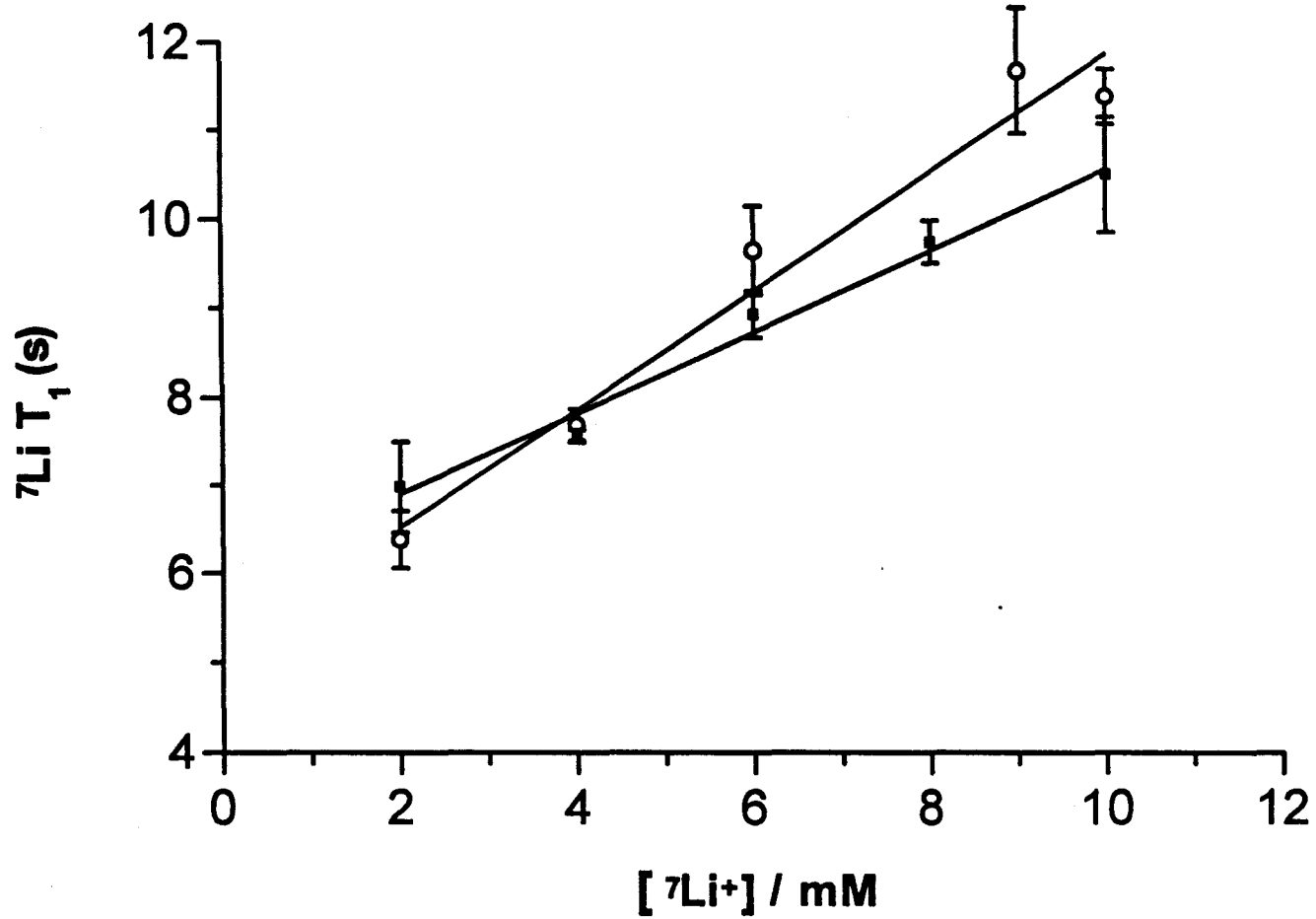
12
10
8
6
4
0
2
4
6
8
10
12
^{7}Li T_1 (s)
[^{7}Li$^+$] / mM

Table 11. ^{7}Li T_1 measurements of Li^+-treated unsealed and cytoskeleton-depleted RBC membranes in the presence of varying amounts of $MgCl_2$.

	^{7}Li T_1 (s)	
$[Mg^{2+}]$ / mM	unsealed membrane	cytoskeleton-depleted membrane
0.0	8.41 ± 0.04	8.94 ± 0.06
0.1	10.46 ± 0.46	10.63 ± 0.88
0.2	10.77 ± 0.41	11.64 ± 0.14
0.4	11.28 ± 0.15	14.07 ± 0.06
0.6	13.16 ± 1.17	14.15 ± 0.63

All samples contained 4.0 mM LiCl and the experiment was conducted at 37 °C in a 10 mm NMR probe. The values reported are the average values ± range obtained from two different samples. The protein concentration of the unsealed and the cytoskeleton-depleted RBC membranes were 6.0 ± 1.0 mg/mL and 4.5 ± 0.8 mg/mL, respectively. The total phospholipid content was comparable in both the samples.

IV.1.3b. ^{23}Na MQF NMR

The evolution of a typical ^{23}Na double quantum filtered (DQF) NMR signal as a function of creation time is shown in Figure 12. The sample used to check the proper functioning of the pulse sequences was 10% agarose containing 150 mM NaCl. In this MQF NMR study the evolution time was maintained constant at 10 μs and the creation time was varied. As the creation time increases the signal begins to evolve and after growing it decays. As a result the intensity of a DQF signal varies with the creation time and this behavior is seen for all the samples including the agarose sample shown in Figure 12; this behavior is consistent with previously published reports (Pekar & Leigh, 1986; Shinar et al., 1993). The signals also have the characteristic MQF line shapes as shown in the figure.

The DQF ^{23}Na NMR signal for an unsealed RBC membrane suspension containing 50 mM NaCl as a function of creation time is shown in Figure 13. At smaller creation times the signal is broad due to two overlapping antiphase resonances whose proportion depends on the creation time. The broad component $T_{2\,1}$ of negative intensity, characteristic of anisotropic motion of the Na^+ ions at the membrane surface is dominant at short creation times, but then disappears. The narrow component $T_{3\,1}$, characteristic of isotropic motion still evolves at longer creation times. This behavior has been observed previously for unsealed RBC membrane ghosts (Shinar et al., 1993) and has been attributed to ionic strength effects on the conformation of the cytoskeleton (Shinar et al., 1993), in particular on the dimer-tetramer equilibrium of spectrin (Knubovets et al., 1996). The cytoskeleton is involved in the anisotropy of Na^+ motion at the membranes, as shown by the observed isotropic DQF spectra ($T_{3\,1}$ component only) of cytoskeleton-depleted membranes in the presence of 5 or 50 mM NaCl. At low ionic strengths or when the unsealed membranes are suspended in 5 mM NaCl, the cytoskeleton detaches itself from the lipid bilayer and as a result of this the DQF signal is composed of $T_{3\,1}$ component only.

Figure 12. ^{23}Na DQF NMR spectra of 150 mM NaCl in 10% agarose gel. The creation time was varied from 1, 3, 5, 10, 15, 20, 30, 40, 50, 70 to 100 ms (from left to right). The evolution time was maintained at 10 μs. All spectra were recorded at 37 °C in a 10 mm broad band probe without spinning the sample. A line broadening of 20 Hz was used.

Figure 13. Variation of the ^{23}Na DQF NMR signal of unsealed RBC membranes containing 50 mM NaCl with the creation time. The creation time was varied from 1, 3, 5, 10, 15, 20, 30, 40, 50, 70 to 100 ms (from left to right). The evolution time was maintained at 10 μs. All spectra were recorded at 37 °C in a 10 mm broad band probe without spinning the sample. A line broadening of 20 Hz was used.

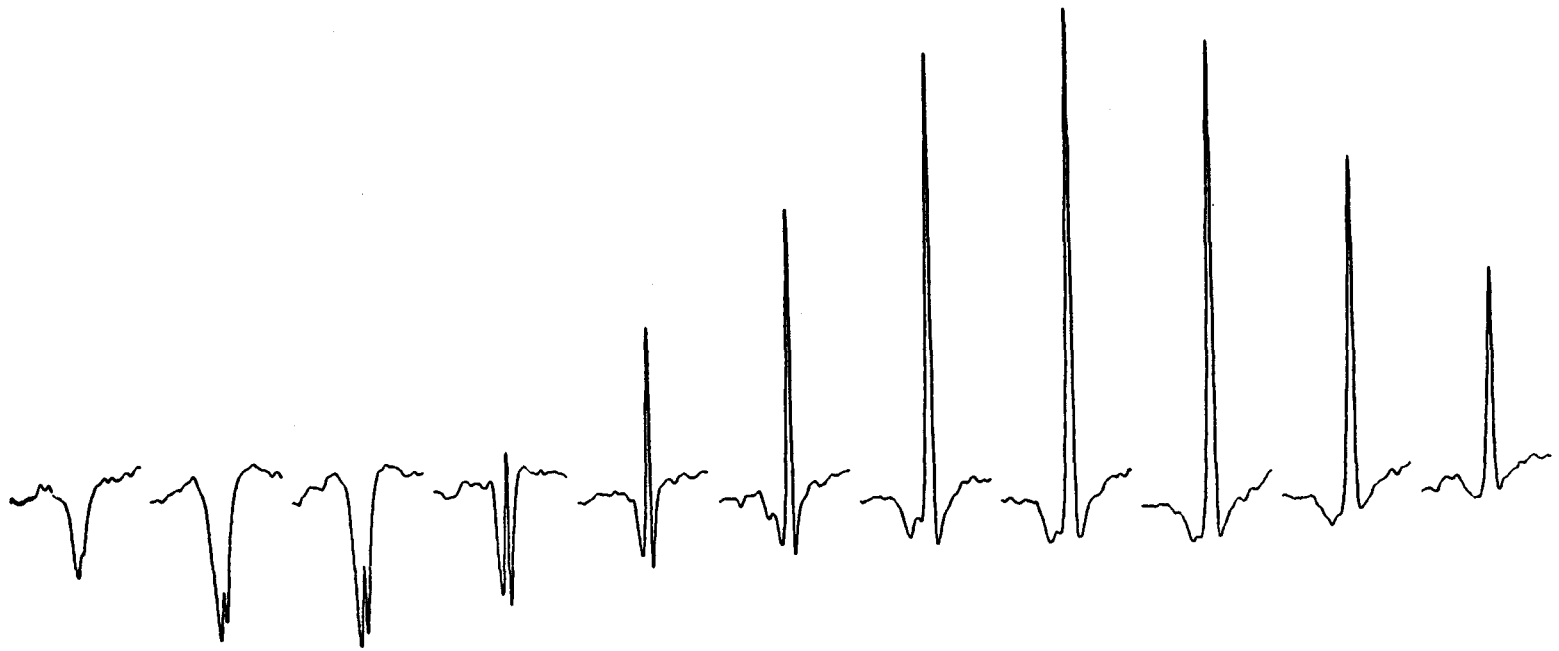

Lithium ion was shown to quench the sodium double quantum signals of both the intracellular and the extracellular compartments in human RBCs (Gullapalli et al., 1992). In this study the effects of the lithium ion on the double and triple quantum filtered signals were investigated; unsealed and cytoskeleton-depleted RBC membranes containing 5 or 50 mM NaCl were titrated with varying amounts of LiCl. This study was conducted to understand the contribution of the cytoskeleton towards binding of Na^+ and Li^+ and to compare the extent of Na^+/Li^+ competition. Figure 14 shows the effect of Li^+ addition on the TQF NMR peak intensity as a function of creation time. Figure 14A represents the triple quantum filtered spectra for the unsealed RBC membrane containing 50 mM NaCl. As for DQF experiments the signal intensity varied with the creation time. However, the TQF signals did not exhibit the negative resonance due to the even ranked tensor $T_{2\,1}$ for the unsealed and cytoskeleton-depleted RBC membranes at the NaCl concentrations used in this study. This observation is consistent with published reports (Shinar et al., 1993). Addition of 40 mM LiCl to the unsealed RBC membranes containing 50 mM NaCl caused the TQF peak intensity to decrease significantly (Figure 14B).

A representative plot to demonstrate the changes in the MQF NMR signal intensity upon addition of increasing amounts of Li^+ is shown in Figure 15. For unsealed membranes containing 50 mM NaCl as the Li^+ concentration was varied from 0 mM to 100 mM, the maximum peak intensity of the TQF signal decreased from 13 to 3 arbitrary units. Similar trends were observed for all membrane samples containing various amounts of NaCl. Peak areas also varied in a similar manner to that of peak intensities. A representative plot as in Figure 16 shows the effect of LiCl addition on the TQF NMR signal of unsealed membranes containing 50 mM NaCl. However, peak areas were not used for quantitative analysis as accurate determination is difficult for membrane samples containing 5 mM NaCl as the signal intensities are very low compared with the 50 mM NaCl samples.

Figure 14. Comparison of the ^{23}Na TQF NMR signals of unsealed RBC membranes containing 50 mM NaCl (A) before and (B) after addition of 40 mM LiCl. The creation time was varied from 1, 3, 5, 7, 9, 11, 13, 15, 17, 20, 24, 28, 32, 35, 40, 50, 80, 110, 150, 200 to 300 ms (from left to right). The evolution time was maintained at 10 μs. All spectra were recorded at 37 °C in a 10 mm broad band probe without spinning the sample. Each NMR measurement was conducted using two different sample preparations and a representative spectra is shown. A line broadening of 20 Hz was used.

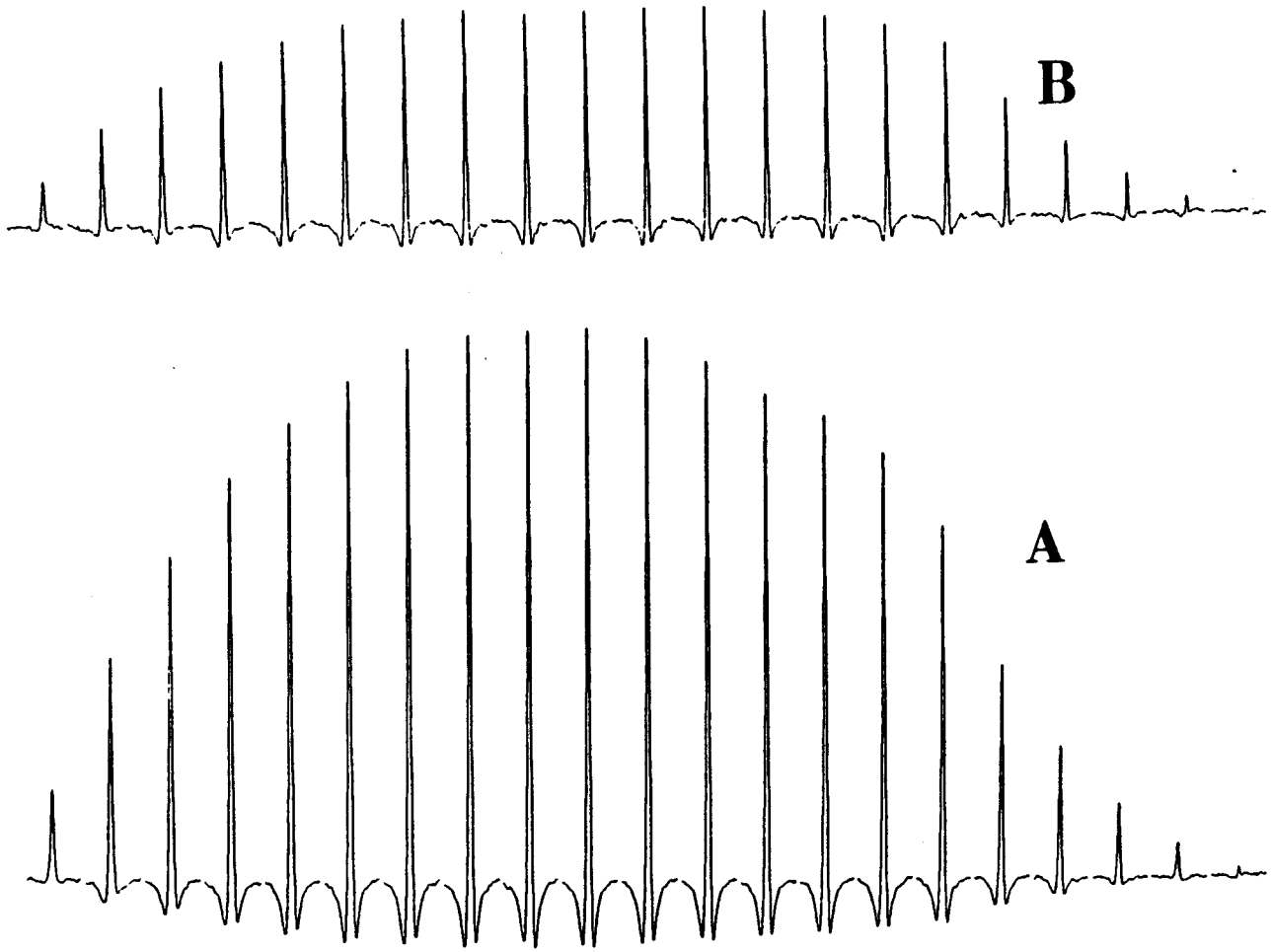
B
A

Figure 15. Plot of the changes in peak intensities of the ^{23}Na TQF NMR signal with creation time upon Li^+ titration. The samples used were unsealed RBC membranes containing 50 mM NaCl. The LiCl concentration used were 0, 10, 20, 40 and 100 mM. The peak intensities were measured after performing a magnitude transformation of the spectrum. NMR measurements were conducted using atleast two different sample preparations and a representative plot is shown here.

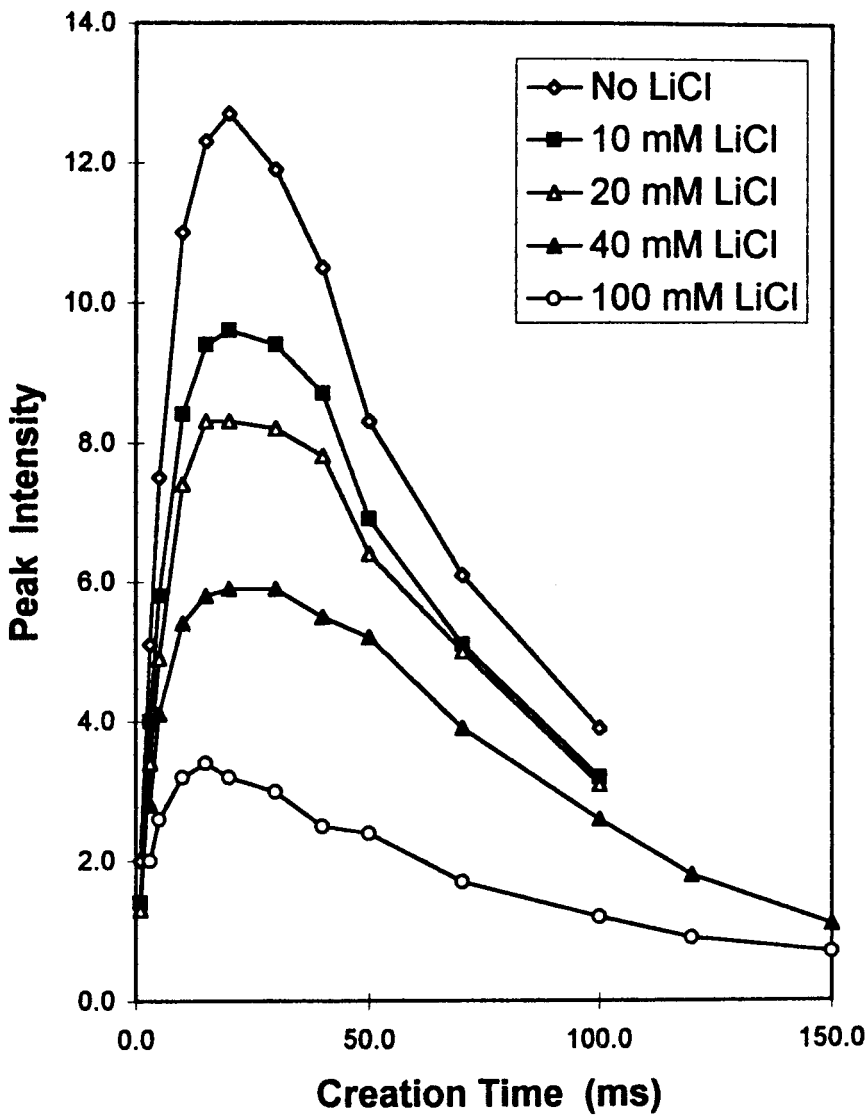
14.0
12.0
10.0
8.0
6.0
4.0
2.0
0.0
Peak Intensity
0.0
50.0
100.0
150.0
Creation Time (ms)
No LiCl
10 mM LiCl
20 mM LiCl
40 mM LiCl
100 mM LiCl

Figure 16. Plot of the changes in peak areas of the ^{23}Na TQF NMR signal with creation time upon Li^+ titration. The samples used were unsealed RBC membranes containing 50 mM NaCl. LiCl concentration used were 0, 10, 20, 40 and 100 mM. The peak areas were measured after performing a magnitude transformation of the spectrum. TQF NMR measurements were conducted using two separately prepared samples and a representative plot is shown here.

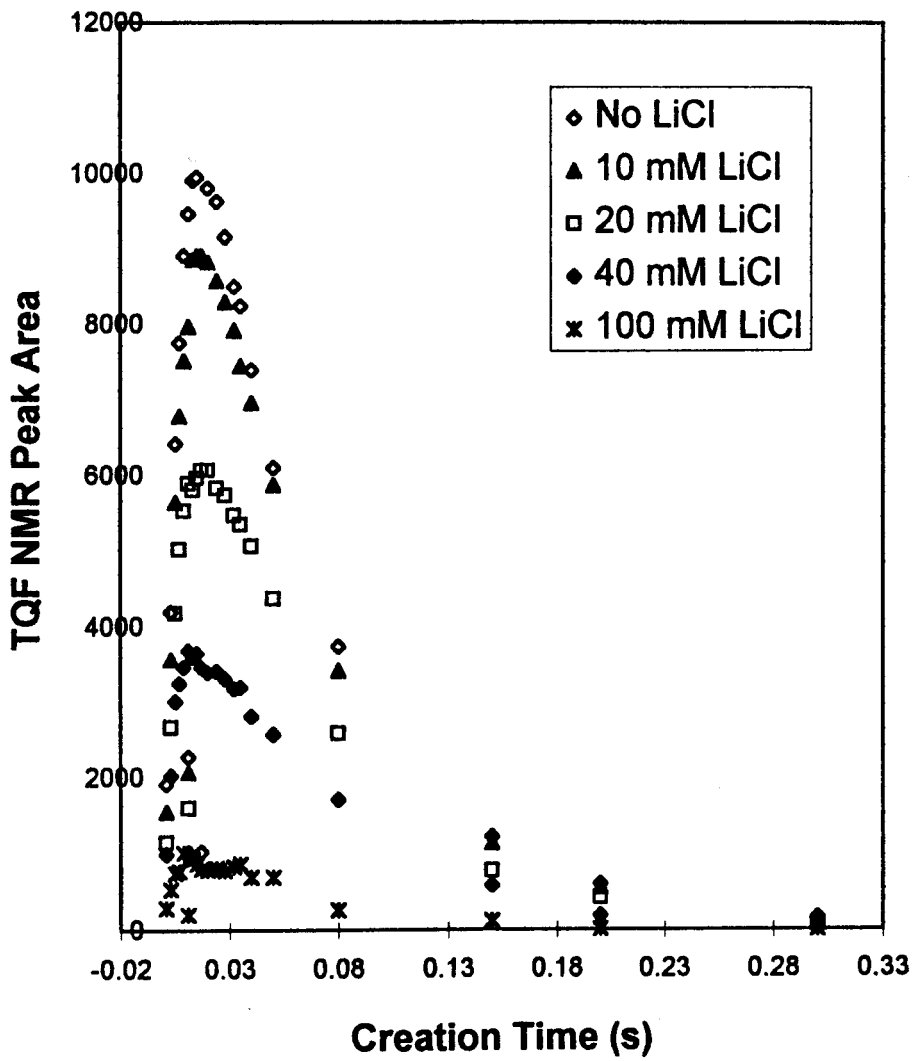
12000
10000
8000
6000
4000
2000
0
TQF NMR Peak Area
-0.02
0.03
0.08
0.13
0.18
0.23
0.28
0.33
Creation Time (s)
No LiCl
10 mM LiCl
20 mM LiCl
40 mM LiCl
100 mM LiCl

In all the above samples the MQF lineshape remains almost independent of the creation time and the experimental TQF signal intensity (peak height) obtained at different creation times were fitted to a double exponential of the form:

$$S(\omega,\tau) = A\ [\ \exp(-\tau / T_{2s}) - \exp(-\tau / T_{2f})] \qquad (7)$$

where, τ is the creation time, parameter A is indicative of the amount of bound Na^+ ions, T_{2f} and T_{2s} are the fast and slow components, respectively of the biexponential spin-spin relaxation time (T_2) (Pekar & Leigh, 1986; Eliav & Navon, 1994). Table 12 lists the calculated values of the parameters A, T_{2f}, and T_{2s}, as well as the values of the creation time τ_{max}, which gives maximum TQF signal intensities (I_{max}). All the experimental data gave good fits to the equation 7, except those for the unsealed RBC membranes with 50 mM NaCl. Equation 7 applies for isotropic samples with zero residual quadrupole splitting, $\omega_Q = 0$, a condition which is found not to apply to these samples, as shown by their ^{23}Na DQF NMR signals (Figure 13). Thus, for these samples a better fit of the signal intensity modulation was obtained with the following equation (Eliav & Navon, 1994):

$$S(\omega,\tau) = A\ [\ \exp(-\tau / T_{2s}) - \exp(-\tau / T_{2f}) \cos(\omega_Q \tau)] \qquad (8)$$

The parameters obtained from this fit are also shown in Table 12, giving much more consistent values, indicating a residual quadrupolar splitting $\omega_Q = 0.52 \pm 0.11$ Hz.

$T_{2\,1}$ parameters were calculated using the equation (Eliav & Navon, 1994):

$$S(\omega,\tau) = B\ [\ \exp(-\tau / T_{2f}) \sin(\omega_Q \tau)] \qquad (9)$$

The parameter B is similar to the parameter A which is directly proportional to the amount of bound Na^+ ions.

It is easy to find visually that the TQF signal intensity for samples containing 50 mM NaCl is much higher than for the samples containing 5 mM NaCl at the same creation time, as this signal intensity is proportional to the SQ magnetization (M_o) which increases with the Na^+

Table 12. ^{23}Na TQF NMR parameters obtained from curve fitting for unsealed and cytoskeleton-depleted RBC membranes in the presence of varying concentrations of NaCl and LiCl.

Sample	[Li^+] / mM	A	T_{2f}[d]	T_{2s}[d]	I_{max}	τ_{max} /ms	ω_Q /Hz	ΔA (%)[a]
Unsealed RBC membranes	0.0	132.2	9.5	159.7	104.0	30	-	0
with 50 mM NaCl[b]	10.0	181.9	9.8	66.4	111.4	21	-	-37.5
	20.0	103.1	9.5	145.1	79.6	27	-	22.0
	40.0	49.5	11.3	164.7	37.9	33	-	62.5
	100.0	13.5	4.7	131.6	11.5	15	-	89.8
Unsealed RBC membranes	0.0	133.8	9.4	158.0	105.2	27	0.50	0
with 50 mM NaCl[c]	10.0	131.5	8.4	142.2	103.5	24	0.52	1.7
	20.0	106.7	11.1	95.1	85.1	21	1.97	20.2
	40.0	67.7	8.1	87.3	48.1	21	0.65	49.4
	100.0	16.2	6.8	85.9	12.0	18	0.41	87.9
Unsealed membranes	0.0	33.8	3.5	57.9	26.5	11	-	0
with 5 mM NaCl	2.0	24.6	5.9	67.9	17.8	16	-	27.3
	4.0	23.1	5.2	66.2	17.2	14	-	31.5
	10.0	12.4	9.6	62.1	7.4	21	-	63.4
Cytoskeleton-depleted	0.0	57.7	10.1	83.8	38.0	24	-	0
membranes with 50 mM NaCl	10.0	37.0	8.2	97.8	27.0	21	-	36.1
	20.0	24.6	5.4	116.0	20.2	18	-	57.5
	40.0	20.8	5.2	86.9	16.3	15	-	64.2
	60.0	13.5	3.4	103.8	11.6	12	-	76.7
Cytoskeleton-depleted	0.0	23.0	2.8	52.9	18.5	8	-	0
membranes with 5 mM NaCl	2.0	17.1	3.8	66.9	13.6	12	-	25.6
	4.0	14.7	3.8	60.8	11.5	12	-	36.1
	10.0	9.7	5.0	80.0	7.5	14	-	58.1

[a]Decrease of the TQF peak intensity given by A value in the presence of LiCl relative to the intensity before LiCl addition. [b]Using equation 7 ($\omega_Q = 0$); [c]Using equation 8, $\omega_Q \neq 0$. [d]The reported relaxation times are in ms.

concentration. However, at a given Na^+ concentration intact RBC membranes gave more intense TQF signals than the cytoskeleton-depleted RBC membranes. The ratio of the TQF to SQ ^{23}Na signal can be quantified by using the parameter A in Table 12. An increase in the NaCl concentration in the suspending medium from 5 to 50 mM resulted in a decrease of the TQF/SQ signal ratio by 2.5 for intact membranes and by 3.8 for cytoskeleton-depleted membranes. This is a reflection of the saturation of the Na^+ binding sites at the membrane as the medium NaCl concentration increases. Cytoskeleton depletion of the membranes was accompanied by a significant decrease of the TQF/SQ signal ratio (50% at 5 mM Na^+, 130% at 50 mM Na^+). Thus the presence of the cytoskeleton network and its ionic strength induced conformational changes strongly affect the $T_{3\,1}$ term (Shinar et al., 1993).

Table 12 also shows the dependence of τ_{max} on Na^+ concentration and the cytoskeleton, which decreases significantly when Na^+ concentration decreases from 50 mM to 5 mM. This is a reflection of the variation of T_{2f} and T_{2s} values, which decreases significantly. The decrease of T_{2f} to very short values reflects a larger percentage of Na^+ ions bound to the membrane at lower concentration, particularly in the absence of the cytoskeleton. Table 12 also shows the various parameters obtained by fitting of the curves of Figure 15 to equations 7 and 8 for various Li^+/Na^+ concentration ratios, performed in the same way as described above in the absence of Li^+. The extent of quenching of the ^{23}Na TQF signal intensity (which results from the $T_{3\,1}$ term) by Li^+ at a given Li^+/Na^+ ratio can be quantitatively evaluated by the parameter ΔA, whose percentage value gives the percentage of TQF peak intensity decrease due to the replacement of Na^+ ions, bound at the isotropic sites at the membrane, by Li^+ ions. At 5 mM NaCl, the percentage of quenching is the same in intact and cytoskeleton-depleted membrane, at all Li^+/Na^+ ratios. However, at 50 mM NaCl, the percentage of quenching is initially higher in the case of cytoskeleton-depleted membrane, but at higher ratios, $Li^+/Na^+ > 0.8$, the percentage of quenching

is comparable in both the systems.

The effect of Li^+ addition on the value of τ_{max} for the TQF signal can also be observed from the data (Table 12). At 5 mM NaCl concentration in the suspension medium, both types of membranes show marked increase of τ_{max} upon Li^+ addition, which results from increased T_{2f} and T_{2s} values. This increase is more pronounced for T_{2f} in intact membranes, and for T_{2s} for cytoskeleton-depleted membranes, leading to a smaller increase of τ_{max} in the second case. At 50 mM NaCl, both types of membranes show a decreased τ_{max}, resulting from an increase of T_{2s}, for normal membranes, and a large decrease of T_{2f}, for cytoskeleton-depleted membranes. At a low NaCl concentration, the observed increase of the relaxation time components upon LiCl addition corresponds to that expected from replacement of Na^+ by Li^+ at the membrane binding sites. At high NaCl concentrations some relaxation times decrease as Li^+ is added, indicating that other effects are operating such as ionic strength effects upon the conformation of the cytoskeleton (Shinar et al., 1993), or preferential Li^+/Na^+ competition for different types of membrane sites.

The line widths at half-height of the TQF signal were found to depend on the creation time, which indicates the presence of non-equivalent Na^+ binding sites in slow chemical exchange at the RBC membranes (Shinar et al., 1993). This heterogeneity was also found through the behavior of the DQF signal. Figure 17 illustrates this behavior of the TQF signal linewidth for cytoskeleton-depleted RBC membranes, showing that it decreases initially very steeply at low creation times and stabilizes for $\tau \geq \tau_{max}$. The presence of increasing amounts of Li^+ causes the limiting linewidth value at high creation time to decrease substantially in intact membranes, indicating a preferential competition of Li^+ for the more anisotropic Na^+ binding sites. The absence of this effect in the cytoskeleton-depleted membranes reflects the role of the cytoskeleton in promoting the Li^+/Na^+ competition for the anisotropic sites. This observation is also supported

Figure 17. A plot showing the variation in line widths of the TQF NMR signal with the creation time at different LiCl concentrations. The sample contained cytoskeleton-depleted RBC membranes suspended in 50 mM NaCl and titrated with 0, 10, 20, 40, and 60 mM LiCl.

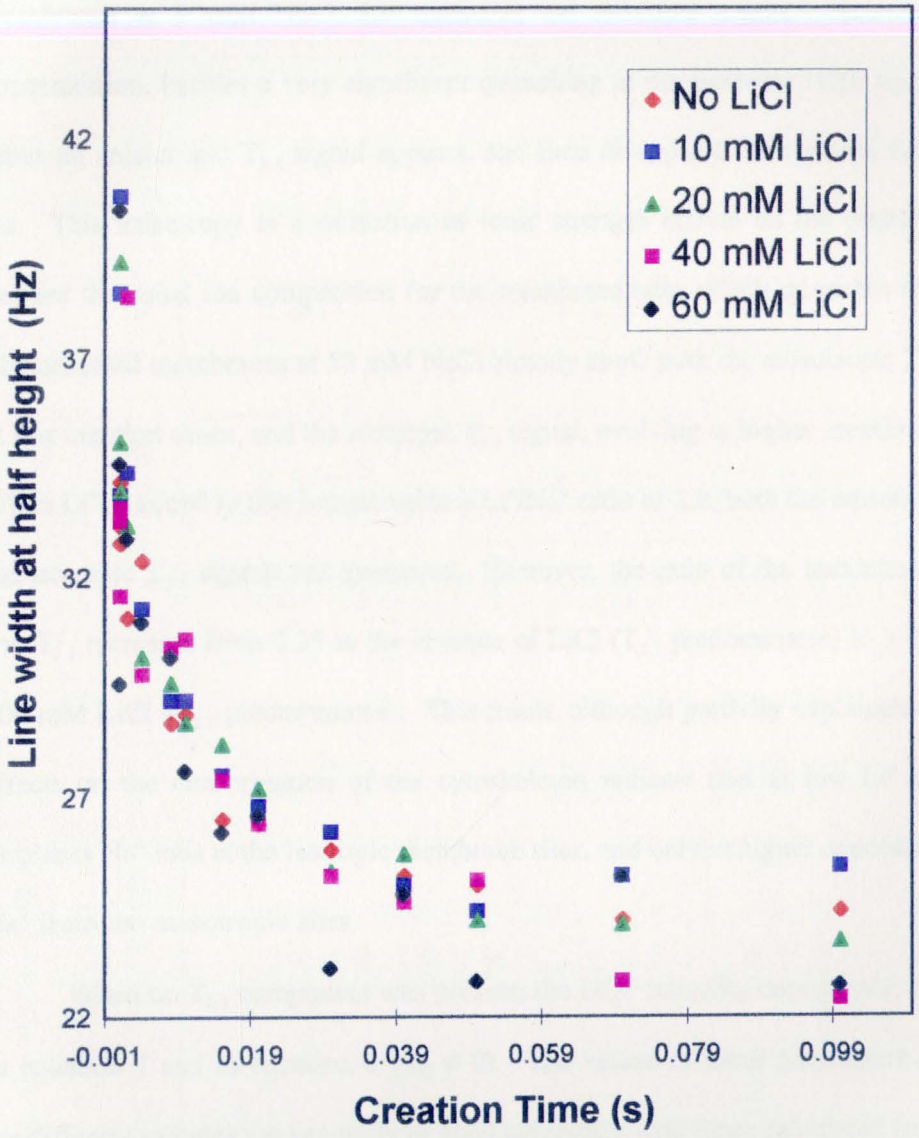
No LiCl
10 mM LiCl
20 mM LiCl
40 mM LiCl
60 mM LiCl
Line width at half height (Hz)
42
37
32
27
22
-0.001
0.019
0.039
0.059
0.079
0.099
Creation Time (s)

by DQF measurements.

A similar approach was applied for DQF signal intensities to obtain the parameters reported in Table 13. The isotropic DQF signal has the same modulation by the creation time as the TQF signal, and therefore it can be described by equation 7. In the case of unsealed membranes at 5 mM NaCl, Li^+ quenches the isotropic signal. However at 40 mM Li^+ concentration, besides a very significant quenching of the isotropic DQF signal, at low creation times an anisotropic $T_{2\,1}$ signal appears, and then disappears for creation times higher than 30 ms. This anisotropy is a reflection of ionic strength effects on the membrane cytoskeleton, besides the usual ion competition for the membrane sites which quenches the isotropic signal. The unsealed membranes at 50 mM NaCl already show both the anisotropic $T_{2\,1}$ signal, evolving at low creation times, and the isotropic $T_{3\,1}$ signal, evolving at higher creation times (Figure 13). When Li^+ is added to this sample up to a Li^+/Na^+ ratio of 2.0, both the anisotropic $T_{2\,1}$ signal and the isotropic $T_{3\,1}$ signals are quenched. However, the ratio of the maximum intensities of $T_{2\,1}$ and $T_{3\,1}$ increases from 0.35 in the absence of LiCl ($T_{3\,1}$ predominates) to 3.0 in the presence of 100 mM LiCl ($T_{2\,1}$ predominates). This result, although partially explainable by ionic strength effects on the conformation of the cytoskeleton indicate that at low Li^+ concentrations, Li^+ displaces Na^+ ions at the isotropic membrane sites, and only at higher concentrations replaces the Na^+ from the anisotropic sites.

When no $T_{2\,1}$ component was present, the DQF intensity dependence with τ curve was fit to equation 7 and to equation 8 ($\omega_Q \neq 0$). The values of these parameters and their trends in the different samples are generally in good agreement with those calculated from the TQF signals (Table 12).

IV.2. NMR Investigation of the Interactions of Li^+ and Mg^{2+} with G Proteins

Table 13. ^{23}Na DQF NMR parameters obtained from curve fitting for unsealed and cytoskeleton-depleted RBC membranes in the presence of varying concentrations of NaCl and LiCl

Sample		[Li^+] / mM	A	T_{2f} /ms	T_{2s} /ms	I_{max}	τ_{max} /ms	ω_Q[e]	ΔA (%)[a]	B
Unsealed RBC membranes										
with 50 mM NaCl	$T_{3\,1}$[b]	0.0	83.6	33.3	43.4	11.4	42	1.5	0	-
		10.0	27.7	37.1	69.9	6.3	51	1.6	66.8	-
		20.0	13.9	49.8	93.5	5.0	66	1.9	83.4	-
		40.0	3.8	90.9	63.6	1.6	99	20.8	95.4	-
	$T_{2\,1}$[d]	0.0	-	5.3	-	7	5	57.0	-	78.2
		10.0	-	6.3	-	6.8	5	43.0	-	75.1
		20.0	-	7.1	-	5.8	7	58.8	-	39.1
		40.0	-	10.0	-	2.9	7	50.6	-	10.1
Unsealed membranes		0.0	39.1	2.7	57.8	32.0	9	-	0	-
with 5 mM NaCl[c]		2.0	29.3	5.1	62.5	21.6	14	-	25.1	-
		4.0	24.3	6.9	68.2	16.9	18	-	37.9	-
		10.0	11.6	7.3	58.5	7.5	17	-	70.3	-
Cytoskeleton-depleted		0.0	65.8	11.1	99.0	44.3	27	-	0	-
membranes with 50 mM NaCl[c]		10.0	23.3	6.3	82.4	17.4	18	-	64.5	-
		20.0	16.9	6.7	89.4	12.7	19	-	74.3	-
		40.0	13.3	6.8	60.9	8.9	17	-	79.8	-
		60.0	10.5	6.3	66.4	7.4	16	-	84.0	-
Cytoskeleton-depleted		0.0	14.6	3.3	59.0	11.6	10	-	0	-
membranes with 5 mM NaCl[c]		2.0	13.1	5.2	66.9	9.8	14	-	10.3	-
		4.0	8.7	3.1	78.3	7.3	11	-	40.4	-
		10.0	7.8	6.3	50.3	6.4	16	-	46.6	-

[a]Decrease of the DQF $T_{3\,1}$ and $T_{2\,1}$ peak intensities are given by A and B values, respectively, in the presence of LiCl relative to the intensity before LiCl addition; [b]Using equation 8; [c]Using equation 7. [d]$T_{2\,1}$ parameters were calculated using equation 9. [e]ω_Q values are in Hz.

As G proteins are involved in signal transduction, detailed metal binding studies with these proteins were conducted to understand the interaction of Li^+ with the proteins at a molecular level. In this study the inactive conformation of the G proteins, the GDP-bound conformation, was used. The purpose of these studies was to identify suitable experimental conditions for various NMR experiments used to probe metal binding to G proteins as well as to characterize the interactions of Li^+ and Mg^{2+} with these proteins. G proteins from different sources were used. Purified transducin, the G protein in visual signal transduction, was used to determine the Li^+ binding constant to this protein. Transducin bound to the ROS membranes also provided a good model system to monitor the Li^+/Mg^{2+} competition mechanism. ^7Li T_1 measurements were used to study the interaction of Li^+ and the Li^+/Mg^{2+} competition hypothesis for $rG_i\alpha_1$. ^{31}P NMR spectroscopic studies of GDP bound to $rG_i\alpha_1$ were used to monitor metal binding to the nucleotide of the protein. Preliminary ^{19}F NMR results of the transition state analog of $rG_i\alpha_1$ are also presented in this section.

IV.2.1. Interactions of Li^+ with T Bound to ROS Membranes and Purified T

In this study ROS membranes with and without T and also purified T were used. ROS membranes were stripped of all soluble proteins and this served as a control; to this sample, T was added to obtain the reconstituted membranes. Thus, two membrane samples without and with T were obtained. ^7Li T_1 measurements were conducted on both these samples to monitor Li^+ binding. Figure 18 shows the ^7Li T_1 values obtained for these two different membrane samples without and with 0.2 mM Mg^{2+}. In both samples as the Li^+ concentration increased, the T_1 values also increased and this is due to an increase in the fraction of free Li^+. The slope of the plots are different due to different Li^+ affinities of the membrane systems used. However, in the presence of Mg^{2+} the T_1 values are much higher than without Mg^{2+} and this is due to Mg^{2+}

Figure 18. ^{7}Li T_1 measurements for bovine ROS membranes without (A) and with (B) heterotrimeric transducin. The ROS membrane concentration was 9.0 ± 0.8 mg/mL and all experiments were conducted at 20 ± 1 °C in a 10 mm NMR probe in a dark room under a dim red light. Dark room conditions were used to prevent photo bleaching of the ROS membranes. Reported values are averages obtained from two different trials.

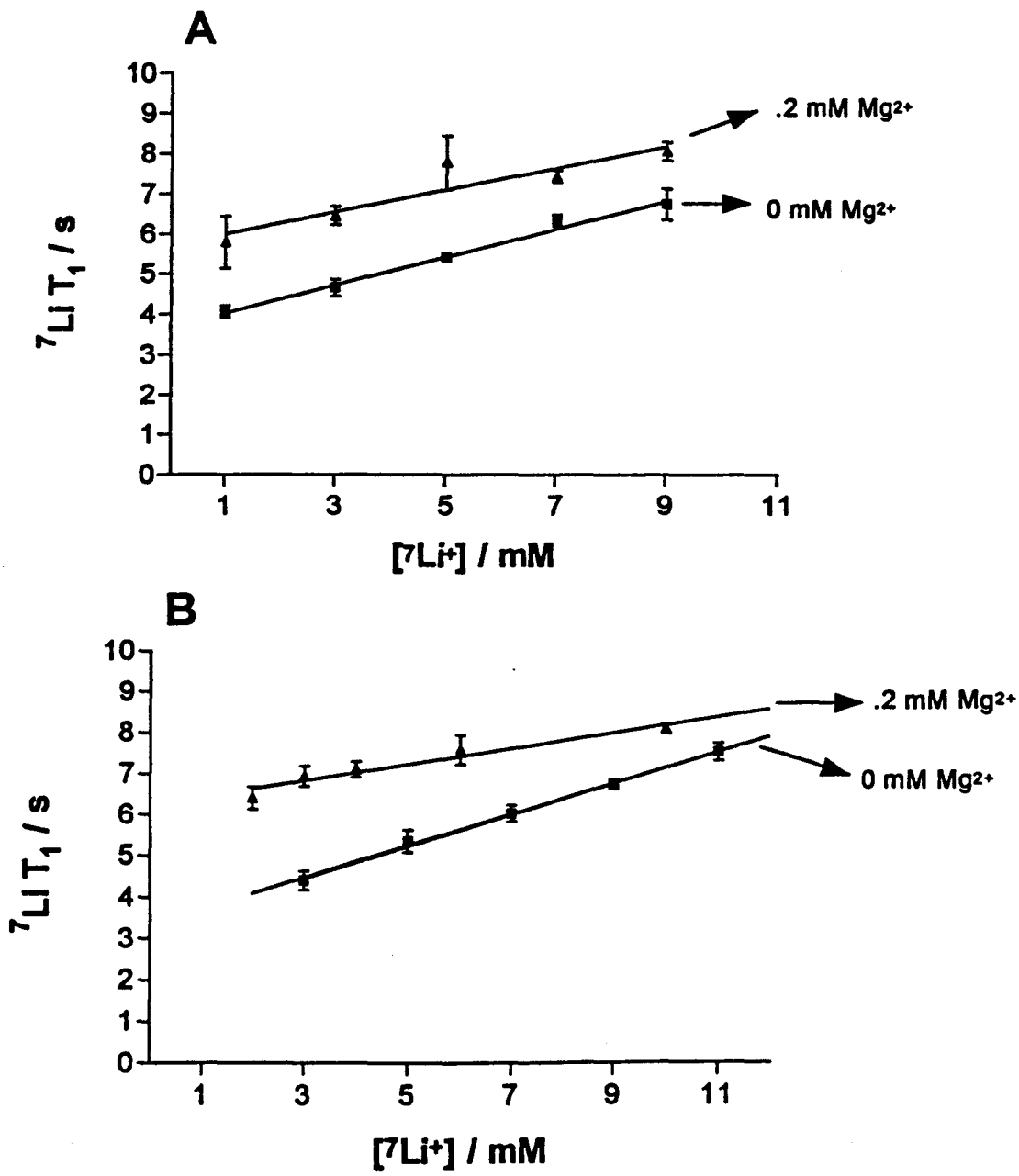
A
10
9
8
7
6
5
4
3
2
1
0
1
3
5
7
9
11
^{7}Li T_1 / s
[^{7}Li$^+$] / mM
.2 mM Mg^{2+}
0 mM Mg^{2+}
B
10
9
8
7
6
5
4
3
2
1
0
1
3
5
7
9
11
^{7}Li T_1 / s
[^{7}Li$^+$] / mM
.2 mM Mg^{2+}
0 mM Mg^{2+}

displacing the bound Li^+. The slope of the plot for the ROS membrane with T is greater. The Li^+ binding constants were calculated for both membrane samples without Mg^{2+} and with increasing amounts of Mg^{2+} and the variation of the K_{app} values upon addition of different amounts of Mg^{2+} are shown in Figure 19. From the figure it is clear that ROS membranes with T have a higher K_{app} value than the membranes without T.

^7Li T_1 measurements were also conducted for purified heterotrimeric transducin. A 0.06 mM GDP bound T sample was titrated with 3, 5, 7, 9, 20, and 30 mM ^7LiCl; the ^7Li values increased from 9.21 ± 0.72 to 13.44 ± 0.33 s (Table 14). The Li^+ affinity constant to the heterotrimeric T was calculated using a James-Noggle plot and it was found to be 122 M^{-1} (r^2 = 0.97). This value of 122 M^{-1} is much smaller than the Li^+ binding constant observed for T bound to the ROS membrane (about 500 M^{-1}). Attempts were made to obtain large amounts of T_α to see if the absence of the βγ-complex changes the Li^+ affinity of the protein. Since each NMR experiment requires 8-10 mg of protein it was not possible to obtain such high yields of T_α within a reasonable period of time.

IV.2.2. ^7Li T_1 Measurements with GDP-Bound $rG_i\alpha_1$

The ^7Li relaxation measurements were conducted with the Mg^{2+}-bound inactive conformation of $rG_i\alpha_1$. Table 15 shows the variation in the ^7Li T_1 and T_2 values as a function of LiCl concentration. As the Li^+ concentration increased from 2.0 to 10.0 mM, the T_1 values increases from 9.30 ± 0.80 to 11.71 ± 0.31 s. The T_1 values are increasing with the changes in Li^+ concentrations and this is due to Li^+ binding to the protein. However, the changes are not reliable to calculate the Li^+ binding constant using a James-Noggle plot as the T_1 values are in the saturation region (9-11 s). The T_2 values also did not change significantly and the R ratio for these samples was close to 3. The R ratio is indicative of the strength of Li^+ interaction and

Figure 19. Variation of K_{app} of ROS membranes with (▲) and without (o) heterotrimeric transducin in the presence of varying concentrations of $MgCl_2$. The ROS membrane concentration was 9.0 ± 0.8 mg/mL. The same dark experimental conditions as in Figure 18 were used. The concentration range of LiCl used was 1-13 mM. The errors in the determination of K_{app} were under 15% and the reported vaules are average values from two different trials.

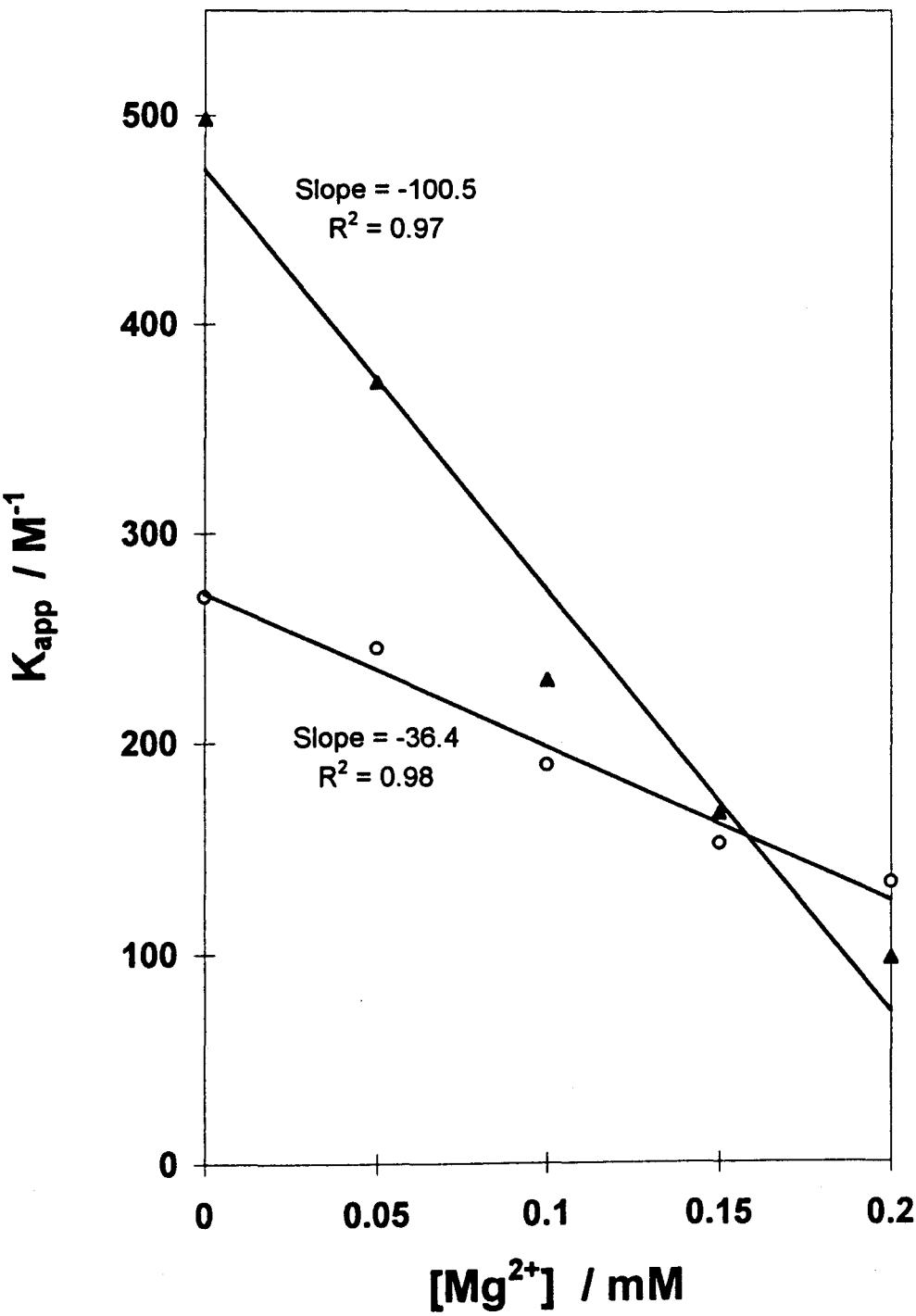
500
400
300
200
100
0
K_{app} / M^{-1}
Slope = -100.5
R^2 = 0.97
Slope = -36.4
R^2 = 0.98
0
0.05
0.1
0.15
0.2
[Mg^{2+}] / mM

Table 14. ^{7}Li NMR spin-lattice relaxation (T_1) measurements of heterotrimeric transducin

$[Li^+]$ / mM	^{7}Li T_1 / s
3	9.21 ± 0.72
5	10.96 ± 0.44
7	11.39 ± 0.41
9	11.98 ± 0.31
20	13.02 ± 0.28
30	13.44 ± 0.33
500 (Free)	15.40 ± 0.60
K_{Li}	122 M^{-1}
	(R^2 = 0.97)

All samples contained 0.06 mM heterotrimeric transducin in 5 mM HEPES buffer at pH 7.5. ^{7}Li NMR relaxation measurements were conducted at 20 ± 1 °C in a 10 mm NMR probe with the sample spinning at 16-18 Hz. The R ratio (T_1/T_2) was close to 4.0 for the above samples.

Table 15. ^{7}Li relaxation measurements of Mg^{2+}-bound $rG_i\alpha_1$ in the GDP bound conformation

$[^{7}Li^{+}]$ / mM	T_1 / s	T_2 / s	R (T_1 / T_2)
2.0	9.30 ± 0.80	3.51 ± 0.44	2.7
4.0	11.54 ± 0.87	3.62 ± 0.14	3.2
6.0	12.16 ± 0.90	3.44 ± 0.36	3.5
10.0	11.71 ± 0.31	3.69 ± 0.18	3.2

The concentration of $rG_i\alpha_1$-GDP used in this experiment was 0.34 mM. The NMR experiment was conducted at 20 ± 1 °C in a 5 mm probe.

it did not change significantly with Li^+ addition.

The $rG_i\alpha_1$ sample containing 10.0 mM LiCl when titrated with increasing amounts of $MgCl_2$ the ^7Li T_1 values increased from 11.71 ± 0.31 to 14.72 ± 0.30 s upon addition of 10 mM $MgCl_2$ (Table 16). The increase in the ^7Li T_1 values upon addition of Mg^{2+} was presumably due to Mg^{2+} displacing the bound Li^+.

The ^7Li relaxation times were high, in the order of 10 - 11 s, for Mg^{2+}-bound $G_i\alpha_1$ and they were not very sensitive to Li^+ addition. A paramagnetic probe was introduced and this was done by replacing Mg^{2+} that is bound to the protein with Mn^{2+}. Incorporation of Mn^{2+} in the protein was checked by ESR spectroscopy and the spectrum is shown in Figure 20. ESR results indicated that the 90% of the sample contained Mn^{2+}-bound to the protein. The activity of the protein was shown to be not affected by this metal ion replacement (Higashijima et al., 1991). This was also verified for the above preparation by conducting a fluorescence activity assay after Mn^{2+} incorporation. The ^7Li relaxation measurements were conducted on the Mn^{2+} derivative of the GDP-bound $rG_i\alpha_1$. The ^7Li relaxation values for this sample were significantly lower than the values obtained for the Mg^{2+}-bound protein. As the LiCl concentration increased from 2 - 100 mM, the T_1 values increased from 1.26 ± 0.08 to 1.99 ± 0.19 s (Table 17). The T_2 values also showed a steady increase while the R ratio decreased with LiCl addition. This trend is a clear indication of Li^+ binding to the Mn^{2+}-derivative of the $rG_i\alpha_1$. The Li^+ binding constant to the Mn^{2+}-derivative of $rG_i\alpha_1$ was calculated using the T_1 values to be 32 ± 3 M^{-1} ($r^2 > 0.92$). This value is significantly smaller than the K_{Li} value obtained for heterotrimeric transducin. The changes in ^7Li T_2 values were also used to generate Li^+ binding constant to the Mn^{2+}-derivative and the calculated value was 35 ± 4 M^{-1} ($r^2 > 0.96$). However, NMR T_2 values are subjected to larger error and therefore they are not routinely used to determine binding constants.

Table 16. ^{7}Li T_1 measurements of Mg^{2+}-bound $rG_i\alpha_1$-GDP in the presence of varying amounts of Mg^{2+}

$[Li^+]$ / mM	$[Mg^{2+}]$ / mM	T_1 / s
10	0	11.71 ± 0.31
	0.5	12.99 ± 0.27
	3	15.21 ± 1.01
	10	14.72 ± 0.30

All samples contained 0.34 mM Mg^{2+}-bound $rG_i\alpha_1$-GDP in 50 mM Tris-Cl buffer at pH 7.9. ^{7}Li T_1 measurements were conducted at 20 ± 1 °C in a 5 mm probe.

Figure 20. ESR spectra of Mn^{2+} free (B) and Mn^{2+} bound to $rG_i\alpha_1$ (A). Spectra were recorded using a Q-band 35 GHz Varian spectrometer with a cylindrical cavity at liquid nitrogen temperature. A 90 μM $MnCl_2$ solution was used as a control and the concentration of $rG_i\alpha_1$ and Mn^{2+} in the protein sample were 0.43 mM and 0.39 mM, respectively. Sample volume used for the ESR measurement was 50 μL.

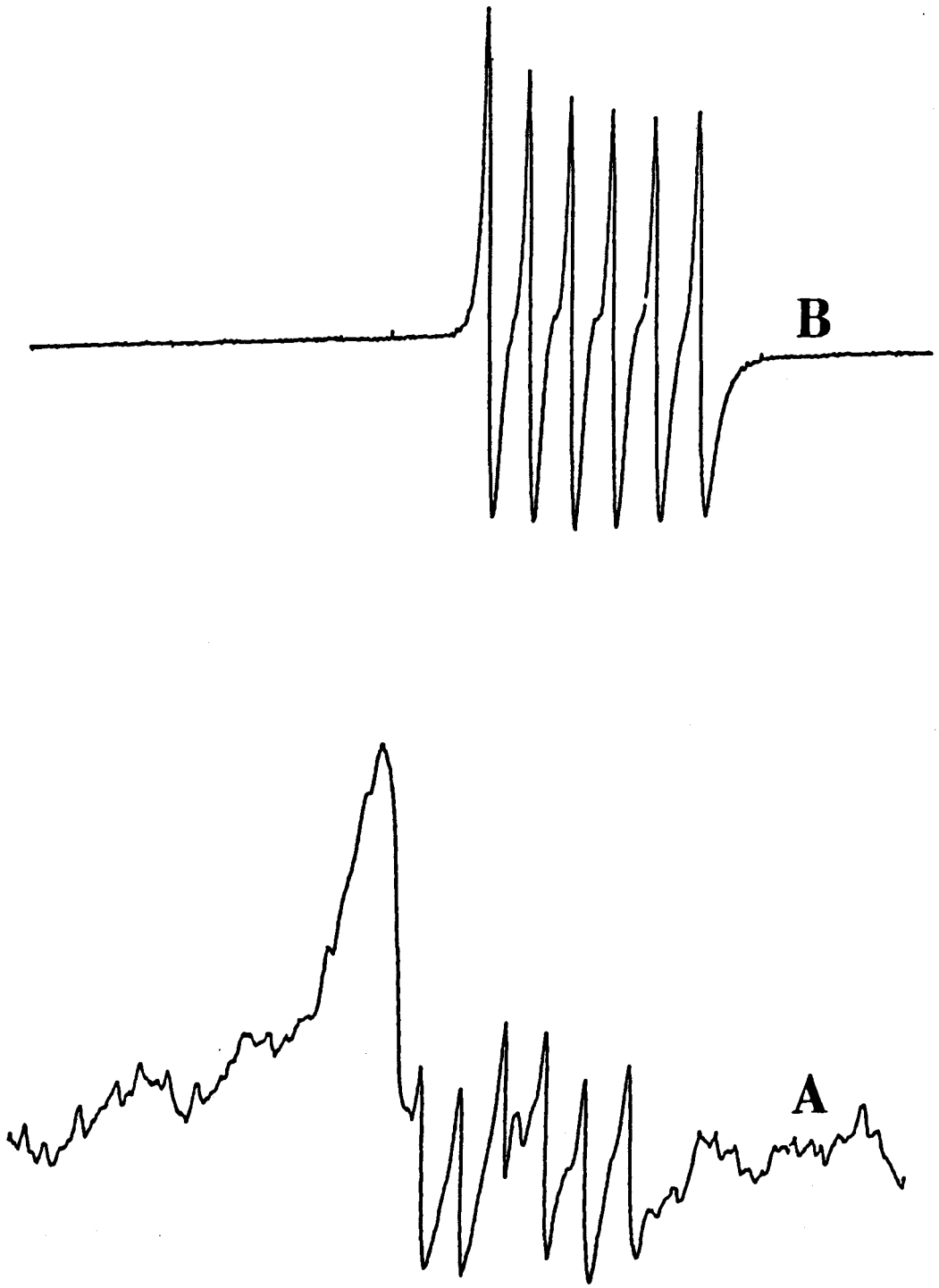
B
A

Table 17. ^{7}Li NMR relaxation measurements of the Mn^{2+}-derivative of $rG_i\alpha_1$-GDP

$[^{7}Li^{+}]$ / mM	T_1 / s	T_2 / s	R (T_1 / T_2)
2	1.26 ± 0.08	0.34 ± 0.03	3.7
8	1.32 ± 0.02	0.49 ± 0.06	2.7
15	1.50 ± 0.06	0.56 ± 0.05	2.7
25	1.61 ± 0.06	0.46 ± 0.08	3.5
50	1.78 ± 0.07	0.65 ± 0.04	2.7
100	1.99 ± 0.19	0.80 ± 0.03	2.5
500 (Free)	2.46 ± 0.07	1.17 ± 0.04	2.1

The concentration of Mn^{2+} derivative of $rG_i\alpha_1$-GDP used in this experiment was 0.4 mM. About 90% of the Mn^{2+} in the NMR sample was found to be bound to $rG_i\alpha_1$ by ESR. The NMR experiment was conducted at 20 ± 1 °C in a 5 mm probe. K_{Li} was calculated from both T_1 and T_2 values using the James-Noggle plot and it was found to be 32 ± 3 M^{-1} (n=2, $r^2 > 0.92$) and 35 ± 4 M^{-1} (n=2, $r^2 > 0.96$), respectively.

IV.2.3. ^{31}P NMR Chemical Shift Measurements with Mg^{2+}-Bound $rG_i\alpha_1$ in the Inactive Conformation

^{31}P NMR spectrum of the Mg^{2+}-bound $rG_i\alpha_1$ in the GDP bound conformation is shown in Figure 21. As in free GDP solution, two ^{31}P NMR resonances, one for the α and the other for the β-phosphate, were obtained for the GDP bound to the protein. However, the signals were very broad and this was due to GDP being in the bound state and also due to the sample being very viscous due to the presence of a high concentration of protein. Overnight accumulations were done to obtain good signal to noise and during long NMR acquisition time there was no hydrolysis of the bound GDP; the absence of an additional ^{31}P NMR resonance downfield to the β-phosphate resonance supports the above observation. The insert of Figure 21 shows the ^{31}P NMR spectrum obtained for $rG_i\alpha_1$.GDP sample spiked with 1 mM GDP. The chemical shifts for the α- and β-phosphate resonances of free GDP were at -4.6 and -9.0 ppm, while the bound GDP resonances appeared at -0.8 and -7.4 ppm. The above observation indicates that the free and bound GDP do not exchange. This behavior is consistent with the published report (Higashijima et al., 1991).

The ^{31}P NMR δ value is sensitive to metal ion addition and we and others have previously explored this technique to investigate metal ion binding and competition (Mota de Freitas et al., 1994). The ^{31}P NMR δ values as well as the line widths at half heights are sensitive to metal ion addition and the values obtained for $rG_i\alpha_1$-GDP upon Li^+ and Mg^{2+} addition are shown in Table 18. The addition of 100 mM LiCl to the GDP-bound $rG_i\alpha_1$ sample caused the $\alpha\beta$ separation to increase from 6.63 to 6.70 ppm; when 0.1 mM Mg^{2+} was added to the sample containing 100 mM LiCl, the $\alpha\beta$ separation increased from 6.70 to 6.88 ppm. The linewidths at half heights also increased with the metal ion addition. However, a free GDP solution (0.6 mM) under the sample experimental conditions gave an $\alpha\beta$ separation of 4.38 ppm when it

Figure 21. ^{31}P NMR spectrum of GDP-bound $rG_i\alpha_1$. The sample contained 0.5 mM $rG_i\alpha_1$.GDP in HED (D_2O) buffer. The spectrum was recorded at room temperature with sample spinning at 16 Hz in a 5 mm NMR probe. The ^{31}P NMR δ is expressed relative to an external reference, 85% orthophosphoric acid. A line broadening of 20 Hz was applied to improve the signal to noise of the spectrum. Insert shows the spectrum obtained for a mixture of free and GDP bound to $rG_i\alpha_1$ and the concentration of free GDP in the protein sample was 1 mM. The assignment of the phosphate resonances are indicated and the subscript f and b refer to GDP-free and GDP-bound forms, respectively.

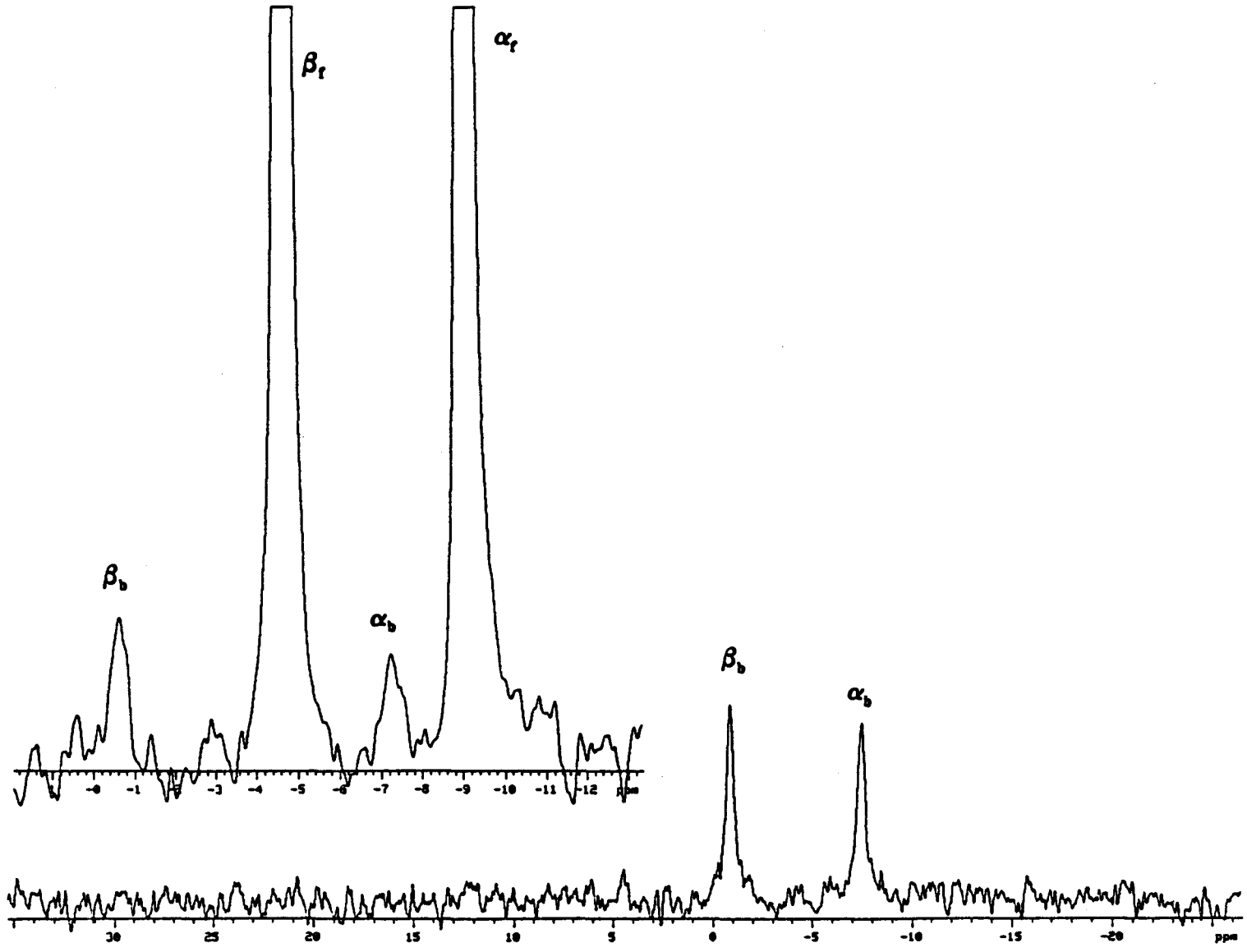
β_f
α_f
β_b
α_b
β_b
α_b
-0 -1 -2 -3 -4 -5 -6 -7 -8 -9 -10 -11 -12 ppm
30 25 20 15 10 5 0 -5 -10 -15 -20 ppm

Table 18. ^{31}P NMR chemical shifts and linewidths of the GDP-bound $rG_i\alpha_1$

	δ (ppm)		$\delta_{\alpha\beta}$ (ppm)	Linewidth (Hz)	
Sample	β	α		β	α
w/o metal ions	-0.80	-7.43	6.63	68.5	77.1
w/ 100 mM Li^+	-0.67	-7.36	6.70	78.2	101.4
w/ 100 mM Li^+ + 0.1 mM Mg^{2+}	-0.63	-7.51	6.88	122	88.0

All samples contained 0.5 mM $rG_i\alpha_1$ in 0.5 mL of HED (D_2O) buffer at pH 7.9. ^{31}P NMR spectra were recorded at room temperature in a 5 mm probe using a VXR-400 NMR spectrometer. The reported δ values are referenced relative to 85% orthophosphoric acid resonance.

contained no metal ions and this value is comparable to the published report (Rong et al., 1992). Under the same experimental conditions, the αβ separation obtained for free GDP (4.38 ppm) is significantly lower than the value obtained for GDP bound to $rG_i\alpha_1$ (6.63 ppm).

IV.2.4. Preliminary ^{19}F NMR Studies of the Transition State Analog of $rG_i\alpha_1$

It was known that the addition of NaF and $AlCl_3$ in the presence of Mg^{2+} transforms the inactive GDP bound conformation of G_i into a transition state analog wherein the AlF_4^- group mimics the γ-phosphate of the GTP; this transition analog provides a good system to understand the active-GTP bound conformation of G_i. When excess AlF_4^- is added the free and the bound F^- resonances are in slow exchange in the ^{19}F NMR time scale giving rise to two signals. As the ^{19}F NMR has a wide δ range the two signals are well resolved. For G_o and G_s, the ^{19}F NMR results indicated two well separated signals for the free and bound AlF_4^-. In this study ^{19}F NMR of the transition state analog of $rG_i\alpha_1$ was used to see if added Li^+ had any effects on the bound F^- signal (Figure 22). ^{19}F NMR spectra of identical samples without protein were also measured and they are presented in Figure 23. Addition of up to 100 mM LiCl changed the δ value of the free F^- resonance by 1.4 ppm (Table 19); however, the δ value of the bound signal changed by about 0.1 ppm and this change was not significant. The area of the bound signal decreased while the area of the free signal increased to a small extent. Addition of LiCl caused the bound signal to broaden. However, there was no clear trend in linewidths as a function of LiCl concentration. For the control sample without protein containing the same amounts of NaF, $AlCl_3$, and $MgCl_2$, the δ value also changed by 1.5 ppm with the addition of 100 mM LiCl.

Figure 22. ^{19}F NMR spectra of Mg^{2+}-bound transition state analog of $rG_i\alpha_1$ titrated with varying amounts of LiCl. All samples contained 0.3 mM $rG_i\alpha_1$ in HED (D_2O) buffer containing 2.5 mM NaF, 3 mM $MgCl_2$, 0.3 mM $AlCl_3$ titrated with (A) 0, (B) 10, (C) 50, and (D) 100 mM LiCl. All spectra were recorded at 21 ± 1 °C in a 5 mm probe. The symbols f and b stands for free and bound F^-, respectively.

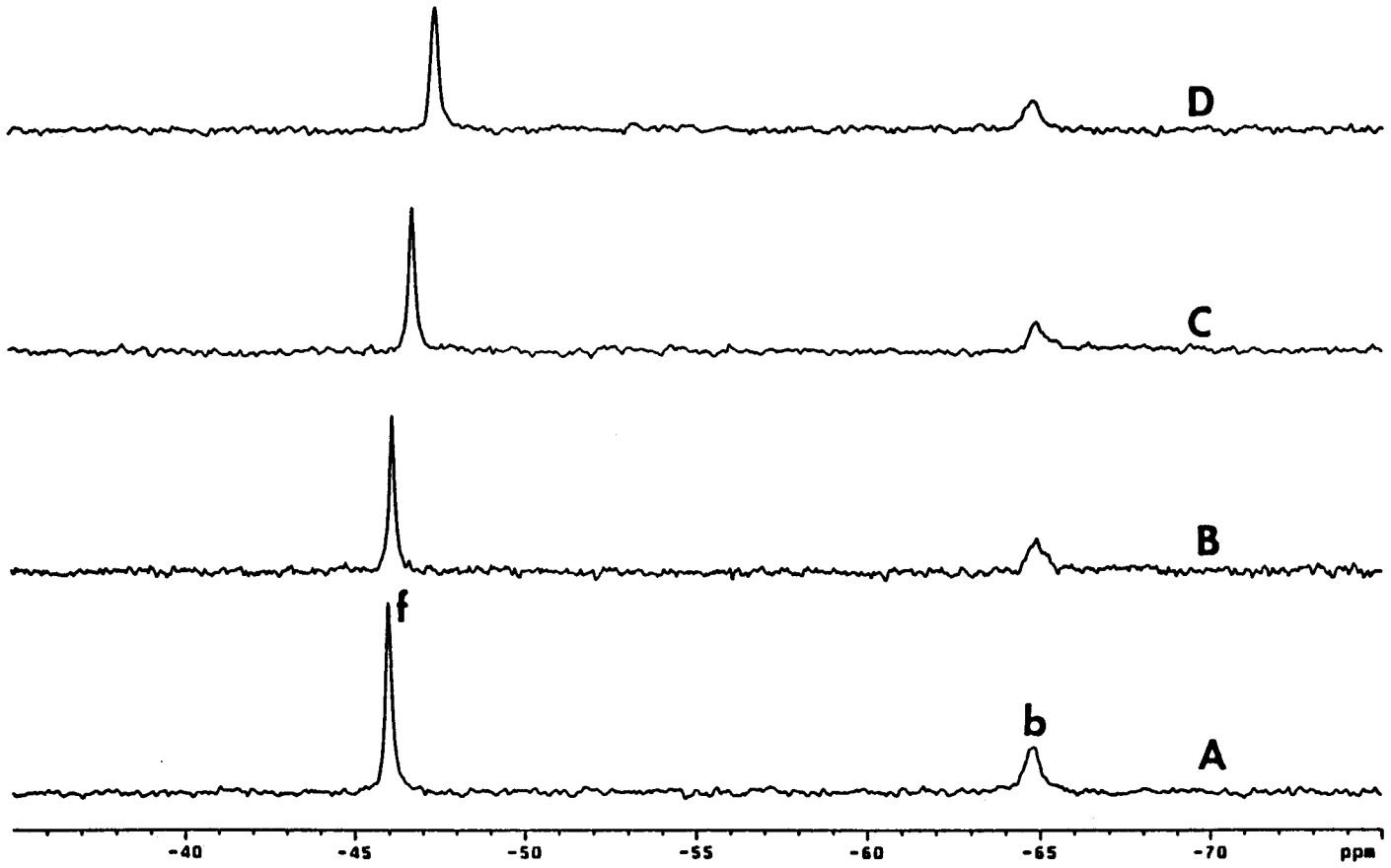
D
C
B
f
b
A
-40
-45
-50
-55
-60
-65
-70
ppm

Figure 23. ^{19}F NMR spectra of a control sample without $rG_i\alpha_1$ titrated with varying amounts of LiCl. All samples contained 0.3 mM $rG_i\alpha_1$ in HED(D_2O) buffer containing 2.5 mM NaF, 3 mM $MgCl_2$, 0.3 mM $AlCl_3$ titrated with (A) 0, (B) 50, and (C) 100 mM LiCl. All spectra were recorded at 21 ± 1 °C in a 5 mm probe.

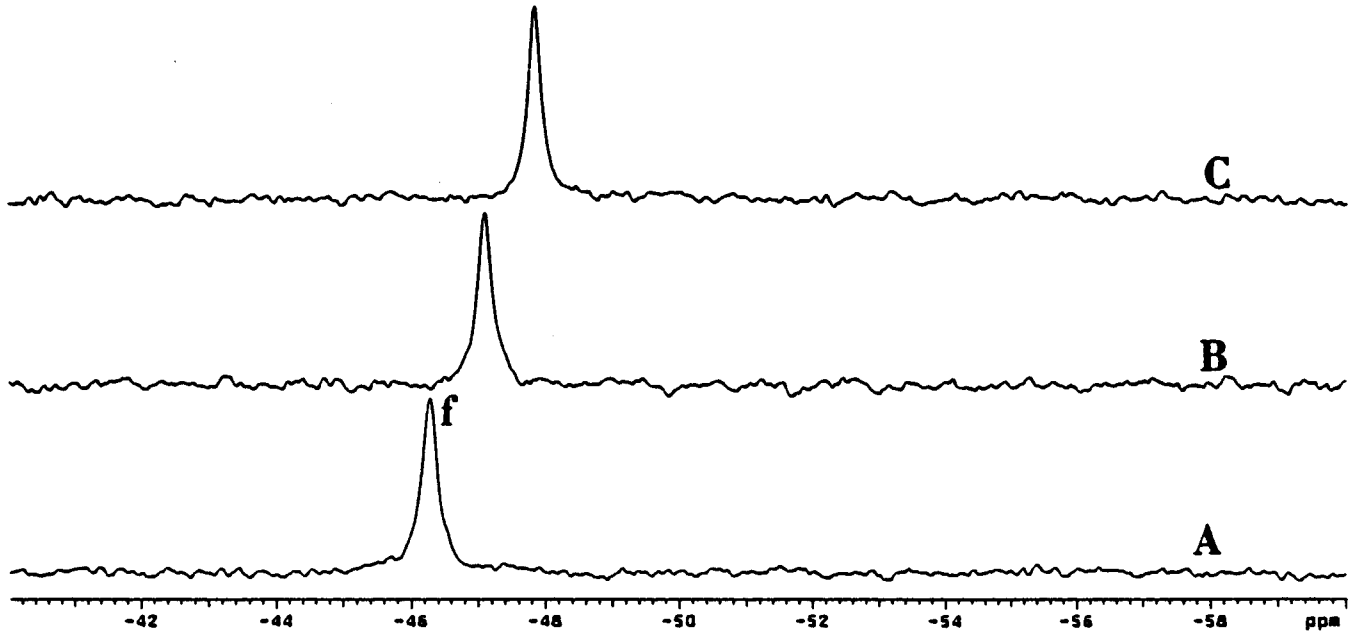
C
B
f
A
-42
-44
-46
-48
-50
-52
-54
-56
-58
ppm

Table 19. ^{19}F NMR chemical shifts, areas and linewidths as a function of added LiCl

Sample	$[^7Li^+]$ / mM	δ (ppm) f	δ (ppm) b	Area (%) f	Area (%) b	Linewidth (Hz) f	Linewidth (Hz) b
$rG_i\alpha_1$.GDP-AlF_4^-	0.0	-46.0	-64.8	64	36	51	165
	10.0	-46.2	-64.9	67	33	46	193
	50.0	-46.7	-64.9	69	31	50	141
	100.0	-47.4	-64.7	70	30	80	176
Without $rG_i\alpha_1$	0.0	-46.3	---	85.1	---	72	---
	50.0	-47.1	---	71.7	---	66	---
	100.0	-47.9	---	78.2	---	57	---

All spectra were recorded using a Varian unity 400 NMR instrument. All samples were maintained at 21 °C in a 5 mm NMR probe. All samples with protein contained 0.3 mM $rG_i\alpha_1$ in HED(D_2O) buffer with 2.5 mM NaF, 3 mM $MgCl_2$, 0.3 mM $AlCl_3$ titrated with LiCl. Control samples without $rG_i\alpha_1$ had the same sample composition except that $rG_i\alpha_1$ was not added.

CHAPTER V

DISCUSSION

V.1. Competition Between Li^+ and Mg^{2+} for the Phosphate Groups in ATP, Human RBC Membranes and Phospholipids

Lithium and magnesium ions have similar ionic radii and there exists a "diagonal relationship" between these elements in the periodic table; as a result, the chemistry of lithium ion often resembles that of magnesium ion. Hence competition between these two ions could occur. Previous reports from our research group have shown evidence for competition between Li^+ and Mg^{2+} ions for Mg^{2+}-binding sites in biomolecules (Abraha et al., 1991; Mota de Freitas et al., 1994a; Ramasamy & Mota de Freitas, 1989; Rong et al., 1992; 1994). Since Mg^{2+} is a cofactor for several enzymes, displacement of Mg^{2+} by Li^+ from biomolecules can affect several biological processes and a combination of several effects could account for the mode of action of lithium ion in the treatment of manic-depression. Therefore this study was devoted to probing the Li^+/Mg^{2+} competition hypothesis systematically for several biomolecules using multinuclear NMR techniques.

An initial study was conducted with ATP and RBC membranes to confirm that there was competition between Li^+ and Mg^{2+} using low temperature ^{31}P NMR spectroscopy. At room temperature, addition of large concentrations of Li^+ (100 mM) to aqueous solutions containing 5.0 mM Tris-ATP and 0.5 mM $MgCl_2$ caused an increase in the $\delta_{\alpha\beta}$ separation measured by ^{31}P NMR spectroscopy (Abraha et al., 1991); this observation was consistent with metal ion

competition for ATP. Whereas the Mg^{2+}-free and Mg^{2+}-bound β-phosphate ^{31}P NMR resonances of ATP are in the fast-exchange domain at room temperature, they are in slow exchange at around 0 °C (Sontheimer et al., 1986). Besides low temperature, a dilute solution of ATP (about 1 mM ATP) can also slow this exchange and give rise to two separate well resolved signals for the β-phosphate at high field NMR although long accumulation times will be needed (Glonek, 1992).

It was reported (Brown et al., 1993) that, at 0 °C, there was no evidence for competition between Li^+ and Mg^{2+} for ATP, based on the relative changes in the areas of the ^{31}P NMR resonances of the β-phosphate groups of free ATP and Mg^{2+}-bound ATP in aqueous solutions of 5.0 mM NaATP and 2.5 mM $MgCl_2$ in the presence and absence of 2.5 mM LiCl. We also found that, for low concentrations of LiCl (2.5, 10, and 20 mM), there were no appreciable increases in the areas of the Mg^{2+}-free and Mg^{2+}-bound β-phosphate ^{31}P NMR resonances of 5.0 mM NaATP (Table 4). This could be due to very high concentration of Mg^{2+} used in this study. However, either in the presence or in the absence of RBC membrane, we observed significant increases in the $[Mg^{2+}]_f$ values for 3.0 mM Na-ATP solutions containing 1.0 mM $MgCl_2$ and $[Li^+]_t \geq 20$ mM (Table 3). Clearly, a large excess of Li^+ over Mg^{2+} is required to make it possible to detect, by ^{31}P NMR spectroscopy, competition between Li^+ and Mg^{2+} for phosphate groups in ATP in the absence of RBC membrane (Figure 6). This is probably due to a difference in charge between lithium and magnesium ions. The extent of competition is greater when ATP samples contain RBC membranes as shown by the increase in area ratio with the addition of LiCl (Table 3). The presence of RBC membranes provide additional binding sites for the Mg^{2+} that is being displaced by Li^+ and thus the extent of competition is greater when the samples contain membranes.

In order to identify the major Li^+ binding sites in RBCs, Rong and co-workers (1993) used

^{7}Li NMR relaxation measurements to measure the R ratio (T_1/T_2) for several RBC components. A larger R ratio was observed for Li^+-treated RBCs (about 20) and for RBC membranes (about 50) and these R ratios were also sensitive to LiCl addition. In a free LiCl solution, the ^{7}Li NMR T_1 and T_2 values are very similar yielding an R ratio close to 1. The higher the R ratio, the greater is the interaction between the metal ion and the ligand. For spectrin, ATP, BPG and hemoglobin (regardless of its oxygenation state) the R ratios were very small (close to 2) and they were virtually independent of Li^+ concentration. These results suggested that the inner leaflet of the RBC membrane provides the major binding sites for Li^+. For a 1.5 mM Li^+-containing phospholipid extract from the RBC membrane, the R ratio was 6.2 and this indicated that the phospholipids in the membrane could be responsible for Li^+ binding (Rong et al., 1993).

^{31}P NMR spectrum of the phospholipids extracted from the RBC membrane provide well resolved resonances for each phospholipid when a suitable solvent system is used. Interaction of the phospholipids with the metal ions caused ^{31}P NMR chemical shift changes, signal broadening, signal quenching or a combination of these effects and the changes in δ values were used to identify the phospholipids that interact most strongly with the metal ions. Mg^{2+} titration of a phospholipid mixture containing PA, PS and CL indicated that CL had the highest, and PA the next highest interaction potential for Mg^{2+} (Merchant & Glonek, 1992).

For human RBC membrane phospholipids, addition of up to 2 mM Mg^{2+} caused the δ value of the PS resonance to change by 0.5 ppm and this was the largest change that was observed (Figure 8 and Table 5); the phospholipid PS interacted most strongly with Mg^{2+} with marked broadening of the PS signal upon Mg^{2+} addition followed by quenching of the signal due to excessive broadening. Qualitatively, the signal that disappears first from the phospholipid spectral profile is considered to be interacting most strongly with the added cation. This observation was consistent with Mg^{2+} binding constant determination which was found to be 221

M^{-1} for PS using equation 3. A pure PS sample under identical experimetal conditions was found to bind Mg^{2+} with a binding constant of 279 M^{-1}. However, other phospholipids, such as PC, PE and Sph bind Mg^{2+} weakly (K_{Mg} in the range of 30 - 200 M^{-1}). The binding constants reported were calculated using the amount of Mg^{2+} added to the mixture and not the amount present in the organic phase.

The effect of Mg^{2+} addition on PI could be investigated only by spiking the phospholipid extract sample with known amounts of PI. The amount of PI added to the extract was adjusted so that the mixture contained equal amounts of PI and PS. Mg^{2+} titration caused the PS and PI δ values to change by 0.43 and 0.56 ppm, respectively (Table 6). The Mg^{2+} binding constant to PI was calculated to be 2.1 X 10^3 M^{-1}. This value is significantly higher than the value obtained for the other anionic phospholipid PS. Thus it was found that the anionic phospholipid PI interacted most strongly with Mg^{2+}; PS and Sph were found to bind Mg^{2+} with intermediate affinity while PE and PC interacted very weakly.

Li^+ titration of human RBC membrane phospholipids caused the ^{31}P NMR chemical shift of all phospholipids to change, except for PC, by 0.1 ppm when 17.6 mM LiCl was added (Figure 8B and Table 7). The changes in ^{31}P NMR chemical shift values for increase in Li^+ concentration are very small when compared to the changes observed for Mg^{2+}. This has to do with the charge on the metal ion; with Mg^{2+} being divalent it interacts more strongly. The Li^+ binding constant to PS was calculated to be 191 M^{-1} whereas for the other neutral phospholipids the K_{Li} values were in the range of 0.03 - 117 M^{-1}. Li^+ binding constant to PI and Sph were calculated to be 105 M^{-1} and 117 M^{-1}, respectively. ^7Li titration also revealed that PS binds Li^+ most strongly; Sph and PI were found to have intermediate interaction with Li^+. From the ^{31}P NMR δ data it is interesting to see that in a phospholipid mixture Li^+ shows a preference for PI while Mg^{2+} does not differentiate between PS and PI (Table 6).

The chemical shift of the individual phospholipids are dependent on the amount of water and methanol in the chloroform layer of the sample. Overlapping resonances in a specific solvent system can be resolved by varying the solvent composition (Branca et al., 1995). If the solvent composition is varied, the chemical shift of the phospholipids will be different and hence the same solvent composition should be maintained all the time to prevent changes in δ values due to solvent composition variations. For all the ^{31}P NMR experiments the solvent composition was fixed constant by dissolving the extracted dried lipid film in chloroform-methanol-0.2 M EDTA reagent in a ratio of 125:8:3. The NMR sample tube was sealed to prevent changes in the solvent composition due to evaporation of the low-boiling solvents such as methanol and chloroform. Instead of carrying out the NMR experiments at 37 °C, all measurements with phospholipids were carried out at 27 °C to minimize the evaporation of the low-boiling solvents.

The aqueous EDTA phase was needed to obtain sharp and well resolved ^{31}P NMR resonances for all the phospholipids (Meneses & Glonek, 1988). As all the resonances fall within a 1 ppm chemical shift range, the presence of paramagnetic ions or the improper solvent system, including the lack of the aqueous EDTA phase, will cause broadening of the signals and several resonances can overlap (Edzes et al., 1992). However prior to metal ion addition, the aqueous EDTA phase was removed as much as possible to prevent EDTA chelation of the added metal ions. Before metal ion titration, ^{31}P NMR spectra were recorded before and after the removal of the aqueous EDTA layer, to see if the δ value changes after the removal of the aqueous phase. However, no significant change in δ value was noticed after the removal of the aqueous phase and this could be because complete removal of the aqueous phase was not possible.

The binding constants reported above for the phospholipids are approximate and only represent the trend observed. This is because the phospholipid extract sample used for metal ion

titration contained two phases, the organic as well as the aqueous EDTA layer. Although prior to metal ion addition attempts were made to remove the EDTA layer, complete removal could not be achieved. Hence the amount of metal ion in the organic phase was different from the amount added as some amount of metal ions were chelated by the EDTA or more soluble in the aqueous phase. Several methods were used to identify the amount of metal ions in the organic phase. Atomic absorption spectroscopy was used to quantify Mg^{2+} concentration in the organic layer by taking an aliquot from the organic layer of the NMR sample. As the solvent system has chloroform the flame was not very stable and the readings obtained were not reliable. Attempts were also made to evaporate the solvent and dissolve the residue in water. The presence of the phospholipids resulted in a suspension instead of a solution. AA results however indicated that only about 50-60% of the Mg^{2+} added was going into the organic layer. AA with flame source was not able to detect Li^+ as an aliquot from the NMR sample was diluted to obtain enough sample. ^7Li NMR was also used to see if it could be used to determine Li^+ in the organic layer. Two resonances were observed for Li^+ in the organic layer. However, when the aqueous phase was eliminated or when there were no phospholipids in the biphasic solvent mixture only one resonance was obtained for Li^+. Previous study probing metal ion interaction with the phospholipids using NMR methods could not determine the amount of metal ion in the organic phase or the binding constants (Merchant & Glonek, 1988); this could be due to the difficulties involved in quantification.

To see if there is competition between Li^+ and Mg^{2+} for the phospholipid extract the phospholipid extract sample was titrated with 0.5 mM Mg^{2+}. Addition of Mg^{2+} caused all the resonances, except PC, to move upfield with the effect being maximum for PS resonance with a 0.2 ppm shift (Figure 9). When titrated with increasing amounts of LiCl the resonances of this sample moved downfield and this effect was observed clearly for the anionic phospholipid PS.

The signal of PS also sharpened and this we believe is due to Li^+ displacing Mg^{2+} from the phosphate head group of the phospholipids. ^6Li NMR T_1 measurements were conducted with the phospholipid extracts both in the presence and absence of $MgCl_2$ (Figure 10). The T_1 values were sensitive to LiCl addition in both samples and this is consistent with ^{31}P NMR results indicating that the phospholipids interact with Li^+. However the samples with Mg^{2+} gave higher T_1 values than the samples without Mg^{2+} at the same Li^+ concentration. This increase in T_1 values in the presence of Mg^{2+} is due to increase in the free Li^+ concentration, and this we believe is due to Mg^{2+} and Li^+ occupying the same binding site. Mg^{2+} is presumably displacing Li^+ from the phosphate head group of the phospholipids. Both the ^{31}P NMR chemical shift measurements and the ^6Li T_1 measurements provide evidence for Li^+/Mg^{2+} competition.

For ^7Li or ^6Li NMR relaxation measurements, the extracted dried phospholipid film was dissolved in a chloroform-methanol solvent mixture in a ratio of 5:2. The aqueous EDTA phase was eliminated since there is only one resonance in ^7Li or ^6Li NMR and the absence of aqueous EDTA phase will affect all the samples to the same extent. Also, since there is no aqueous phase, the amount of Li^+ is the amount that is added and therefore this eliminates the need to quantify the amount of metal ion in the organic phase. The Li^+ binding constant to the phospholipid extract without Mg^{2+} was calculated to be 45 ± 5 M^{-1} ($n=2$, $r^2 > 0.90$) using the James-Noggle plot (Table 10). This value is lower than the binding constant determined for the unsealed RBC membranes which is close to 200 M^{-1} (Rong et al., 1993). However, the James-Noggle plots do not provide any information regarding the number of binding sites.

Although the phospholipids provide major binding sites for the metal ions, the removal of the lipids from the membrane skeleton could have decreased their affinity for the metal ions. This prompted us to characterize the role played by the cytoskeleton towards metal ion binding and competition. To identify if the cytoskeleton underlying the lipid bilayer plays any significant

role in metal ion binding and competition, NMR studies were conducted with unsealed and cytoskeleton-depleted membranes. ^{7}Li NMR T_1 measurements were conducted for unsealed and cytoskeleton-depleted human RBC membranes titrated with increasing amounts of LiCl (Figure 11). Removal of the cytoskeleton did not affect the sensitivity of the ^{7}Li T_1 values to the changes in LiCl concentration and this indicated that the removal of the cytoskeleton did not prevent Li^+ binding to the membranes. The Li^+ affinity constant to the cytoskeleton-depleted membrane was found to be two-fold higher than the value determined for the unsealed membranes. This increase in Li^+ affinity for the cytoskeleton-depleted membranes could be due to exposure of the anionic phospholipids. The inner leaflet of the RBC membranes contain greater percentage of the negatively charged phospholipids (PI and PS) and the removal of the spectrin-actin network could allow for easy interaction between Li^+ and the anionic phospholipids in the lipid bilayer. The competition between Li^+ and Mg^{2+} (Table 11) as well as the competition between Li^+ and Na^+ was found to be present even after the removal of the cytoskeleton. Hence it was clear that the cytoskeleton had no major role in Li^+ binding as well as in Li^+/Mg^{2+} or Li^+/Na^+ competition. Since it is not possible to observe MQF signal for ^{7}Li, SQ T_1 measurements were used in this study.

The contribution of the cytoskeleton towards alkali metal ions, in particular, Li^+ and Na^+ binding was studied in detail using a ^{23}Na MQF NMR spectroscopy. A free NaCl solution does not provide a MQF NMR signal while addition of any substance that can bind Na^+ will give rise to MQF NMR signal. The observance of the MQF NMR signal is due to motional restriction of the Na^+ and thus MQF ^{23}Na NMR provides a great tool to address this question of cytoskeleton involvement towards Li^+ and Na^+ binding. Unsealed RBC membranes containing 5 or 50 mM NaCl and cytoskeleton-depleted membranes with 5 or 50 mM NaCl were used in this study. When an unsealed RBC membrane is in a low ionic strength medium (5 mM NaCl),

cytoskeleton detaches itself from the bilayer (Shinar et al., 1993). However, at 50 mM NaCl concentration, the unsealed membrane has the cytoskeleton attached to the lipid bilayer. Thus these four different membrane samples provide a good system to compare and understand the contribution of the cytoskeleton towards Li^+ and Na^+ binding.

The DQF signal arises from the forbidden transition with a selection rule $\Delta m = \pm 2$. This is a weak transition and hence a high field NMR or long accumulation time will aid in the observation of this signal. Since ^{23}Na T_1 values are in the millisecond range, usually between 40 and 70 ms, the delay time required for the complete relaxation of the nuclei is extremely small and this is one of the reason why no one has ever observed a ^7Li MQF NMR signal. The ^{23}Na DQF NMR signal intensity variation with the creation time of the unsealed membrane sample containing 50 mM NaCl is shown in Figure 13. The observance of the negative signal is due to the formation of the second rank tensor $T_{2\,1}$ which arises when the quadrupolar interaction between the nuclei and the surrounding is not averaged to zero (Eliav et al., 1992). The formation of the second or even ranked tensor which results in the appearance of a broad negative DQF signal has been shown to provide a good method to detect anisotropic motion of bound ions in biological systems. Removal of the cytoskeleton of the unsealed membranes at 50 mM NaCl caused the even ranked tensor $T_{2\,1}$ to vanish and the DQF spectra exhibited a sharp positive resonance resulting from the odd ranked tensor $T_{3\,1}$ which is indicative of the isotropy of the Na^+ ion motion in the membrane system. In human RBCs, anisotropic motion of the intracellular Na^+ ion was found to be due to their interaction with the plasma membrane and to depend on the integrity of its cytoskeleton network (Knubovets et al., 1996; Shinar et al., 1993). Variation of the ionic strength of the medium also affects the anisotropic motion dramatically by affecting the cytoskeletal spectrin dimer/tetramer equilibrium (Knubovets et al., 1996), and this is the reason for the disappearance of $T_{2\,1}$ when the NaCl concentration was 5 mM in the

unsealed membrane samples.

The NMR TQF signal arises also due to the forbidden transition with a selection rule $\Delta m = \pm 3$. However the TQF NMR is much more sensitive than the DQF NMR. The theoretical signal intensities of the TQF NMR spectra are 50% greater than the DQF NMR signal intensities for same samples under identical experimental conditions (Jaccard et al., 1986). Hence TQF ^{23}Na NMR is more popular and widely used in *in vivo* studies. The TQF NMR signal of the unsealed membranes containing 50 mM NaCl does not give rise to the overlapped antiphase resonances (Figure 14). This is because TQF spectra give only the isotropic signal resulting from $T_{3\ 1}$, whose maximum intensity is affected by ionic strength and the presence of the cytoskeleton network (Shinar et al., 1993). Thus this TQF NMR can not distinguish between isotropic or anisotropic behavior of the ^{23}Na nuclei in the biological system. The TQF signal intensity decreased with LiCl addition and this was due to the displacement of Na^+ by Li^+ from the Na^+ isotropic binding sites of the membrane (Figure 15). The dependence of the extent of competition between these two ions on the ionic strength, the affinity of the lithium ion to the membrane and the presence and integrity of the cytoskeleton is expressed by the parameter ΔA (Table 12). At the same Li^+/Na^+ ratio the extent of competition is higher at 50 mM NaCl than at 5 mM NaCl. This could be due to the saturation of the membrane binding sites by Na^+ ions at this high concentration, as Li^+ addition causes immediate displacement since no vacant sites are available for Li^+ to bind. However, the percentage of quenching is comparable in intact and cytoskeleton-depleted membranes, indicating clearly that the cytoskeleton contributes very little towards Li^+ and Na^+ binding at the isotropic sites (Table 12).

There is a strong indication of the presence of non-equivalent Na^+ binding sites in slow chemical exchange (Shinar et al., 1993). This binding site heterogeneity is reflected by the dependence of the TQF and DQF signal linewidths on the creation time (Figure 17). Increasing

Li^+ concentrations caused the limiting linewidth value at high creation time to decrease substantially in intact membranes, indicating at high Li^+/Na^+ ratios a preferential competition of Li^+ for the more anisotropic Na^+ binding sites. The absence of this effect in the cytoskeleton-depleted membranes reflects the role of the cytoskeleton in promoting the Li^+/Na^+ competition for the anisotropic sites. This observation was supported by DQF measurements of the unsealed RBC membranes at 50 mM NaCl. The DQF measurements of this sample indicates that Li^+ ions replace Na^+ ions preferentially at the isotropic membrane sites, and only at higher concentrations replaces the anisotropic sites. This could possibly due to the isotropic sites being low affinity and the anisotropic sites being of high affinity sites for cations.

Our results from ^{23}Na MQF NMR experiments with the unsealed and the cytoskeleton-depleted membranes demonstrates that the cytoskeleton plays only a small role towards Na^+ and Li^+ binding as well as Na^+/Li^+ competition for RBC membranes. However, the presence of the cytoskeleton is responsible for the anisotropic motion of the bound Na^+ ions in the unsealed RBC membranes, leading to the presence of isotropic and anisotropic sites. The cytoskeleton network affects the extent of Li^+ competition at the anisotropic, high affinity sites. The above information could not have been obtained using SQ relaxation measurements.

V.2. Competition between Li^+ and Mg^{2+} for the metal binding domain in G Proteins

Lithium ion was shown to block the activities of G_i and G_s, the two G proteins that inhibit and stimulate the enzyme adenylate cyclase respectively (Avissar at el., 1988). It was proposed by these authors that G proteins may provide a common site for both the antimanic and antidepressant therapeutic effects of lithium ion. Several recent studies have also provided evidence for the hyperfunctional G proteins or abnormal amounts of G proteins in the membranes of bipolar patients relative to those present in normal individuals. Since these G proteins require

Mg^{2+} for their structure and function, Li^+ could compete at the Mg^{2+}-binding sites. Avissar and co-workers (1991) have also found evidence for competition between Li^+ and Mg^{2+} ions for low-affinity Mg^{2+}-binding sites in G proteins present in membranes from rat cerebral cortex. Hence a systematic study of Li^+/Mg^{2+} competition hypothesis was conducted using G proteins from different sources by extending the previously established multinuclear NMR methods which were developed for small molecules (Abraha et al., 1991; Mota de Freitas et al., 1994a; Rong et al., 1993).

In our studies, G proteins from two different sources were used. To test the competition hypothesis it is the Mg^{2+}-binding domain that is important. X-ray crystallographic data on transducin and other G_α subunits suggest that the Mg^{2+} binding sites are highly conserved within the superfamily of G proteins (Coleman et al., 1994a; 1994b; Lacal & McCormick., 1993; Lambright et al., 1994). The amino acid side chains that are involved in the Mg^{2+} coordination are the same for transducin and G_α (Figure 24). However, outside the Mg^{2+}-binding domain there is only 68% homology between the α-subunit of transducin and $rG_i\alpha_1$. Hence to investigate the Li^+/Mg^{2+} competition hypothesis G protein from any source could be used. For our studies transducin from bovine retinas and $rG_i\alpha_1$ expressed in *E.Coli* were chosen. The criterion for choosing these two systems was easy isolation and purification techniques involved in obtaining milligram amounts of protein within a short period of time. Since for each NMR experiment 10-15 mg of protein was needed, systems that allow easy and quick purification techniques were used. The isolation and purification of His_6-$rG_i\alpha_1$ was very fast as it involved a single step Ni^{2+}-NTA affinity column chromatography after which the protein was about 90% pure. This column chromatography was followed by FPLC to obtain about 30 mg of $rG_i\alpha_1$ within 3-4 days. In about 3 to 4 days, 20-25 mg of transducin could be obtained from bovine retinas.

To address the question of effect of Li^+ on the function of G proteins, comparison of the

Figure 24. Mg^{2+}-binding sites of various G proteins. Magnesium ions are represented by pink circles and the red cross sign indicates the water molecules that are coordinated to Mg^{2+}.

Mg^{2+}-binding Sites of T_α and $G_i\alpha_1$

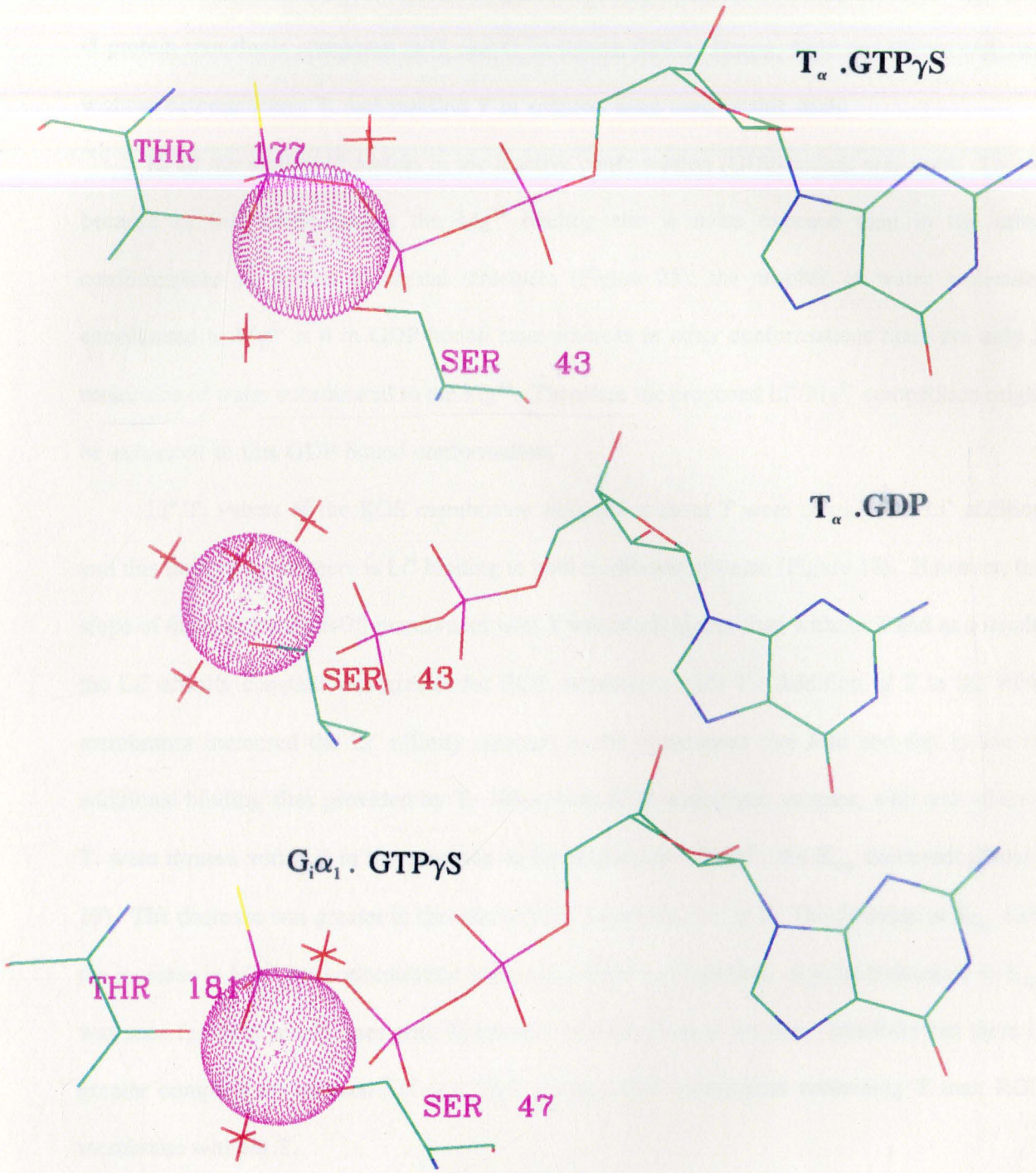

binding properties of Li^+ and Mg^{2+} in purified G protein preparations as well as G proteins embedded in cell membranes were investigated. The ROS membrane contains large amounts of G protein transducin compared to G_i and G_s in human RBCs. Hence, ROS membrane with and without heterotrimeric T, and purified T in solution were used in this study.

In all our studies G protein in the inactive conformation (GDP-bound) was used. This is because in this conformation the Mg^{2+} binding site is more exposed than in the other conformations as shown in crystal structures (Figure 25); the number of water molecules coordinated to Mg^{2+} is 4 in GDP bound state whereas in other conformations there are only 2 molecules of water coordinated to the Mg^{2+}. Therefore the proposed Li^+/Mg^{2+} competition might be enhanced in this GDP bound conformation.

Li^+ T_1 values of the ROS membranes with and without T were sensitive to Li^+ addition and this indicated that there is Li^+ binding to both membrane systems (Figure 18). However, the slope of the plot for the ROS membranes with T was much higher than without T and as a result, the Li^+ affinity constant was greater for ROS membranes with T. Addition of T to the ROS membranes increased the Li^+ affinity constant to the membranes two fold and this is due to additional binding sites provided by T. When both ROS membrane samples, with and without T, were titrated with Li^+ in the presence of fixed amounts of Mg^{2+}, the K_{app} decreased (Figure 19). The decrease was greater in the case of ROS membranes with T. The decrease in K_{app} with the increase in Mg^{2+} ion concentration is due to Li^+/Mg^{2+} competition. A greater decrease in K_{app} was seen for ROS membranes with T; based on this experiment we can conclude that there is greater competition between Li^+ and Mg^{2+} for the ROS membranes containing T than ROS membrane without T.

To quantify the interaction between Li^+ and the heterotrimeric transducin in solution, ^7Li T_1 measurements were conducted using purified T in solution. The ^7Li T_1 values were sensitive

Figure 25. Crystal structure of Mg^{2+}-bound $rG_i\alpha_1$-GDP. The magnesium ion (blue circle) in the inactive conformation is well exposed than in other conformations.

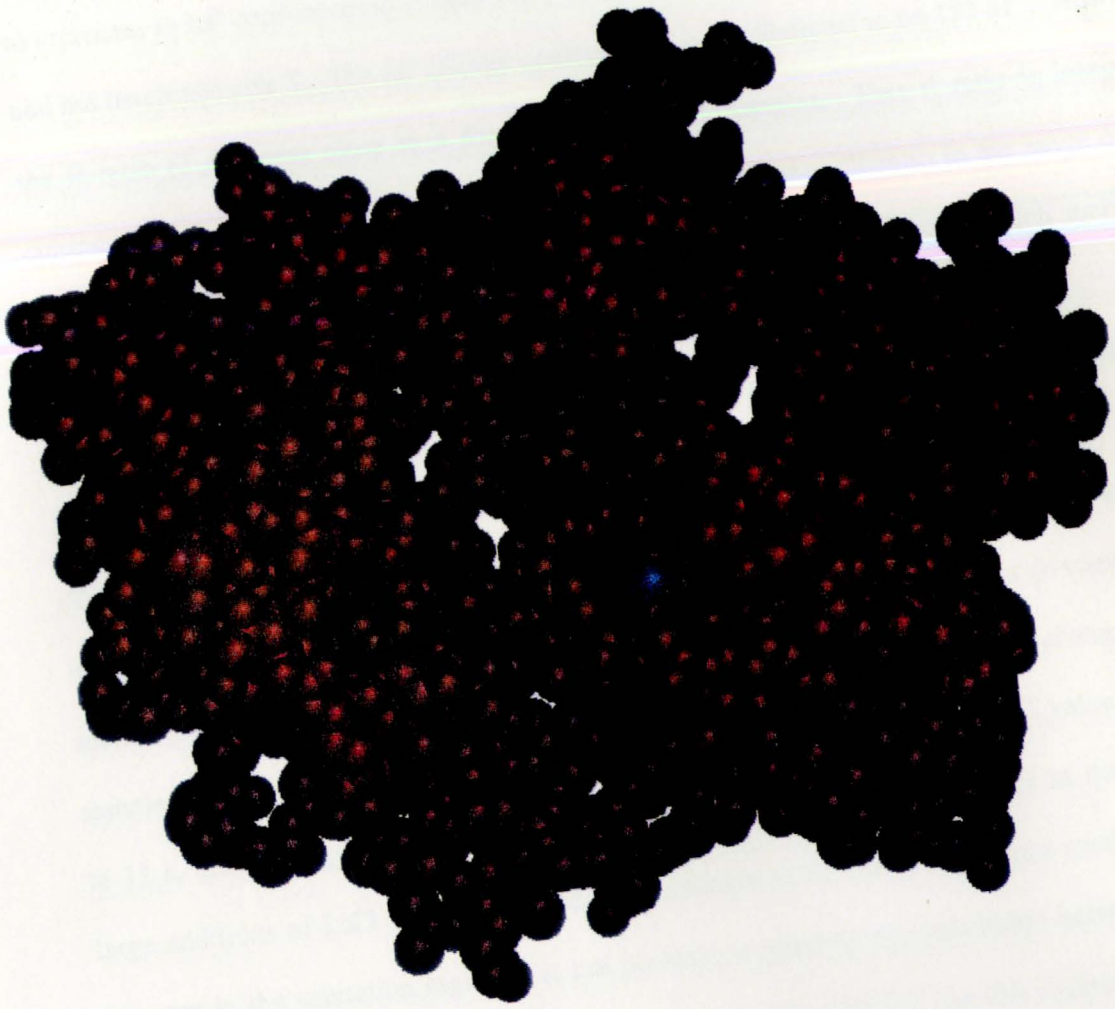

to increases in Li^+ concentration (Table 14). This indicates that there is interaction between Li^+ and the heterotrimeric T. The Li^+ affinity constant to T was calculated to be 122 M^{-1}. However, the R ratio (T_1/T_2) was close to 4 for Li^+ containing T samples. This R ratio is low when compared to the R ratio obtained for Li^+-treated RBC membranes (R ratio in the range of 50). This low R ratio could be due to the high molecular weight of the protein which makes the molecule to tumble slowly.

To identify the contribution of the βγ-complex towards Li^+ binding, Li^+ titrations were conducted with $rG_i\alpha_1$ samples. The ^7Li T_1 values were only slightly sensitive to Li^+ addition (Table 15). The protein concentration was varied from 0.1 - 0.9 mM and the ^7Li T_1 measurements were conducted with increasing amounts of Li^+ at each protein concentration to see if by changing the protein concentration the ^7Li T_1 response to Li^+ addition changed. In all samples the T_1 values were in the saturation range (10 to 14 s). When the ^7Li T_1 values are close to 11 s, the binding sites are saturated with Li^+ and in order to see a change in the T_1 values large additions of LiCl will be required. The changes in T_1 values were very small and since they are in the saturation region it is not possible to quantify the interaction between Li^+ and $rG_i\alpha_1$. The T_2 values were also not very sensitive to Li^+ addition and this indicates weak Li^+ binding. The ^7Li NMR R ratio (T_1/T_2) for all Mg^{2+}-bound $rG_i\alpha_1$ samples were close to 3 and this once again proves that the binding is very weak. These results indicate that the Li^+ affinity for $rG_i\alpha_1$ is very weak and this system might not be good to quantify the interaction.

Introduction of a paramagnetic probe, in this case replacement of bound Mg^{2+} by Mn^{2+} aided in probing and in the quantification of weak Li^+ binding to $rG_i\alpha_1$. The presence of a paramagnetic probe in the protein resulted in shorter relaxation times for bound Li^+ relative to free Li^+ in solution; the T_1 values decreased from 9 s to around 1 s upon replacement with Mn^{2+} (Table 17). The ^7Li NMR T_1 and T_2 values were sensitive to Li^+ addition and they increased

systematically. The Li^+ affinity constant was calculated to be 32 ± 3 M^{-1} ($r^2 > 0.92$, n=2). This is much lower than the value of 122 M^{-1} obtained for heterotrimeric transducin. The decrease in Li^+ affinity for $rG_i\alpha_1$ could be due to the absence of the βγ-complex which could provide additional binding sites.

To investigate if there is competition between Li^+ and Mg^{2+}, Mg^{2+}-bound $rG_i\alpha_1$ containing 10 mM LiCl was titrated with increasing amounts of Mg^{2+}. As the Mg^{2+} concentration increased the ^7Li T_1 values also increased (Table 16). However, when 10 mM Mg^{2+} was added the binding sites were saturated with the Mg^{2+} ions and hence no changes in the T_1 value was observed. This experiment was also conducted at different Li^+ concentrations; the LiCl concentration was fixed at 2 mM and as the Mg^{2+} concentration increased from 0 to 0.1 mM, the ^7Li T_1 values increased from 9.96 to 13.92 s for the protein concentration at 0.9 mM. An increase in ^7Li T_1 values with Mg^{2+} addition is a clear indication that Li^+ and Mg^{2+} bind at the same sites. These results clearly suggest that there is competition between Li^+ and Mg^{2+} for the Mg^{2+} binding sites on the G protein $rG_i\alpha_1$.

NMR relaxation times are sensitive to the presence of paramagnetic ions and therefore extra precaution was taken during dialysis and sample preparations. As the relaxation times are dependent on viscosity of the samples, prior to NMR measurements samples were dialyzed extensively to remove the added glycerol. Suitable buffer compositions for dialysis and NMR samples were determined by carrying out ICP-ES analysis on the NMR samples after the experiments; ideal conditions for sample preparations were deduced in order to maintain the metal ion contaminants to minimal amounts. For ^{19}F and ^{31}P NMR, the water in the protein samples was exchanged with HED (D_2O) buffer to obtain a good lock signal so that chemical shift changes observed are not due to field drift.

^{31}P NMR chemical shift separation between α- and β-phosphate resonances of free and

GDP bound to $rG_i\alpha_1$ are not comparable even when the experimental conditions are identical. This is because the ^{31}P NMR δ values are sensitive to metal ion addition as well as the changes in the torsion angle. Binding of the nucleotide to the protein could have caused the torsion angle as well as the chemical environment to change due to which the $\alpha\beta$ separation values are not comparable. Previous ^{31}P NMR chemical shift studies of ADP and ATP bound to several different proteins indicated that the $\alpha\beta$ separation values are different for free and nucleotide that is bound (Gorenstein, 1984).

The addition of 100 mM LiCl to $rG_i\alpha_1$ sample caused the ^{31}P NMR linewidths to increase and this indicates that there is interaction between Li^+ and $rG_i\alpha_1$ (Table 18). The changes in the chemical shift observed upon metal ion addition does not provide any evidence for competition between Li^+ and Mg^{2+}. However, similar approach was used previously for free GDP in solution and from the changes in δ value observed upon metal ion addition, evidence for Li^+/Mg^{2+} competition was obtained (Rong et al., 1992). Since $rG_i\alpha_1$ contains one mole of Mg^{2+} per mole of protein, it will be interesting to see if reconstituted protein sample with lesser amounts of Mg^{2+} would provide a better system to investigate Li^+/Mg^{2+} competition mechanism using ^{31}P NMR spectroscopy.

The ^{19}F NMR spectrum of the transition analog of $rG_i\alpha_1$ was in slow exchange in the NMR time scale and this allowed for the observation of the bound F^- signal (Figure 22). The LiCl titration caused the δ value of the free F^- resonance to move upfield; however the bound resonance did not change in δ. Addition of 10 mM LiCl caused the bound signal to broaden and this could be because of the bound signal going to an intermediate exchange case in the NMR time scale. If the same sample is run at low temperature it might be possible to get two resonances for the bound signal as the Li^+ complex will be in slow exchange.

Li^+ binding constant to this transition state analog could not be determined using ^7Li NMR

relaxation measurements. To obtain this transition state analog besides NaF and $AlCl_3$, mM amounts of Mg^{2+} are required (Higashijima et al., 1991), which interferes with the ^7Li NMR relaxation measurements. When this sample was titrated with LiCl, the T_1 values were closer to the value obtained for free LiCl in solution (about 20 s) and hence no attempt was made to characterize this transition state analog of $rG_i\alpha_1$. The presence of large amounts of Mg^{2+} (mM amounts) in the NMR samples will increase the observed ^7Li T_1 and T_2 values and further addition of LiCl will not change the relaxation values. Large amounts of Mg^{2+} also interferes with the ^{31}P NMR chemical shift measurements by binding tightly to the phosphate head groups of the nucleotide; in order to see an effect due to Li^+ addition a very large excess of Li^+ over Mg^{2+} might be required as shown in our low-temperature ^{31}P NMR experiments (Table 3 and 4). Hence in our studies often, instead of therapeutically relevant Li^+ concentrations, much higher concentrations of LiCl were used. This is one of the limitations of this technique used in probing Li^+ binding as well as the competition mechanism.

In summary, this study indicated that there is competition between Li^+ and Mg^{2+} for ATP, human RBC membranes, phospholipids and G proteins. This study also identified that the phospholipids PS and PI bind Li^+ and Mg^{2+} most strongly while the neutral phospholipid PC does not contribute towards metal ion binding. This observation provides an explanation for the higher Li^+ binding constants obtained for the RBC membranes from manic-depressive patients undergoing Li^+ therapy as their cell membranes contain a greater percentage of the anionic phospholipids (Mota de Freitas et al., 1994b). Novel ^{23}Na MQF NMR experiments along with established ^7Li NMR relaxation measurements pointed out that the cytoskeleton of RBCs do not contribute significantly toward alkali metal ion binding or the competition mechanism. Multinuclear NMR methods developed for small molecules to probe Li^+ binding as well as Li^+/Mg^{2+} competition were extended to 41 kDa $rG_i\alpha_1$ and the results obtained provide supporting

evidence for competition between Li^+ and Mg^{2+} for G proteins in the GDP bound conformation. However, the Li^+ interaction with G proteins was found to be rather weak with a K_{Li} value in the range of 30 M^{-1} for $rG_i\alpha_1$.

APPENDIX I

DERIVATION OF EQUATION 1

Area of the peak that is due to Mg^{2+}-ATP = β_2

Area of the peak that represents both Li^+-ATP and free ATP = β_1

Chemical shift of free-ATP as well as the Li^+-ATP peak = δ

Mole fraction of Li^+-ATP = X_b'

Mole fraction of Mg^{2+}-ATP = X_b

Chemical shift of the Li^+-ATP resonance saturated with Li^+ = δ_b

Chemical shift of the free ATP peak before Li^+ addition = δ_f

$$\delta = X_b' \, \delta_b + X_f \, \delta_f \qquad (a)$$

where, $X_b' + X_f + X_b = 1$

Equation (a) can be written as $\delta = (1 - X_f - X_b) \, \delta_b + X_f \, \delta_f$ (b)

Since $\beta_1 / \beta_2 = (X_b' + X_f) / X_b$, $X_b = \beta_2 / (\beta_1 + \beta_2)$, in Equation (b) this value can be used.

$$Mg^{2+} + ATP \text{ ----------> } Mg^{2+}\text{-ATP}$$

where $K_\beta = [Mg^{2+}\text{-ATP}] / [Mg^{2+}]_f \, [ATP]_f$ (c)

Rearranging the Equation (c) and dividing the numerator and the denominator with $[ATP]_{total}$, equation (d) is obtained:

$$[Mg_{2+}]_f = X_b / (X_f \, K_\beta) \qquad (d)$$

substituting for X_b and X_f in Equation (d) the following Equation (1) is obtained.

$$[Mg^{2+}]_f = [\beta_2 \, (\delta_b - \delta_f)] / [\beta_1 \, (\delta_b - \delta) - \beta_2 \, \delta] \, K_\beta \qquad (1)$$

APPENDIX II

Use of HPLC to Determine the Phospholipid Composition of Human RBC Membranes

We have used ^{31}P NMR spectroscopy to determine the composition of different phospholipids present in human RBC membranes (Mota de Freitas et al., 1990). This method has been validated against TLC methods for several other systems (Edzes et al., 1992) but not with human RBC membranes. This HPLC study was therefore designed to compare the HPLC method with ^{31}P NMR spectroscopy.

The HPLC method developed for the determination of membrane composition of rat hepatocytes by Kurumi and co-workers (1991) was used. RBC membranes were prepared using the method described in Chapter III and the phospholipids were extracted from 1.5 mL of packed membranes using chloroform-methanol solvent mixture (total volume 21 mL) in a ratio of 2:1 and KCl (10 mL) was used to remove the non-lipid impurities from the organic phase. About 2 mL of the extract was dried by passing a stream of nitrogen gas and the dried lipids were dissolved in 500 μL of dichloromethane. Injection volume for HPLC analysis ranged between 6-10 μL. A Waters HPLC system with a variable wavelength absorbance detector fixed at 203 nm equipped with a TSK Gel Silica 60 column (5 μm particle size; ID, 4.7 mm X 25 cm; Tosoh Co.) was used. The different phospholipids were eluted using a solvent system composed of acetonitrile-methanol-85% phosphoric acid (130:5:1.7) at a flow rate of 1 mL/min.

The HPLC profile obtained is shown in Figure 26. The peak assignments were made by spiking the samples with known pure phospholipids. The HPLC analysis indicates that the human RBC membranes contain 22% PE, 29% PC, 3% PI, 28% PS and 9% Sph. However the literature value (Surgenor, 1974) shows that the human RBC membranes contain 29% PE, 29% PC, 2% PI, 14% PS and 26% Sph. Our ^{31}P NMR phospholipid analysis is consistent with the

Figure 26. HPLC profile of phospholipids extracted from human RBC membranes. The extracted phospholipids were dissolved in dichloromethane and 9 μL was injected into the column and the flow rate used for the separation was 1 mL/min. The mobile phase contained acetonitrile-methanol-85% phosphoric acid in a ratio of 130:5:1.7. The peak S is due to the solvent front and the peak U stands for the unidentified component. The peak assignments are indicated in the chromatogram.

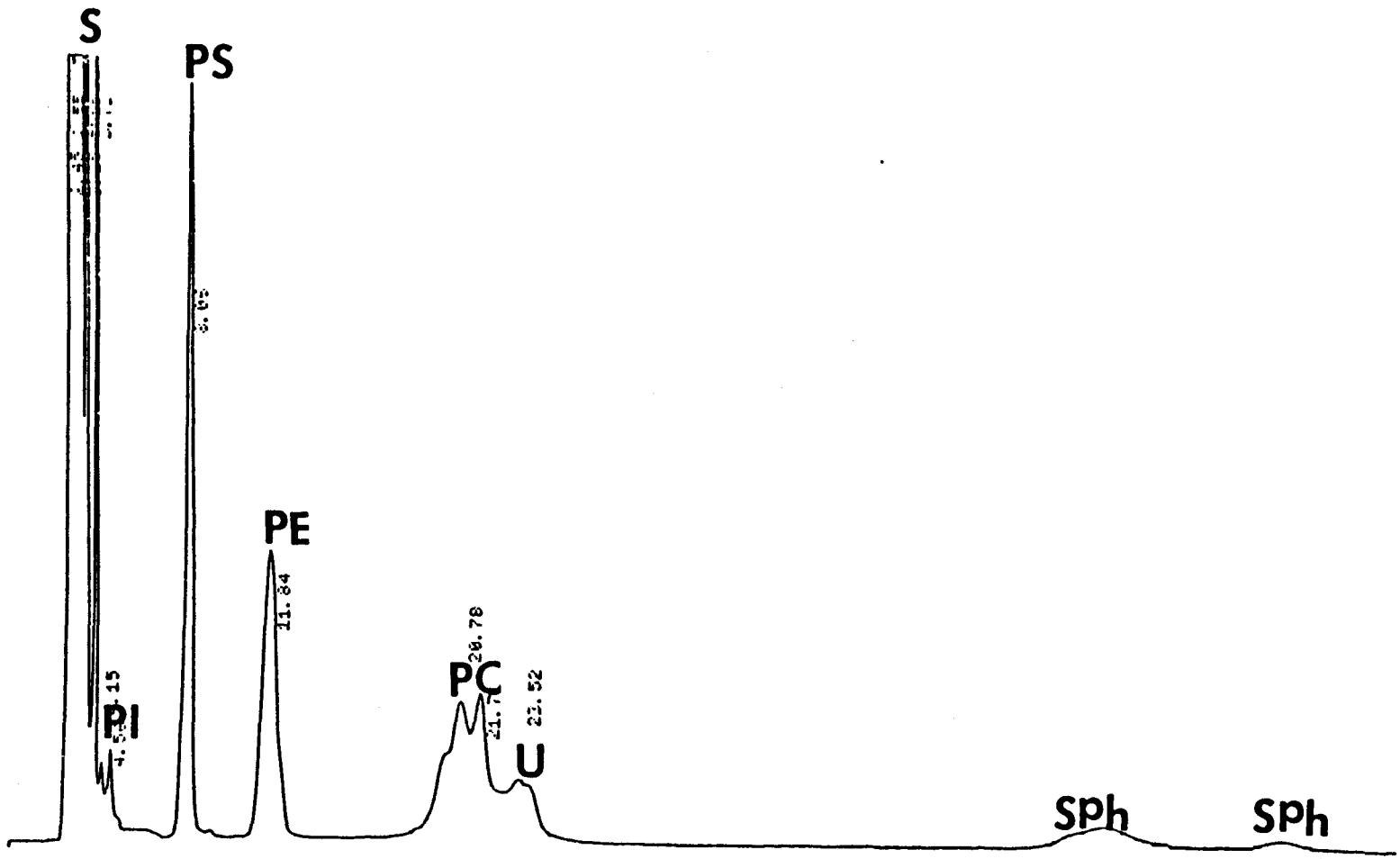
S
PS
PE
PI
PC
U
SPh
SPh
11.84
20.78
22.52

literature reports. However, in our HPLC analysis the percentage of PS was very high while the percentage of Sph was much lower than the reported values. This problem could not be addressed using the reported experimental conditions. No attempts were made to modify the composition of the mobile phase or use a different column.

BIBLIOGRAPHY

Abraha, A., Mota de Freitas, D., Castro, M.M.C.A., Geraldes, C.F.G.C. Competition between Li^+ and Mg^{2+} for ATP and ADP in aqueous solution: a multinuclear NMR study. J. Inorg. Biochem., 1991; 42: 191-198.

Allison, J.H., Stewart, M.A. Reduced brain inositol in lithium-treated rats. Nature, 1971; 233: 267-268.

Avissar, S., Schrieber, G., Danon, A., Belmaker, R.H. Lithium inhibits adrenergic and cholinergic increases in GTP binding in rat cortex. Nature, 1988; 331: 440-442.

Avissar, S., Murphy, D.L., Schreiber, G. Magnesium reversal of lithium inhibition of β-adrenergic and muscarinic receptor coupling to G proteins. Biochem. Pharmacol., 1991; 41: 171-175.

Baraban, J.M., Worley, P.F., Snyder, S.H. Second messenger systems and psychoactive drug action: focus on the phosphoinositide system and lithium. Am. J. Psychiatry, 1989; 146: 10, 1251-1260.

Berridge, M.J., Downes, C.P., Hanley, M.R. Neural and developmental actions of lithium: a unifying hypothesis. Cell, 1989; 59: 411-419.

Bock, J.L., Wenz, B., Gupta, R.K. Changes in intracellular Mg adenosine triphosphate and ionized Mg^{2+} during blood storage: detection by ^{31}P nuclear magnetic resonance spectroscopy. Blood, 1985; 65: 1526-1530.

Bollag, D.M., Edelstein, S.J. in Protein Methods, 1991; pp 50-55, Wiley, New York.

Bourne, H.R., Sanders, D.A., McCormick, F. The GTPase superfamily: conserved structure and molecular mechanism. Nature, 1991; 349: 117-127.

Bramham, J., Riddell, F.G. The effect of lithium therapy upon the composition of the human erythrocyte membrane. J. Inorg. Biochem., 1995; 57: 23-32.

Branca, M., Culeddu, N., Fruianu, M., Serra, M.V. ^{31}P nuclear magnetic resonance analysis of phospholipids in a ternary homogeneous system. Anal. Biochem., 1995; 232: 1-6.

Brown, S.G., Hawk, R.M., Komoroski, R.A. Competition between Li(I) and Mg(II) for ATP binding: A ^{31}P NMR study. J. Inorg. Biochem., 1993; 49: 1-8.

Bull, T.E. Nuclear magnetic relaxation of spin = 3/2 nuclei involved in chemical exchange. J. Magn. Reson., 1972; 8: 344-353.

Bull, T.E., Andrasko, J., Chiancone, E., Forsen S. Pulsed nuclear magnetic resonance studies on ^{23}Na, ^{7}Li and ^{35}Cl binding to human oxy- and carbonmonoxy haemoglobin. J. Mol. Biol., 1973; 73: 251-259.

Burk, S.C., Papastavros, M.Z., McCormick, F., Redfield A.G. Identification of resonances from an oncogenic activating locus of human N-RAS-encoded p21 protein using isotope-edited NMR. Proc. Natl. Acad. Sci. USA, 1989; 86: 817-820.

Burstein, D., Fossel, E.T. Nuclear magnetic studies of intracellular ions in perfused frog heart. Am. J. Physiol., 1987; 252: H 1138-1146.

Cade, J.F.J. Lithium salts in the treatment of psychotic excitement. Med. J. Aust., 1949; 36: 349-352.

Campbell, M.K. Hormones and second messengers. In "Biochemistry", 1995; second edition: 566-577.

Canessa, M., Adragna, N.C., Solomon, H.S., Connolly, T.M., Tosteson, T.M. Increased sodium-lithium countertransport in red cells of patients with essential hypertension. New Engl. J. Med., 1980; 302: 772-776.

Chi, Y., Mota de Freitas, D., Sikora, M., Bansal, V.K. Correlations of Na^+-Li^+ exchange activity with Na^+ and Li^+ binding and phospholipid composition in erythrocyte membranes of white hypertensive and normotensive individuals. Hypertension, 1996; 27: 456-464.

Codina, J., Hildebrandt, J., Sekura, R., Birnbaumer, M., Bryan, J., Manclark, C., Iyengar, R., Birnbaumer, L. N_s and N_i, the stimulatory and inhibitory regulatory components of adenylate cyclases. J. Biol. Chem., 1984; 259: 5871-5886.

Coleman, D.E., Berghuis, A.M., Lee, E., Linder, M.E., Gilman, A.G., Sprang, S.R. Structures of active conformations of $G_{i\alpha 1}$ and the mechanism of GTP hydrolysis. Science, 1994a; 265: 1405-1412.

Coleman, D.E., Lee, E., Mixon, M.B., Linder, M.E., Berghuis, A.M., Gilman, A.G., Sprang, S.R. Crystallization and preliminary crystallographic studies of $G_{i\alpha 1}$ and mutants of $G_{i\alpha 1}$ in the GTP and GDP-bound states. J. Mol. Biol., 1994b; 238: 630-634.

Corfu, N.A., Tribolet, R., Sigel, H. Comparison of self-association properties of the 5'-triphosphates of inosine (ITP), guanosine (GTP), and adenosine (ATP). Eur. J. Biochem., 1990; 191: 721-735.

Cullis, P.R., Hope, M.J. Physical properties and functional roles of lipids in membranes. In "Biochemistry of Lipids and Membranes" (Vance, D.E & Vance, J.E., eds.). Benjamin/Cummings Publ. Co., Menlo Park. 1985; 25-72.

Damonte, G., Sdraffa, A., Zocchi, E., Guida, L., Polvani, C., Tonetti, M., Benatti, U., Boquet, P., Flora, A.D. Multiple small molecular weight guanine nucleotide-binding proteins in human erythrocyte membranes. Biochem. Biophys. Res. Commn., 1990; 166: 1398-1405.

Edzes, H.T., Teerlink, T., Van Der Knaap, M.S., Valk, J. Analysis of phospholipids in brain tissue by ^{31}P NMR at different compositions of the solvent system chloroform-methanol-water. Magn. Reson. Med., 1992; 26: 46-59.

Eliav, U., Shinar, H., Navon, G. The formation of a second-rank tensor in ^{23}Na double-quantum-filtered NMR as an indicator for order in a biological tissue. J. Magn. Reson., 1992; 98: 223-229.

Eliav, U., Navon, G. Analysis of double-quantum-filtered NMR spectra of ^{23}Na in biological tissues. J. Magn. Reson., 1994; 103: 19-29.

Evans, T., Brown, M.L., Fraser, E.D., Northup, J.K. Purification of the major GTP-binding proteins from human placental membranes. J. Biol. Chem., 1986; 261: 7052-7059.

Fairbanks, G., Steck, T.L., & Wallach, D.F.H. Electrophoretic analysis of the major polypeptides of the human erythrocyte membrane. Biochemistry, 1971; 10: 2606-2617.

Fanger, B.O. Adaptation of the Bradford protein assay to membrane-bound proteins by solubilizing in glucopyranoside detergents. Anal. Biochem., 1987; 162: 11-17.

Frausto da Silva, J.J.R., Williams, R.J.P. Possible mechanism for the biological action of lithium. Nature, 1976; 263: 237-239.

Frazer, A., Mendels, J., Brunswick, D., London, J., Pring, M., Ramsey, A., Rybakowski J. Erythrocyte concentrations of lithium ion: Clinical correlates and mechanisms of action. Am. J. Psychiatry, 1978; 135: 1065-1069.

Fukada, Y., Takao, T., Oghuro, H., Yoshizawa, T., Akino, T., Shimonishi, Y. Farnesilated subunit of photoreceptor G protein indispensable for GTP binding. Nature, 1990; 346: 658-660.

Fung, B.K., Hurley, J.B., Stryer, L. Flow of information in the light-triggered cyclic nucleotide cascade of vision. Proc. Natl. Acad. Sci. USA, 1981; 78: 152-156.

Geisler, A., & Mork, A. The interaction of lithium with magnesium-dependent enzymes. In R. O. Bach and V. S. Gallicchio (eds.) Lithium and Cell Physiology. New York: Springer-Verlag, 1990: pp 125-136.

Gilman, A.G. G proteins: Transducers of receptor-generated signals. Ann. Rev. Biochem., 1987; 56: 615-649.

Glonek, T. ^{31}P NMR of Mg-ATP in dilute solutions: complexation and exchange. Int. J. Biochem., 1992; 24: 1533-1559.

Gorenstein, D.G. Phosphorous-31 chemical shifts: Principles and emperical observations: In David G Gorenstein (ed.) Phosphorous-31 NMR principles and applications. New York: Academic Press Inc., 1984: 7-36.

Greiner, C.A.M., Greiner, J.V., Hebert, E., Berthiaume, R.R., Glonek, T. Phospholipid analysis of mammalian optic nerve tissue: A ^{31}P nuclear magnetic resonance spectroscopic study. Opthalmic Res., 1994; 26: 264-274.

Gullapalli, R. P., Hawk, R. M., Komoroski, R. A. Effect of lithium on double-quantum behavior of ^{23}Na in normal human erythrocytes. Magn. Reson. Med., 1992; 27: 1-12.

Hall, A. The cellular functions of small GTP-binding proteins. Science, 1990; 249: 635-640.

Hepler, J.R., Gilman, A.G. G Proteins. TIBS Lett., 1992; 17: 383-387.

Higashijima, T., Graziano, M.P., Suga, H., Kainosho, M., Gilman, A.G. ^{19}F and ^{31}P NMR spectroscopy of G protein α subunits. Mechanism of activation by Al^{3+} and F^-. J. Biol. Chem., 1991; 266: 3396-3401.

Hu, J.-S., Redfield, A.G. Mapping the nucleotide-dependent conformational change of human N-ras p21 in solution by heteronuclear-edited proton-observed NMR methods. Biochemistry, 1993; 32: 6763-6772.

Hubbard, P.S. Nonexponential nuclear magnetic relaxation by quadrupole interactions. J. Chem. Phys., 1970; 53, 985-989.

Hucho, F. In "Neurochemistry: Fundamentals and concepts", 1986; 25-27.

Hutchinson, R.B., Huntley, J.J.A., Zhou, H.Z., Ciesla, D.J., Shapiro, J.I. Changes in double quantum filtered sodium intensity during prolonged ischemia in the isolated perfused heart. Magn. Reson. Med., 1993; 29: 391-395.

Ikeda, K., Kikuchi, A., Takai, Y. Small molecular weight GTP-binding proteins in human erythrocyte ghosts. Biochem. Biophys. Res. Commn., 1988; 156: 889-897.

Jaccard, G., Wimperis, S., Bodenhausen, G. Multiple-quantum NMR spectroscopy of S = 3/2 spins in isotropic phase: a new probe for multiexponential relaxation. J. Chem. Phys., 1986; 85: 6282-6893.

James, T.L., Noggle, J.H. ^{23}Na nuclear magnetic resonance relaxation studies of sodium ion interaction with soluble RNA. Proc. Natl. Acad. Sci. USA, 1969; 62: 644-649.

Jefferson, J.W., Greist, J.H., Baudhuin, M. Lithium in psychiatry. In R. O. Bach (ed.) Lithium: Current Applications in Science, Medicine and Technology. New York: Wiley, 1985.

Jelicks, L.A., Gupta, R.K. On the extracellular contribution to multiple quantum filtered ^{23}Na NMR of perfused rat heart. Magn. Reson. Med., 1993; 29: 130-133.

John, J., Sohmen, R., Feuerstein, J., Linke, R., Wittinghofer, A., Goody, R.S. Kinetics of interaction of nucleotides with nucleotide-free H ras p21. Biochemistry, 1990; 29: 6058-6065.

Jope, R.S., Williams, M.B. Lithium and brain signal transduction systems. Biochem. Pharmacol., 1994; 47: 429-441.

Kaziro, Y., Itoh, H., Kozasa, T., Nakafuku, M., Satoh, T. Structure and function of signal-transducing GTP-binding proteins. Annu. Rev. Biochem., 1991; 60: 349-400.

Kikuchi, A., Yamashita, T., Kawata, M., Yamamoto, K., Ikeda, K., Tanimoto, T., Takai Y. Purification and characterization of a novel GTP-binding protein with a molecular weight of 24,000 from bovine brain membranes. J. Biol. Chem., 1988; 263: 2897-2904.

Knubovets, T., Shinar, H., Eliav, U., Navon, G. A ^{23}Na multiple-quantum-filtered NMR study of the effect of the cytoskeleton conformation on the anisotropic motion of sodium ions in red blood cells. J. Magn. Reson., 1996; 110: 16-25.

Krengel, U., Schlichting, I., Scherer, A., Schumann, R., Frech, M., John, J., Kabsch, W., Pai E.F., Wittinghofer, A. Three-dimensional structure of H-ras p21 mutants: molecular basis for their inability to function as signal switch molecules. Cell, 1990; 62: 539-548.

Kurumi, Y., Adachi, Y., Itoh, T., Kobayashi, H., Nanno, T., Yamamoto, T. Novel high-performance liquid chromatography for determination of membrane phospholipid composition of rat hepatocytes. Gastroenterol. Japonica. 1991; 26: 628-632.

Lacal, J.C., McCormick, F. The ras Superfamily of GTPases. Baco Raton: CRC, 1993.

Lambright, D.G., Noel, J.P., Hamm, H.E., Sigler, P.B. Structural determinants for activation of the α-subunit of a heterotrimeric G protein. Nature, 1994; 369: 621-628.

Lee, E., Linder, M., Gilman, A.G. Expression of G-protein α subunits in *Escherichia coli*. Methods Enzymol., 1994; 237: 146-164.

Lochrie, M.A., Hurley, J.B., Simon, M.I. Sequence of the alpha subunit of photoreceptor G protein: homologies between transducin, ras, and elongation factors. Science, 1985; 228: 96-99.

Lyon, R. C., McLaughlin, A. C. Double-quantum-filtered ^{23}Na NMR study of intracellular sodium in the perfused liver. Biophys. J., 1994; 67: 369-376.

Mallinger, A.G., Yoa, J.K., Brown, A.S., Dippold, C.S. Analysis of complex mixtures of phospholipid classes from cell membranes using two-dimensional thin-layer chromatography and scanning laser densitometry. J. Chromatogr., 1993; 614: 67-75.

Manji, H.K. G proteins: implications for psychiatry. Am. J. Psychiatry, 1992; 149: 746-760.

Manji, H.K., Chen, G., Shimon, H., Hsiao, J.K., Potter, W.Z., Belmaker, R. H. Guanine nucleotide binding proteins in bipolar affective disorder. Effects of long-term lithium treatment. Arch. Gen. Psychiatry, 1995; 52: 135-144.

Medynski, D.C., Sullivan, K., Smith, D., Van Drop, C., Chang, F.H. Amino acid sequence of the alpha subunit of transducin deduced from the cDNA sequence. Proc. Natl. Acad. Sci. USA, 1985; 82: 4311-4315.

Meltzer, H.L. Is there a specific membrane defect in bipolar disorders? Biol. Psychiatry, 1991; 30: 1071-1074.

Meneses, P., Glonek, T. High resolution ^{31}P NMR of extracted phospholipids. J. Lipid. Res., 1988; 29: 679-689.

Merchant, T.E., Glonek, T. ^{31}P NMR of tissue phospholipids: competition for Mg^{2+}, Ca^{2+}, Na^{+} and K^{+} cations. Lipids, 1992; 27: 551-559.

Milburn, M.V., Tong, L., DeVos, A.M., Brunger, A., Yamaizumi, Z., Nishimura, S., Kim, S.-H. Molecular switch for signal transduction: structural differences between active and inactive forms of protooncogenic ras proteins. Science, 1990; 247: 939-945.

Miller, A.-F., Halkides, J., Redfield, A.G. An NMR comparison of the changes produced by different guanosine 5'-triphosphate analogs in wild-type and oncogenic mutant p21 *ras*. Biochemistry, 1993; 32: 7367-7376.

Mork, A. Actions of lithium on second messenger activity in the brain. The adenylate cyclase and phosphoinositide systems. Lithium, 1990; 1: 131-147.

Mota de Freitas, D., Silberberg, J., Espanol, M.T., Dorus, E., Abraha, A., Dorus, W., Elenz, E., Whang, W. Measurement of lithium transport in RBC from psychiatric patients receiving lithium carbonate and normal individuals by ^{7}Li NMR spectroscopy. Biol. Psychiatry, 1990; 28: 175-184.

Mota de Freitas, D. Alkali metal NMR. In J.F. Riordan and B.L. Vallee (eds.) Methods Enzymol., 1993; 227: 78-106.

Mota de Freitas, D., Amari, L., Srinivasan, C., Rong, Q., Ramasamy, R., Abraha, A., Geraldes, C.F.G.C., Boyd, M.K. Competition between Li^{+} and Mg^{2+} for the phosphate groups in the human erythrocyte membrane and ATP: an NMR and fluorescence study. Biochemistry, 1994a; 33: 4101-4110.

Mota de Freitas, D., Abraha, A., Rong, R., Silberberg, J., Whang, W., Borge, G.F., Elenz, E. Relationship between lithium ion transport and phospholipid composition in erythrocytes from bipolar patients receiving lithium carbonate. Lithium, 1994b; 5: 29-39.

Naccarato, W.F., Ray, R.E., Wells, W.W. Biosynthesis of myo-inositol in rat mammary gland. Isolation and properties of the enzymes. Arch. Biochem. Biophys., 1974; 164: 194-

201.

Navon, G., Werrmann, J.G., Maron, R., Cohen, S.M. ^{31}P NMR and triple quantum filtered ^{23}Na NMR studies of the effects of inhibition of Na^+/H^+ exchange on intracellular sodium and pH in working and ischemic hearts. Magn. Reson. Med., 1994; 32: 556-564.

Newton, C., Pangborn, W., Nir, S., Papahadjoupoulos, D. Specificity of Ca^{2+} and Mg^{2+} binding to phosphatidylserine vesicles and resultant phase changes of bilayer membrane structure. Biochim. Biophys. Acta, 1988; 506: 281-287.

Noel, J.P., Hamm, H.E., Sigler, P. The 2.2 Å crystal structure of transducin-α complexed with GTPγS. Nature, 1993; 366: 654-663.

Northup, J., Sternweis, P., Smigel, M., Schleifer, L., Ross, E., Gilman, A. Purification of the regulatory component of adenylate cyclase. Proc. Natl. Acad. Sci. USA, 1980; 77: 6516-6520.

Olate, J., Allende, J.E. Structure and function of G proteins. Pharmac. Ther., 1991; 51: 403-419.

Pai, E.F., Kabsch, W., Krengel, U., Holmes, K.C., John, J., Wittinghofer, A. Structure of the guanine-nucleotide-binding domain of the Ha-ras oncogene product p21 in the triphosphate conformation. Nature, 1989; 341: 209-214.

Pai, E.F., Krengel, U., Pestsko, G.A., Goody, R.S., Kabsch, W., Wittinghofer, A. Refinement of crystal structure of the triphosphate conformation of H-ras p21 at 1.35 Å resolution: implications for the mechanism of GTP hydrolysis. EMBO J., 1990; 9: 2351-2359.

Panchalingam, K., Sachedina, S., Pettegrew, J.W., Glonek, T. Al-ATP as an intracellular carrier of Al(III) ion. Int. J. Biochem., 1991; 23: 1453-1469.

Pekar, J., Leigh, J.S. Jr. Detection of biexponential relaxation in sodium-23 facilitated by double-quantum filtering. J. Magn. Reson., 1986; 69: 582-584.

pET system manual. In "Novagen", 1995; fifth edition: 22-24.

Pettegrew, J.W., Post, J.F.M., Panchalingam, K., Withers, G., Woessner, D.E. ^7Li NMR study of normal human erythrocytes. J. Magn. Res., 1987; 71: 504-519.

Pollack, S.J., Atack, J.R., Knowles, M.R., McAllister, G., Ragan, C.I., Baker, R., Fletcher, S.P., Iversen, L.I., Broughton, H.B. Mechanism of inositol monophosphatase, the putative target of lithium therapy. Proc. Natl. Acad. Sci. USA, 1994; 91: 5766-5770.

Post, J.F.M., Wilkinson, D.A. ^7Li NMR investigations of lithium phospholipid interactions. J. Colloid Interface Sci., 1991; 143: 174-179.

Prigodich, R.V., Haake, P. Association phenomena .5. Association of cations with nucleoside diphosphate and triphosphate studied by P-31 NMR. Inorg. Chem., 1985; 24: 89-93.

Ramasamy, R., Mota de Freitas, D. Competition between Li^+ and Mg^{2+} for ATP in human erythrocytes. FEBS Lett., 1989; 244: 223-226.

Ramasamy, R., Mota de Freitas, D., Bansal, V.K., Labotka, R. Nuclear magnetic resonance studies of lithium transport in erythrocyte suspensions of hypertensives. Clin. Chim. Acta, 1990; 188: 169-176.

Ramsey, T.A., Frazer, A., Mendels, J., Dyson, L. The erythrocyte lithium-plasma ratio in patients with primary affective disorder. Arch. Gen. Psychiatry, 1979; 36: 457-461.

Rawis, R.L. G-proteins: Research unravels their role in cell communication. C&EN News, December 1987; 26-39.

Reddy, R., Bolinger, L., Shinnar, M., Noyszewski, E., Leigh, J.S. Detection of residual quadrupolar interaction in human skeletal muscle and brain *in vivo* via multiple quantum filtered sodium NMR spectra. Magn. Reson. Med., 1995; 33: 134-139.

Rens-Domiano, S., Hamm, H.E. Structural and functional relationships of heterotrimeric G-proteins. FASEB J., 1995; 9: 1059-1066.

Riddell, F.G., Arumugam, S. Surface charge effects upon membrane transport processes: the effects of surface charge on the monensin-mediated transport of lithium ions through phospholipid bilayers studied by ^7Li NMR spectroscopy. Biochim. Biophys. Acta, 1988; 945: 65-72.

Rong, Q., Mota de Freitas, D., Geraldes, C.F.G.C. Competition between lithium and magnesium ions for guanosine di- and triphosphates in aqueous solution: a nuclear magnetic resonance study. Lithium, 1992; 3: 213-220.

Rong, Q., Espanol, M., Mota de Freitas, D., Geraldes, C.F.G.C. ^7Li NMR relaxation study of Li^+ binding in human erythrocytes. Biochemistry, 1993; 32: 13490-13498.

Rong, Q., Mota de Freitas, D., Geraldes, C.F.G.C. Competition between lithium and magnesium ions for the substrates of second messenger systems: a nuclear magnetic resonance study. Lithium, 1994; 5: 147-156.

Roux, M., Bloom, M. Ca^{2+}, Mg^{2+}, Li^+, Na^+, and K^+ distributions in the headgroup region of binary membranes of phosphatidylcholine and phosphatidylserine as seen by deuterium NMR. Biochemistry, 1990; 29: 7077-7089.

Schou, M. Biology and pharmacology of lithium ion. Pharmacol. Rev., 1957; 9: 17-58.

Schlichting, I., Almo, S.C., Rapp, G., Wilson, K., Petratos, K., Lentfer, A., Wittinghofer, A., Kabsch, W., Pai, E.F., Petsko, G.A., Goody, R.S. Time-resolved X-ray crystallographic study of the conformational change in Ha-ras p21 protein on GTP hydrolysis. Nature, 1990; 345: 309-315.

Schreiber, G., Avissar, S., Danon, A., Belmaker, R.H. Hyperfunctional G proteins in mononuclear leukocytes of patients with mania. Biol. Psychiatry, 1991; 29: 273-280.

Schwartz, R.S., Chiu, D.T.Y., Lubin, B. In Erythrocyte Membranes 3: Recent Clinical and Experimental Advances (Kruckeberg W. C, Eaton J. W, Aster J, Brewer G. J., eds.), 1984, pp. 89-122, Alan R. Liss, Inc., New York.

Shinar, H., Knubovets, T., Eliav, U., Navon, G. Sodium interaction with ordered structures in mammalian red blood cells detected by Na-23 double quantum NMR. Biophys. J., 1993; 64: 1273-1279.

Singer, S.J., Nicolson, G.L. The fluid mosaic model of the structure of cell membranes. Science, 1972; 175: 720-731.

Skiba, N.P., Bae, H., Hamm, H.E. Mapping of effector binding sites of transducin α-subunit using $G\alpha_t/G\alpha_{i1}$ chimeras. J. Biol. Chem., 1996; 271: 413-424.

Smithers, G.W., Poe, M., Latwesen, D.G., Reed, G.H. Electron paramagnetic resonance measurements of the hydration of Mn(II) in ternary complexes with GDP and *ras* p21 proteins. Arch. Biochem. Biophys., 1990; 280: 416-420.

Sondek, J., Lambright, D.G., Noel, J.P., Hamm, H.E., Sigler, P.B. GTPase mechanism of G proteins from the 1.7-Å crystal structure of transducin α.GDP.AlF_4^-. Nature, 1994; 372: 276-279.

Sondek, J., Bohm, A., Lambright, D.G., Hamm, H.E., Sigler, P.B. Crystal structure of a G_A protein βγ dimer at 2.1 Å resolution. Nature, 1996; 379: 369-374.

Sontheimer, G.M., Kuhn, W., Kalbitzer, H.R. Observation of Mg^{2+}.ATP and uncomplexed ATP in slow exchange by ^{31}P NMR at high magnetic fields. Biochem. Biophys. Res. Commun., 1986; 134: 1379-1386.

Spiegel, A.M., Backlund Jr, P.S., Butrynski, J.E., Jones, T.L.Z., Simonds, W.F. The G protein connection: molecular basis of membrane association. TIBS, 1991; 16: 338-341.

Steck, T.L., Kant, J.A. Preparation of impermeable ghosts and inside-out vesicles from human erythrocyte membranes. Methods Enzymol., 1974; 31: 172-180.

Sternweis, P., Robishaw, J. Isolation of two proteins with high affinity for guanine nucleotides from membranes of bovine brain. J. Biol. Chem., 1984; 259: 13806-13813.

Stryer, L. Visual excitation and recovery. J. Biol. Chem., 1991; 266: 10711-10714.

Stryer, L. Membrane structure and dynamics. In "Biochemistry", 1995; fourth edition: 278-289.

Surgenor, M. In Red Blood Cell, Academic Press, New York, 1974.

Tanabe, T., Nukada, T., Nishikawa, Y., Sugimoto, K., Suzuki, H. Primary structure of the alfa-subunit of transducin and its relationship to *ras* proteins. Nature, 1985; 315: 242-245.

Ting, T.D., Goldin, S.B., Ho, Y.-K. Purification and characterization of bovine transducin and its subunits. Methods Neurosci., 1993; 15: 180-195.

Tong, L., DeVos, A.M., Milburn, M.V., Kim, S.-H. Crystal structure at 2.2 Å resolution of the catalytic domains of normal and an oncogenic mutant complexed with GDP. J. Mol. Biol., 1991; 217: 503.

Urry, W., Trapane, L., Venkatachalam, C.M., McMichens, R.B. Ion interactions at membranous polypeptide sites using nuclear magnetic resonance: determining rate and binding constants and site locations. Methods Enzymol., 1989; 171: 286-287.

Wall, M.A., Coleman, D.E., Lee, E., Iniguez-Lluhi, J.A., Posner, B.A., Gilman, A.G., Sprang, S.R. The structure of the G protein heterotrimer $G_{i\alpha 1}\beta_1\gamma_2$. Cell, 1995; 83: 1047-1058.

Yatsunami, K., Khorana, H.G. GTPase of bovine rod outer segments: the amino acid sequence of the alpha subunit as derived from the cDNA sequence. Proc. Natl. Acad. Sci. USA, 1985; 82: 4316-4320.

Young, L.T., Li, P.P., Kamble, A., Siu, K.P., Warsh, J.J. Postmortem cerebral cortex G_s α-subunit levels are elevated in bipolar affective disorder. Brain Res., 1991; 533: 323-326.

Young, L.T., Li, P.P., Kamble, A., Siu, K.P., Warsh, J.J. Mononuclear leukocyte levels of G proteins in depressed patients with bipolar disorder or major depressive disorder. Am. J. Psychiatry, 1994; 151: 594-596.

Zachariah, C. Multinuclear NMR study of anion binding to copper zinc superoxide dismutase, and of lithium transport and binding in cultured neuroblastoma cells. Ph.D. Dissertation, Loyola University of Chicago, 1996.

VITA

The author, Chandra Srinivasan, was born on January 21, 1969 in Bangalore, India. She obtained her Bachelor of Science degree in 1989 from St. Joseph's college, Bangalore. The author continued to work in the same college and obtained her Master of Science degree in Chemistry in 1991. She was supported by a Bangalore University Scholarship from 1986 until 1991. In the Fall of 1991, she was admitted to the Graduate program at Loyola University Chicago. She received a graduate teaching assistantship from August 1991 - 1994. From August 1994 until August 1995 she was supported by a NIMH grant awarded to Prof. Duarte Mota de Freitas. The author was awarded the Arthur J. Schmitt dissertation fellowship for a period from September 1995 until May 1996. The author was also elected in 1995 to "Alpha Sigma Nu", the National Jesuit Honor Society.

LIST OF PUBLICATIONS

A. Refereed Articles:

1. "Competition between Li^+ and Mg^{2+} for the phosphate groups in the human erythrocyte membrane and ATP: An NMR and fluorescence study," D. Mota de Freitas, L. Amari, C. Srinivasan, Q. Rong, R. Ramasamy, A. Abraha, C.F.G.C. Geraldes, and M.K. Boyd. *Biochemistry* **1994**, 33: 4101-4110.

2. "pH determinations in sulfonate buffers by ^{17}O and ^{33}S NMR." A. Aldridge, C. Srinivasan and D. Crumrine (Submitted).

B. Abstracts:

1. "NMR study of the competition between lithium and magnesium ions for Human RBC membrane phospholipids." C. Srinivasan and D. Mota de Freitas. ISMAR-95, Sydney, Australia; July 1995.

2. "Competition between Li^+ and Mg^{2+} for the metal binding domain in G proteins." D. Mota de Freitas, C. Srinivasan and L. Amari. Lithium Symposium, Malta; November 1995.

3. "pH Determinations in Sulfonate Buffers by ^{17}O and ^{33}S NMR" A. Aldridge, C. Srinivasasn, D.S. Crumrine, 36th Experimental NMR Conference, Boston, MA; March 1995.

4. "The pH Dependence of HEPES ^{33}S NMR in the Presence of BSA" A. Aldridge, C. Srinivasan, D.S. Crumrine, 37th Experimental NMR Conference, Pacific Grove, CA; March 1996.

APPROVAL SHEET

The dissertation submitted by Chandra Srinivasan has been read and approved by the following committee:

Duarte E. Mota de Freitas, Ph.D., Director
Professor, Chemistry
Loyola University Chicago

David S. Crumrine, Ph.D.
Associate Professor, Chemistry
Loyola University Chicago

Evan B. Stubbs, Ph.D.
Assistant Professor, Neurology
Loyola University Medical Center / V.A. Hines Hospital

Poluru L. Reddy, Ph.D.
Assistant Professor (Research), Pathology and Laboratory Medicine
Northwestern University, The Evanston Hospital

The final copies have been examined by the director of the dissertation and the signature which appears below verifies the fact that any necessary changes have been incorporated and the dissertation is now given final approval by the committee with reference to content and form.

The dissertation is, therefore, accepted in partial fulfillment of the requirements for the degree of Doctor of Philosophy.

7/3/96
Date

Director's Signature